Chem Soc Rev

Metal Carbonyl Clusters: Synthesis and Catalysis

Journal:	*Chemical Society Reviews*
Manuscript ID	CS-REV-02-2021-000161.R2
Article Type:	Review Article
Date Submitted by the Author:	04-Jun-2021
Complete List of Authors:	Cesari, Cristiana; University of Bologna, Chimica Industriale "Toso Montanari" Shon, JongHwa; UC Davis, Chemistry Zacchini, Stefano; Universita di Bologna, Dipartimento di Chimica Industriale "Toso Montanari" Berben, Louise; UC Davis, Chemistry

Metal Carbonyl Clusters of Groups 8 – 10: Synthesis and Catalysis

Cristiana Cesari,[‡2] Jong-Hwa Shon,[‡1] Stefano Zacchini,*[2] Louise A. Berben*[1]

[1] *Department of Chemistry, The University of California, Davis CA, 95616, United States*
[2] *Dipartimento di Chimica Industriale "Toso Montanari", Università di Bologna, Viale Risorgimento 4, 40136 Bologna, Italy*

[‡] These authors contributed equally.

Corresponding Authors
laberben@ucdavis.edu, stefano.zacchini@unibo.it

Abstract. In this review article, we discuss advances in the chemistry of metal carbonyl clusters (MCCs) spanning the last three decades, with an emphasis on the more recent reports and those involving Groups 8 – 10 elements. Synthetic methods have advanced and been refined, leading to higher-nuclearity clusters and a wider array of structures and nuclearities. Our understanding of the electronic structure in MCCs has advanced to a point where molecular chemistry tools and other advanced tools can probe their properties at a level of detail that surpasses that possible with other nanomaterials and solid-state materials. MCCs therefore advance our understanding of structure–property–reactivity correlations in other higher-nuclearity materials. With respect to catalysis, this article focuses only on homogeneous applications, but it includes both thermally and electrochemically driven catalysis. Applications in thermally driven catalysis have found success where the reaction conditions stabilise the compounds toward loss of CO. In more recent years, MCCs, which exhibit delocalised bonding and possess many electron-withdrawing CO ligands, have emerged as very stable and effective for reductive electrocatalysis reactions since reduction often strengthens M–C(O) bonds and since room-temperature reaction conditions are sufficient for driving the electrocatalysis.

1. Introduction

A review article describing clusters and their analogies with surfaces was published in 1979 by Muetterties and Rhodin and coworkers; the second page states, “With such riches, a comprehensive review of chemical bonding in metal clusters compared to metal surfaces is neither practical nor appropriate here. ... The largest subgroup comprises the metal carbonyl clusters and the size range

within this subgroup extends through the full, established range for clusters of 3 to 30."[1] Now 42 years later, the size range of homoleptic metal carbonyl clusters (MCCs) has expanded, ranging from 3 to 56; since then, hundreds of papers reporting the activity targeting the many aspects of MCC chemistry have been published. Numerous other reviews have appeared since that time,[2345678910111213141516] and a comprehensive review is certainly not practical or appropriate in the foregoing pages of this article. Hence, we will focus our insights on synthetic methods for obtaining Groups 8 – 10 MCCs and on their use as homogeneous catalysts and as homogeneous electrocatalysts. We will feature work published in the most recent decades, and we will provide a view of future interesting directions in the field. We have decided to exclude MCCs of Groups 5 – 7 because they span a smaller range of clusters, and examples of their synthesis and catalysis are primarily older work.

The work of Hieber defined the beginning of modern metal-carbonyl chemistry and at the same time, of modern organometallic hydride chemistry with the reports of reactions surrounding $Fe(CO)_5$ and the synthesis of $H_2Fe(CO)_4$ in 1931.[15] The chemistry of MCCs developed rapidly in the 1970s and 1980s, whereas there was a marked decline in publications on this topic in the 1990s. A renewed interest started in the noughties,[16] due to the intense research in the more general field of molecular nanoclusters and ultra-small metal nanoparticles.[17181920212122] Within this framework, the recent research in MCC chemistry has focused on the synthesis and structural characterization of metal carbonyl nanoclusters (high-nuclearity MCCs), the investigation of their physical properties in relationship with their molecular structure and composition, and their applications in catalysis and electrocatalysis. Because high temperatures may initiate CO ligand loss, electrocatalysis enables catalysis at room temperature, where MCC decomposition is less likely. Electrochemical reduction reactions in MCCs are particularly promising because the many CO ligands are very efficient at stabilising any electrons added to the cluster core to initiate reductive electrocatalytic reaction cycles. Some of these aspects will be covered in this review. General references, covering the full scope of MCC chemistry, may be found in the cited literature.

In the first part of this review, we discuss in detail the synthesis of MMCs from Groups 8 – 10; after general principles, we illustrate representative examples from recent work. In the Electronic Supporting Information (ESI), we also tabulate many of the known MCCs with citations to their syntheses. To further narrow the scope of the review, we mainly focus our attention on the syntheses of homometallic and homoleptic MCCs. Only a few examples of significant heterometallic and heteroleptic MCCs and of MCCs containing main-group elements will be discussed. The readers can find pertinent references throughout the text. In the second part of this review, we discuss both homogeneous catalysis and homogeneous electrocatalysis, along with the

relative advantages of using MCCs to promote these processes. To clarify, homogeneous refers to the fact that the (electro)catalysts are in solution-phase along with reactants and other additives; unless specified, "catalysis" refers to reactions requiring thermal activation while "electrocatalysis" requires an applied potential. Heterogeneous catalysis, where the electrocatalyst is not in the same phase as the reactants, falls outside the scope of this review; however, we recognise that MCCs have been supported by various matrices to modify their catalytic activities, and some of that work has been summarised in review articles or books.[2324252627] For instance, Pt_{12} and Pt_{13} clusters have been selectively synthesised within dendrimer templates and show dramatically different catalytic activities in the oxygen reduction reaction, which occurs at the cathode of fuel cells.[28] MCCs have also been employed for the preparation of Pt clusters of controlled sizes inside metal–organic frameworks and employed for catalysis and electrocatalysis.[29]

2. Metal Carbonyl Clusters: Synthesis

2.1 General Principles

Methodologies for the syntheses of MMCs may be grouped into four broad categories,[5] which can be applied to both homo- and hetero-metallic species (Scheme 1):

1) Direct (reductive) carbonylation;
2) Thermal methods;
3) Redox methods;
4) Other chemically induced methods.

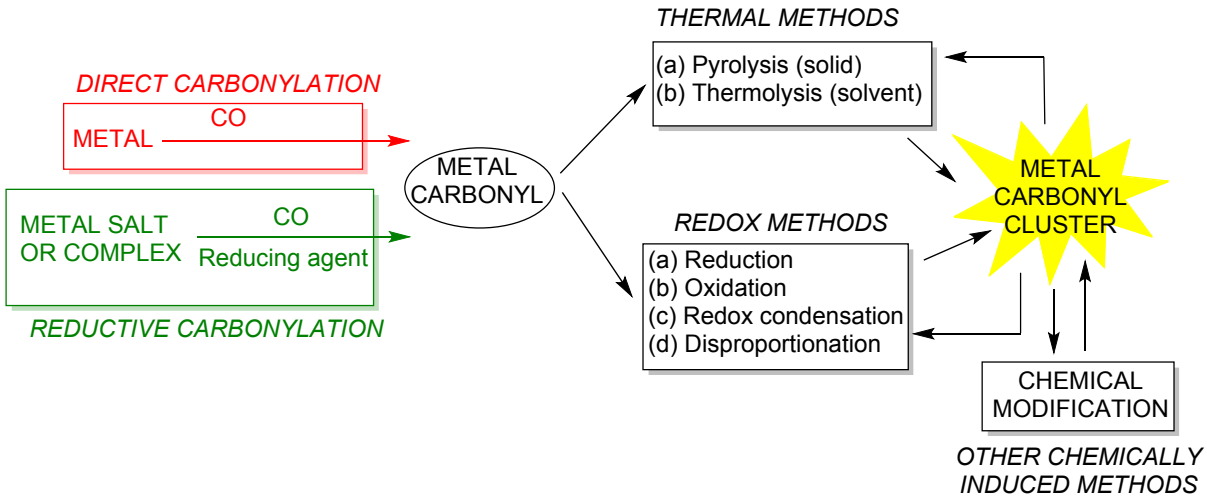

Scheme 1. General methods for the synthesis of MCCs.[5] MCCs can be obtained from non-carbonyl precursors by direct or reductive carbonylation. Low nuclearity metal carbonyls can be transformed into larger MCCs through thermal and redox methods. Moreover, MCCs can be used as starting

material in thermal, redox or other chemically induced methods for the preparation of further MCCs.

It must be remarked that the distinction among these four categories is mainly based on the experimental conditions adopted; from a mechanistic point of view (when a mechanism may be devised), they are often overlapping. For instance, heating a metal carbonyl in the presence of a base is usually classified as a thermal method, even if the mechanism may also involve redox reactions. Syntheses of category (1) start from a non-carbonyl precursor, whereas those of categories (2)–(4) employ carbonyl species.

Compared to C–C bonds, M–M interactions are weaker and non-directional. As a consequence, MCCs adopt a rich variety of structures even in the case of species with similar compositions. The products obtained are highly dependent on the experimental conditions, which, therefore, must be very carefully controlled. A tailored synthesis of a particular structure is still a dream. Nonetheless, it is nowadays possible to outline some general guidelines for the preparation of MCCs with a given composition and for inducing their growth up to the nanometric level.[2,3,5,6,8-11,30] Moreover, isolated MCCs can be modified and functionalised with ancillary ligands to induce new properties, to be anchored onto supports, or to be transformed into nanostructured catalysts.[2,3,5,6,8-11,30]

Infrared (IR) monitoring of the reactions is a very useful tool. Reactions are often accompanied by the formation of side products, such as small carbonyl complexes (*e.g.*, $Ni(CO)_4$, $[Co(CO)_4]^-$, $Ni(CO)_3(PPh_3)$, $[Rh(CO)_4]^-$), bulk metals, metal salts, and other MCCs. Separation and purification of the major product is mainly achieved using solvent extraction, owing to the solubility differences of the product and side products in water and organic solvents. In the case of anionic MCCs, this may be enhanced by choosing suitable tetra-substituted-ammonium or -phosphonium cations. For less charged and neutral MCCs, chromatography is sometimes employed. The resulting yields vary case by case, but many MCCs can be obtained on the hundreds-of-milligram or even gram scale.

Direct (reductive) carbonylation. Direct and reductive carbonylation are the major methods for the preparation of metal carbonyls starting from non-carbonyl precursors.[2,3,5] Direct carbonylation of a finely divided metal under CO works only in a few cases, such as with Fe, Ni, and Co. Reductive carbonylation is a more general procedure, which requires the reduction of a metal salt under CO atmosphere. The reducing agent (H_2, Na, CO itself, *etc.*), temperature, and CO pressure employed depend on the metal. In some cases, harsh conditions are required, and in other cases, the reactions may be performed at room temperature (RT) with 1 atm of CO. For instance,

ambient reductive carbonylation may be used for the synthesis of $Rh_4(CO)_{12}$,[31] $Ir_4(CO)_{12}$,[32] $[Rh(CO)_4]^-$, [33] $[Ir(CO)_4]^-$,[33] and the $[Pt_{3n}(CO)_{6n}]^{2-}$ (n = 1–10).[34] Even if $Ru_3(CO)_{12}$ may be prepared with CO at atmospheric pressure,[35] the high-pressure synthesis is often more convenient.[36] The use of CO as a reducing agent is summarised by the half-reaction (Equation 1); a suitable amount of base is used to tune the reducing ability of CO.

$$CO + 2OH^- \rightarrow CO_2 + H_2O + 2e \quad (1)$$

Reductive carbonylation may also be used in the solid state.[37] Moreover, reductive carbonylation of Pd salts in the presence of PR_3 has been extensively used by Dahl and Mednikov for the synthesis of Pd-CO-PR_3 clusters (see the ESI: Scheme S1).[13]

Thermal methods. CO elimination from a MCCs is an endothermic process with a favourable entropic term; therefore, it is usually promoted by thermal methods, in the solid phase (pyrolysis) and in solution (thermolysis). Other than decomposition, four possible events may follow CO elimination from a MCC, with event (4) as the most common:[2]

1) No reaction. In very few cases, the same cluster cage can be stabilised by different numbers of CO ligands, as in the case of $[Rh_{12}Sn(CO)_{27-x}]^{4-}$ (n = 0, 1, 2) [38] and $[Ni_9CoC_2(CO)_{16-x}]^{3-}$ (x = 0, 1).[39]
2) Permutation. Elimination of two CO ligands from the trigonal bipyramidal (TBP) $[PtRh_4(CO)_{14}]^{2-}$ generates the TBP $[PtRh_4(CO)_{12}]^{2-}$ with the migration of Pt from an equatorial to an apical position.[40]
3) Intramolecular condensation. In some cases, CO elimination induces a structural rearrangement of the cluster with retention of the nuclearity. This is exemplified well by the trigonal prismatic (TP) MCCs, $[M_6C(CO)_{15}]^{2-}$ and $[Co_6N(CO)_{15}]^-$ (M = Co, Rh), which are transformed into octahedral (O_h) clusters, $[M_6C(CO)_{13}]^{2-}$ and $[Co_6N(CO)_{13}]^-$, after elimination of two carbonyl ligands.[41] The number of M–M bonds increases from 9 (TP) to 12 (O_h), and because of this, the process may be referred to as an intramolecular condensation where M–CO bonds are replaced by M–M bonds.
4) Intermolecular condensation. This is the most common process observed after heating a MCC. In this case, CO elimination produces an unsaturated species, which condenses with a second cluster fragment resulting in a higher-nuclearity MCC. Several examples will be given in the following sections.

Heating a MCC may also promote CO dismutation to C and CO_2, resulting in carbide MCCs.[2,3,5,6,8-11,30] Thermal reactions of neutral clusters are often unselective, leading to mixtures of products. As demonstrated by Chini, the use of an anionic cluster as starting material or the addition of a base to a neutral carbonyl in thermal decomposition often provides better selectivity.[42]

Redox methods. Redox reactions used for the synthesis of MCCs include reduction, oxidation, redox condensation, and disproportionation.[2,3,5,6,8-11,30] Multivalent MCCs can undergo reversible redox reaction without any major structural rearrangements;[6] examples include $[Ni_{22-x}Pd_{20+x}(CO)_{48}]^{n-}$ (n = 5–8),[43] $[Pt_{33}(CO)_{38}]^{n-}$ (n = 0–9), and $[Pt_{40}(CO)_{40}]^{n-}$ (n = 4–11).[44] In general, redox reactions on non-multivalent (electron-precise) MCCs or the use of excess redox reagents on multivalent MCCs lead to irreversible processes yielding new MCCs or complete decomposition.

Reduction of a MCC can be performed by (1) direct addition of electrons, for instance, using alkali metals; or (2) nucleophilic attack of the C-atom of a coordinated carbonyl by OH^- ions. In the latter case, the first product is a metallacarboxylic acid $[MCOOH]^-$, which is readily transformed into a hydridocarbonylate $[MH]^-$ upon CO_2 elimination or a metallacarboxylate $[MCOO]^{2-}$ upon deprotonation.[45] Following further deprotonation or CO_2 elimination, $[MH]^-$ and $[MCOO]^{2-}$ are both transformed into the dianion $[M]^{2-}$, which can be stable or undergo redox condensation to larger MCCs (Scheme 2). This approach was developed by Hieber,[15] who demonstrated that different Fe carbonyl cluster anions could be obtained from the treatment of $Fe(CO)_5$ with base. This method is very versatile; it can be used for the preparation of low-nuclearity carbonylates and hydridocarbonylates as well as larger MCCs.

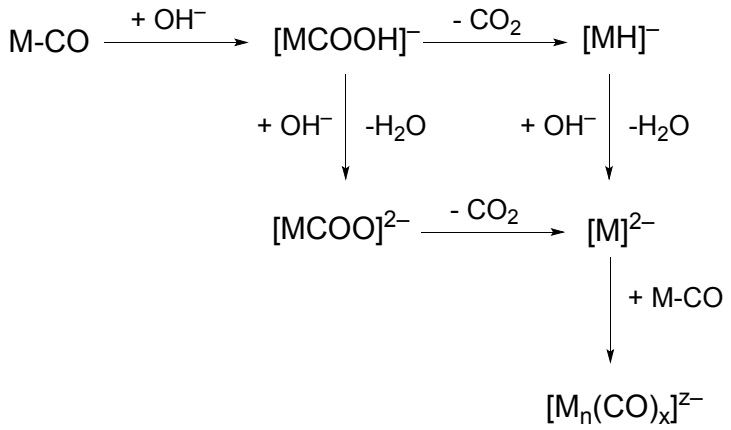

Scheme 2. Condensation induced by reduction. The process is initiated by OH^- nucleophlic attack on a CO ligand and eventually leads to the hydride $[MH]^-$ or the dianion $[M]^{2-}$. This, in turn, can undergo to a condensation reaction resulting in the higher nuclearity metal carbonyl $[M_n(CO)_x]^{z-}$.

When reduction of the MCC is achieved by the direct addition of electrons, the M–M and M–CO bonds often cleave, with the resulting species undergoing fragmentation or condensation to larger species. Alternatively, reduction can simply result in the replacement of a CO ligand with two negative charges with or without structural rearrangement. Indeed, $[M]^{2-}$ may be stable or undergo redox condensation (Scheme 2).

Oxidation of MCCs with innocent (non-coordinating) reagents, such as tropilium tetrafluoroborate or ferrocenium ions, may result in the formation of new M–M bonds with or without CO loss, as in the dimerisation of $[Ir_6(CO)_{15}]^{2-}$ to $[Ir_{12}(CO)_{26}]^{2-}$,[46] $[Pt_{19}(CO)_{22}]^{4-}$ to $[Pt_{38}(CO)_{44}]^{2-}$,[47] or $[Co_6C(CO)_{15}]^{2-}$ to $[Co_{11}C_2(CO)_{23}]^{n-}$ (n = 1–3).[48] Using coordinating oxidants such as H^+ and $[ML_x]^{n+}$, the reaction may proceed through oxidation or formation of a Lewis-type acid–base adduct. In order to increase the nuclearity of MCCs of a few metal atoms, the latter process has been widely employed through the addition of $[ML]^+$ fragments (M = Cu, Ag, Au; L = neutral ligand).[3,9,30] In some cases (*vide infra*), the reaction of MCCs with metal salts or complexes may result in larger MCCs *via* redox condensation. The use of H^+ ions (from acids or hydrolysis of $[M(H_2O)_x]^{n+}$ ions) may result in the oxidation of the MCC or the formation of isostructural MCCs containing hydride ligands. For instance, $[Rh_7(CO)_{16}]^{3-}$ is oxidised by $MCl_2{\cdot}xH_2O$ salts (M = Ni, Zn, Cd) to $[HRh_{14}(CO)_{25}]^{3-}$, $[Rh_{15}(CO)_{27}]^{3-}$, $[Rh_{15}(CO)_{25}(MeCN)_2]^{3-}$, and $[Rh_{17}(CO)_{37}]^{3-}$.[49] Although oxidation usually results in larger clusters, in a few cases oxidative degradation is observed. For example, treatment of $[H_2Co_{20}Pd_{16}C_4(CO)_{48}]^{4-}$ with strong acids affords $[HCo_{15}Pd_9C_3(CO)_{38}]^{2-}$ and, eventually with excess acid, $[Co_{13}Pd_3C_3(CO)_{29}]^{-}$.[50,51,52] In several cases, polyhydride clusters may be interconverted by simple acid–base reactions. For instance, protonation of $[Co_6(CO)_{15}]^{2-}$ affords $[HCo_6(CO)_{15}]^{-}$,[53] while stepwise protonation of $[Co_{15}Pd_9C_3(CO)_{38}]^{3-}$ results in $[H_2Co_{15}Pd_9C_3(CO)_{38}]^{2-}$, $[HCo_{15}Pd_9C_3(CO)_{38}]^{-}$, and $H_3Co_{15}Pd_9C_3(CO)_{38}$; these reactions may be reversed by the addition of base.

Redox condensation was introduced and rationalised by Paolo Chini, and it represents one of the most powerful and versatile procedures for MCC preparation.[54] Redox condensation involves a comproportionation reaction between an MCC anion and a more oxidised species (not necessarily a cluster nor even a carbonyl compound), which can be either cationic, neutral, or anionic (Scheme 3; also see ESI: Figure S1). Redox condensation can be used for the preparation of homo- and hetero-metallic MCCs, even when the second metal does not form a carbonyl compound, such Pd, Cu, Ag, Au, Hg, or main-group metals.

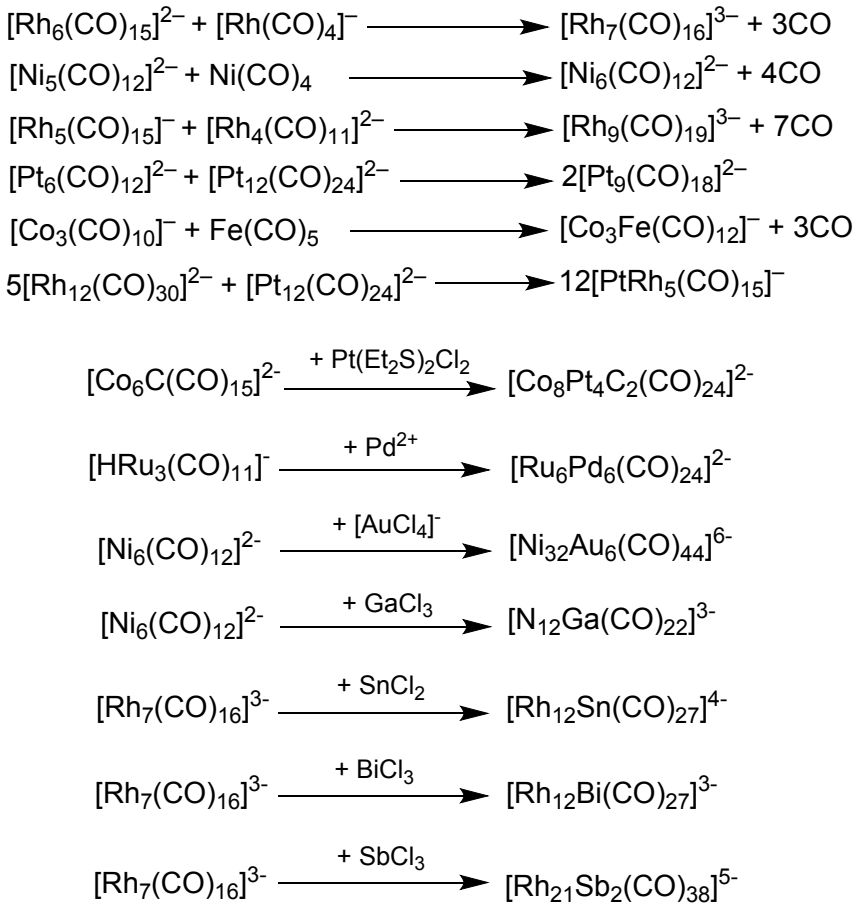

Scheme 3. Some representative examples of redox condensation. Balanced equations have been written only when the complete stoichiometry of all the reagents and products are known.

Disproportionation is the reverse of redox condensation, and it may be promoted in neutral $M_x(CO)_y$ carbonyls by using polar solvents or bases. Disproportionation can result in (a) $[ML_6]^{2+}[M_a(CO)_b]^{2-}$ ionic couples, (b) isocarbonyls adducts, or (c) xenophilic clusters (Scheme 4).[55] An example of case (a) is represented by $[Fe(DMF)_6][Fe_4(CO)_{13}]$, which is formed after heating $Fe(CO)_5$ in DMF (*N*,*N*-dimethylformamide). Xenophilic clusters (case (c)) contain a direct M–M bond between a metal centre in a formal negative oxidation state and a second metal in a positive oxidation state, *e.g.*, $Fe_4(CO)_8(py)_4$[56] and $[Mn][Mn_7(THF)_6(CO)_{12}]_2$ (THF = tetrahydrofuran; see ESI: Figure S2).[57]

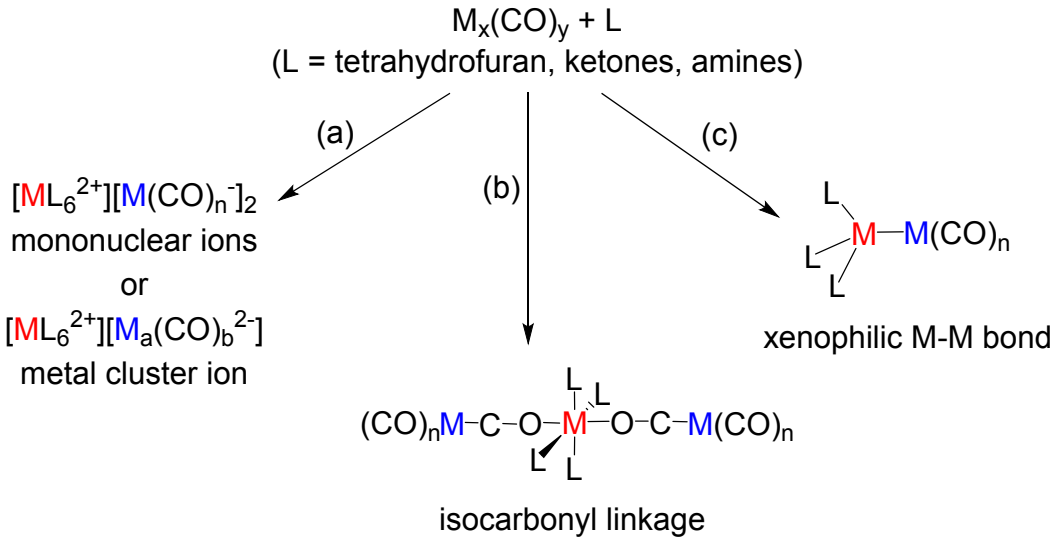

Scheme 4. Disproportionation of neutral metal carbonyls can result in (a) ionic couples, (b) isocarbonyl adducts, or (c) xenophilic clusters (M, black: metal in formal oxidation state = 0; M, red: formal oxidation state > 0; M, blue: formal oxidation state < 0).[55]

Other chemically induced methods. MCCs can be modified by additional chemical reactions. The addition of soft nucleophiles (*e.g.*, CO, PR_3, RC≡CR, $R_2C{=}CR_2$, pyridine, NO_2^-, halides) may result in the formation of addition or substitution products, cluster breakdown, or even condensation; the particular reaction route depends on the MCC, the nature of the nucleophile, the stoichiometry of the reaction, and experimental conditions.[2,3,5,6,8-11,30] Moving from cationic to neutral and anionic MCCs, CO-substitution with stronger σ-donors becomes less favoured. The addition of soft nucleophiles typically causes the removal of ML_x fragments (*e.g.*, $Ni(CO)_4$, $Ni(CO)_2(PR_3)_2$, $[Rh(CO)_2I_2]^-$), forming lower-nuclearity MCCs, but in a few cases, nucleophilic attack promotes condensation, resulting in higher-nuclearity clusters (Scheme 5). For instance, CO-induced cluster condensation is observed after exposing $[Ni_{10}Rh_2C(CO)_{20}]^{2-}$ to CO under ambient conditions, resulting in the bis-acetylide $[Ni_6Rh_8(C_2)_2(CO)_{24}]^{4-}$ (Figure 1).[58]

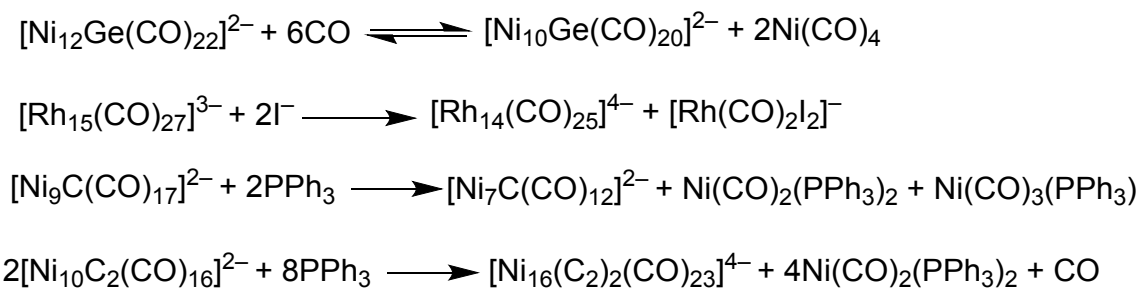

Scheme 5. Some representative reactions of MCCs with soft nucleophiles.

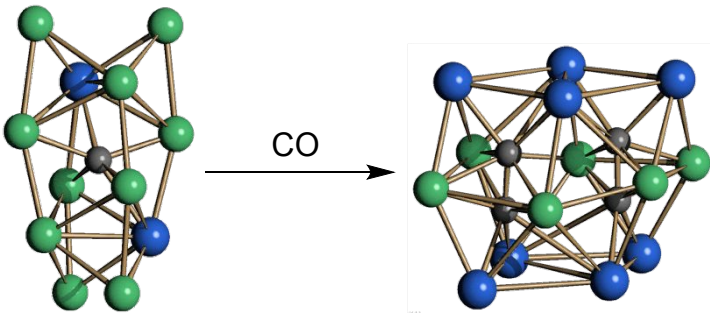

Figure 1. CO-induced condensation of $[Ni_{10}Rh_2C(CO)_{20}]^{2-}$ to $[Ni_6Rh_8(C_2)_2(CO)_{24}]^{4-}$ (green, Ni; blue, Rh; grey, C). CO ligands have been omitted for clarity.[58]

As a final remark, main-group elements are most often introduced into MCCs by redox condensation using suitable EX_n compounds (E = main-group element; X = halide). Chalcogens can also be introduced using elemental O_2, S_8, Se, or Te, or using chalcogen-containing EO_x^{2-} molecules under reducing conditions.[2,3,5,6,8-12,30,59,60] Suitable reagents for the synthesis of nitride-containing MCCs from metal carbonyls are NO^+, NO_2^-, N_3, and NCO^-. Carbide MCCs represent the largest class of MCCs containing a main-group element. They can be prepared by three main methods: [2,3,5,6,8-11,30,61]

1) Thermal disproportionation of CO to C and CO_2. This method is very effective in the case of Re, Fe, Ru, and Os carbonyls.
2) CO splitting by the reduction of a bridging CO ligand. In this case, a CO ligand that C-bonded to a metal is activated by O-coordination to a Lewis acid, such as RCO^+ (generated from RCOCl). The resulting M–C–O–C(O)R is then reduced to a metal carbide following elimination of $RCOO^-$. This method has been applied mainly to Fe and Co clusters.
3) Reaction of MCC anions with carbon halides (*e.g.*, CCl_4, C_2Cl_4, C_2Cl_6, C_3Cl_6). This method is largely employed for the synthesis of Co-, Rh-, and Ni-carbide MCCs.

In the following sections, sample syntheses of MCCs from the Groups 8–10 metals will be illustrated. For each metal, the synthesis of MCCs that can be further employed as precursors for the preparation of new species will be summarised with key details. These include neutral clusters, homometallic MCCs, species containing main-group elements, and heterometallic MCCs. Some representative (not exhaustive) examples on how these species might be employed for the preparation of new MCCs will then be briefly outlined.

2.2 Iron Carbonyl Clusters

$Fe(CO)_5$ can be obtained in very large scale by the direct carbonylation of Fe metal. It is the best commercially available starting material for the preparation of other iron carbonyls (Scheme 6). The photolysis of $Fe(CO)_5$ in acetic acid affords the almost insoluble $Fe_2(CO)_9$,[62] which was probably the first structurally characterised carbonyl compound containing a direct M–M bond, even if supported by bridging carbonyls. $Fe_3(CO)_{12}$ has been obtained by three different methods:[63] (a) thermal treatment of $Fe_2(CO)_9$, (b) oxidation of $[HFe(CO)_4]^-$, and (3) reaction of $[HFe_3(CO)_{11}]^-$ with strong acids.

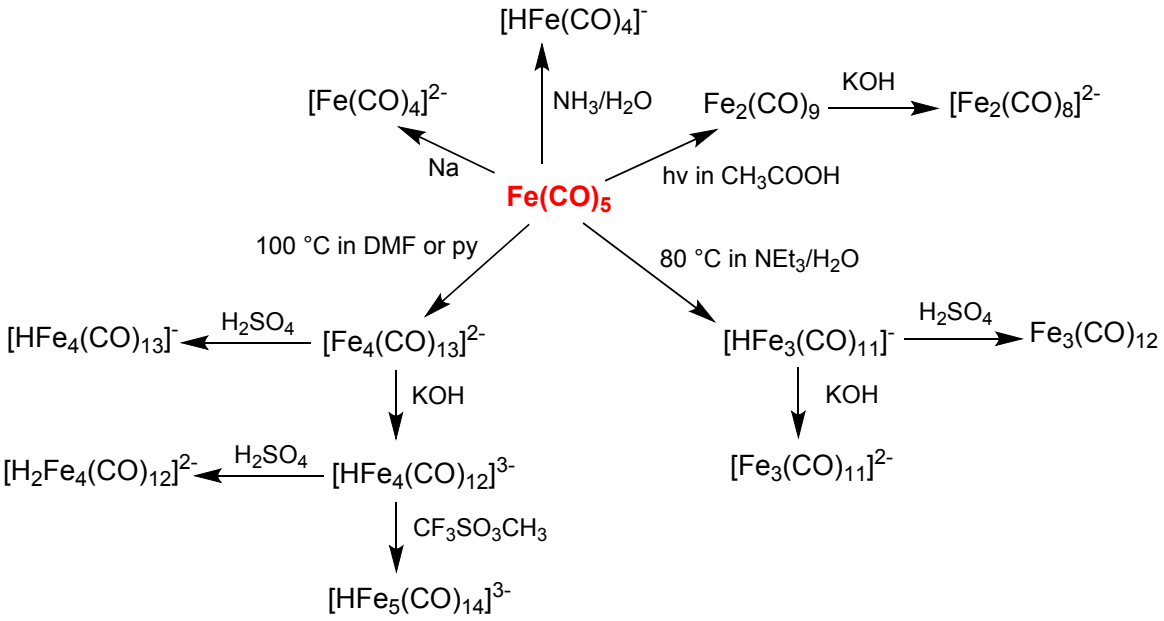

Scheme 6. Synthesis of carbonylferrates and hydridocarbonylferrates from $Fe(CO)_5$ (DMF = N,N-dimethylformamide, py = pyridine). Anionic Fe carbonyls are obtained by a combination of redox and thermal reactions as well as the use of acids and bases. See Table S1 in ESI for a full list with references.

Carbonylferrates and hydridocarbonylferrates. Based on the seminal work of Hieber,[15] several carbonylferrates and hydridocarbonylferrates have been prepared and structurally characterised:[45] $[Fe(CO)_4]^{2-}$, $[Fe_2(CO)_8]^{2-}$, $[Fe_3(CO)_{11}]^{2-}$, $[Fe_4(CO)_{13}]^{2-}$, $[HFe(CO)_4]^-$, $[HFe_2(CO)_8]^-$, $[HFe_3(CO)_{11}]^-$, $[HFe_4(CO)_{13}]^-$, $[HFe_4(CO)_{12}]^{3-}$, $[HFe_5(CO)_{14}]^{3-}$, and $[H_2Fe_4(CO)_{12}]^{2-}$ (see ESI for a full list with references: Table S1). The paramagnetic species $[Fe_2(CO)_8]^{\bullet-}$, $[Fe_3(CO)_{12}]^{\bullet-}$, and $[Fe_3(CO)_{11}]^{\bullet-}$ have been confirmed and characterised by electron paramagnetic resonance studies on (^{13}C, ^{57}Fe) isotopically enriched samples.[6465] In contrast, variable-temperature (VT) multinuclear nuclear magnetic resonance (NMR) studies indicate that the purported dihydrides $H_2Fe_3(CO)_{11}$ and $H_2Fe_4(CO)_{13}$ should be reformulated to $HFe_3(CO)_{10}(CO\text{-}H)$ and $HFe_4(CO)_{12}(CO\text{-}H)$.[66]

Carbonylferrates and hydridocarbonylferrates are usually obtained from neutral Fe carbonyls by reduction, treatment with base, or disproportionation. Several procedures have been reported,

with some species having multiple synthetic routes. Scheme 6 shows only some of the most significant examples. Reduction of $Fe(CO)_5$ with Na/benzophenone in THF affords the Collman's reagent $Na_2[Fe(CO)_4]$. Depending on the specific reaction conditions, treatment of $Fe(CO)_5$ with OH^- conveniently yields $[HFe(CO)_4]^-$ or $[HFe_3(CO)_{11}]^-$; the former is produced with NH_3 in water at RT, while the latter with NEt_3 in water at 80 °C. In contrast, $[Fe_4(CO)_{13}]^{2-}$ is prepared in high yields from the disproprtionation of $Fe(CO)_5$ in either DMF or pyridine (py) at 100 °C (see ESI: Scheme S2).

Isonuclear carbonylferrates and hydridocarbonylferrates are easily interconverted by simple acid–base reactions. For instance, $[Fe_3(CO)_{11}]^{2-}$ is quantitatively protonated to $[HFe_3(CO)_{11}]^-$ by stoichiometric amounts of strong acids, and the reaction is reversed by using 1.2-M KOH in methanol. Interestingly, the reaction of $[HFe_3(CO)_{11}]^-$ or $[Fe_4(CO)_{13}]^{2-}$ with 6-M KOH results in $[HFe_4(CO)_{12}]^{3-}$.[67] The unique hydride of $[HFe_4(CO)_{12}]^{3-}$ is μ_3-coordinated to a triangular face of the cluster. This coordination is retained after the addition of two $[AuPPh_3]^+$ fragments, yielding $[HFe_4(CO)_{12}(AuPPh_3)_2]^-$;[68] however, further addition of $[AuPPh_3]^+$ produces the neutral $HFe_4(CO)_{12}(AuPPh_3)_3$, and concomitantly, the hydride migrates from the triangular face to the tetrahedral cavity (Scheme 7).

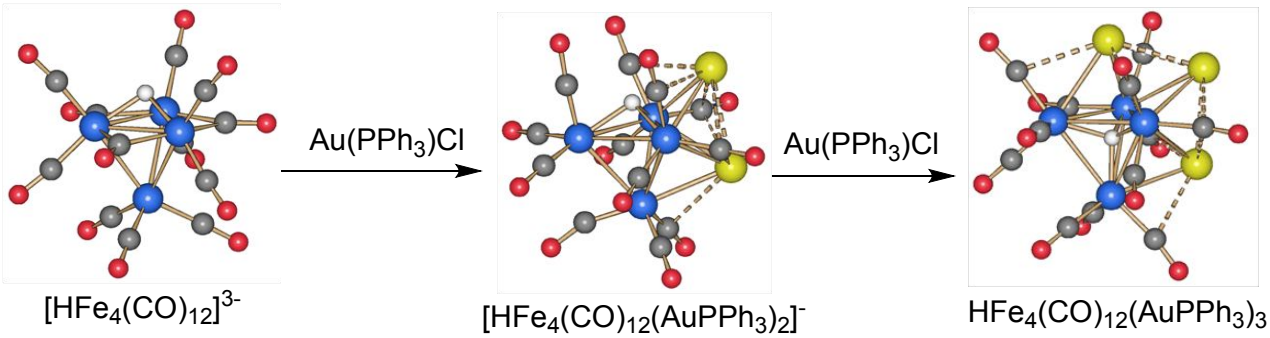

Scheme 7. Hydride migration in $[HFe_4(CO)_{12}]^{3-}$ induced by the addition of $[Au(PPh_3)]^+$ fragments (blue, Fe; yellow, Au; grey, C; red, O; white, H). The surface μ_3-H hydride ligand of $[HFe_4(CO)_{12}]^{3-}$ and $[HFe_4(CO)_{12}(AuPPh_3)_2]^-$ is moved to the tetrahedral cavity of $HFe_4(CO)_{12}(AuPPh_3)_3$ upon the addition of a third $[Au(PPh_3)]^+$ fragment.[68] PPh_3 ligands have been omitted for clarity.

Iron Carbide Carbonyl Clusters. By heating $Fe(CO)_5$ in quinoline at 160–180 °C, both CO and metal disproportionation are observed, resulting in the carbide cluster $[Fe_6C(CO)_{16}]^{2-}$ (Equation

2).[69] The same cluster can be alternatively obtained by heating $Fe(CO)_5$ and $[Fe(CO)_4]^{2-}$ in diglyme at 160 °C.

$$7Fe(CO)_5 + 6quinoline \rightarrow [Fe(quinoline)_6]^{2+} + [Fe_6C(CO)_{16}]^{2-} + 17CO + CO_2 \quad (2)$$

$[Fe_6C(CO)_{16}]^{2-}$ is a very versatile reagent for the preparation of other Fe carbide carbonyl clusters (Scheme 8). Its reaction with NaOH in dimethylsulfoxide (DMSO) affords the highly reduced $[Fe_6C(CO)_{15}]^{4-}$.[70] Moreover, $[Fe_6C(CO)_{16}]^{2-}$ is oxidised by Fe^{3+} ions in H_2O to form $Fe_5C(CO)_{15}$, which, in turn, is transformed into $[Fe_5C(CO)_{14}]^{2-}$ after reaction with $[Fe(CO)_4]^{2-}$.[71] In contrast, the reaction of $[Fe_6C(CO)_{16}]^{2-}$ with Fe^{3+} in MeOH results in the μ_4-(methoxycarbonyl)methylidyne cluster $[Fe_4(CO)_{12}C(CO_2Me)]^-$;[72] which can be further transformed into $Fe_4C(CO)_{13}$ by reaction with CF_3SO_3H or into $[HFe_4C(CO)_{12}]^-$ by reaction with $BH_3 \cdot THF$.[7374] The related $[Fe_4C(CO)_{12}]^{2-}$ dianion can be obtained using a strong base to deprotonate $[HFe_4C(CO)_{12}]^-$ or using Na to reduce the $[Fe_4(CO)_{12}(COC(O)CH_3)]^-$ adduct, which is prepared from the reaction of $[Fe_4(CO)_{13}]^{2-}$ and CH_3COCl.[61]

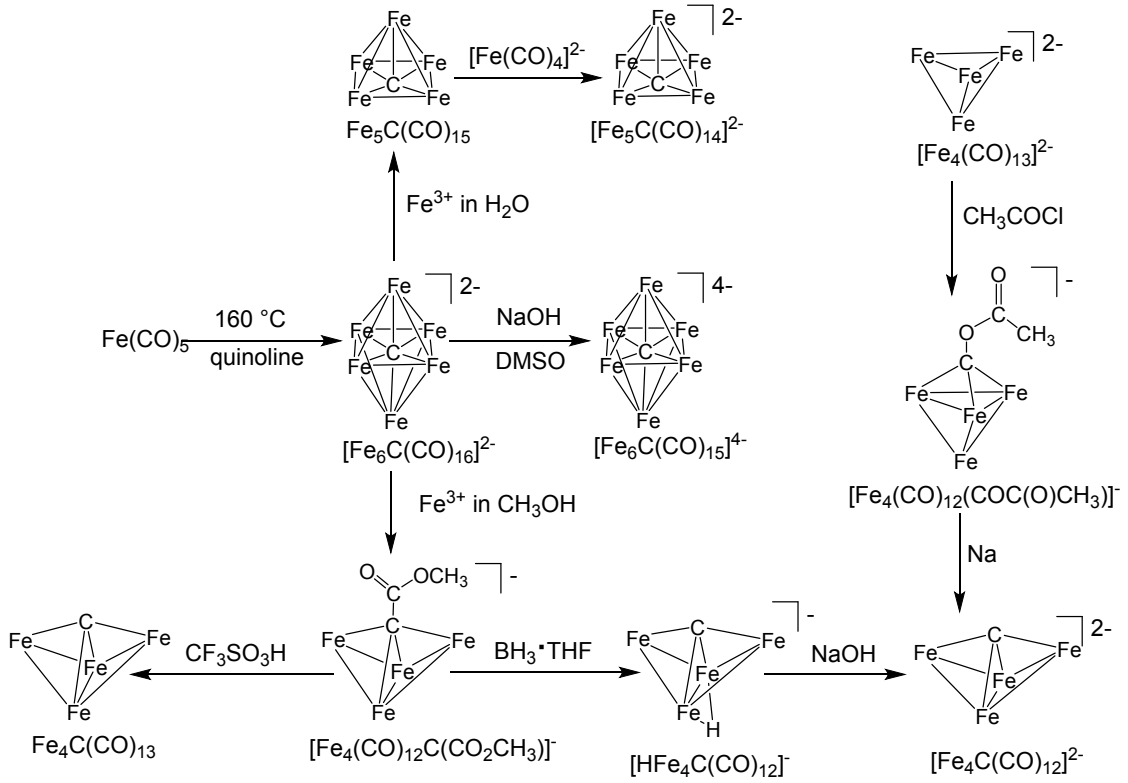

Scheme 8. Synthesis of Fe carbide carbonyl clusters. All the species have been isolated and fully characterized.[61,69-74] $[Fe_6C(CO)_{16}]^{2-}$ is prepared directly from $Fe(CO)_5$ by thermal treatment. Other Fe carbide carbonyl clusters can be obtained from $[Fe_6C(CO)_{16}]^{2-}$ using redox reactions.

Alternatively, $[Fe_4C(CO)_{12}]^{2-}$ can be prepared starting from $[Fe_4(CO)_{13}]^{2-}$ in a two steps reaction by CO scission. CO ligands have been omitted for clarity.

$[Fe_6C(CO)_{16}]^{2-}$, $[Fe_6C(CO)_{15}]^{4-}$, $[Fe_4C(CO)_{12}]^{2-}$, and $[Fe_5C(CO)_{14}]^{2-}$ react with metal carbonyls and metal complexes affording several heterometallic carbide clusters, *via* redox condensation, metal replacement, or formation of Lewis-type acid–base adducts.[7576] A recent advance in this area is the reaction of $[Fe_5C(CO)_{14}]^{2-}$ with $[Mo(CO)_3(chpt)]$ (chpt = cycloheptatriene) to afford the heterometallic carbide $[Fe_5MoC(CO)_{17}]^{2-}$, which displays selective alkyne reduction.[77] The first Fe carbide–sulfide clusters, $Fe_6C(CO)_{16}(S)$ and $[Fe_6C(CO)_{14}(S)]^{2-}$, were also obtained recently (Scheme 9).[78] The addition of SO_2 to $[Fe_6C(CO)_{16}]^{2-}$ results in $[Fe_6C(CO)_{15}(SO_2)]^{2-}$, which is then O-methylated by MeOTf (methyltriflate = methyl trifluoromethanesulfonate) to $[Fe_6C(CO)_{15}(SO_2Me)]^{-}$. Demethoxylation with BF_3 results in $Fe_6C(CO)_{15}(SO)$, which spontaneously converts in solution into $Fe_6C(CO)_{16}(S)$ at RT. Reduction with Na/naphthalene eventually affords $[Fe_6C(CO)_{14}(S)]^{2-}$.

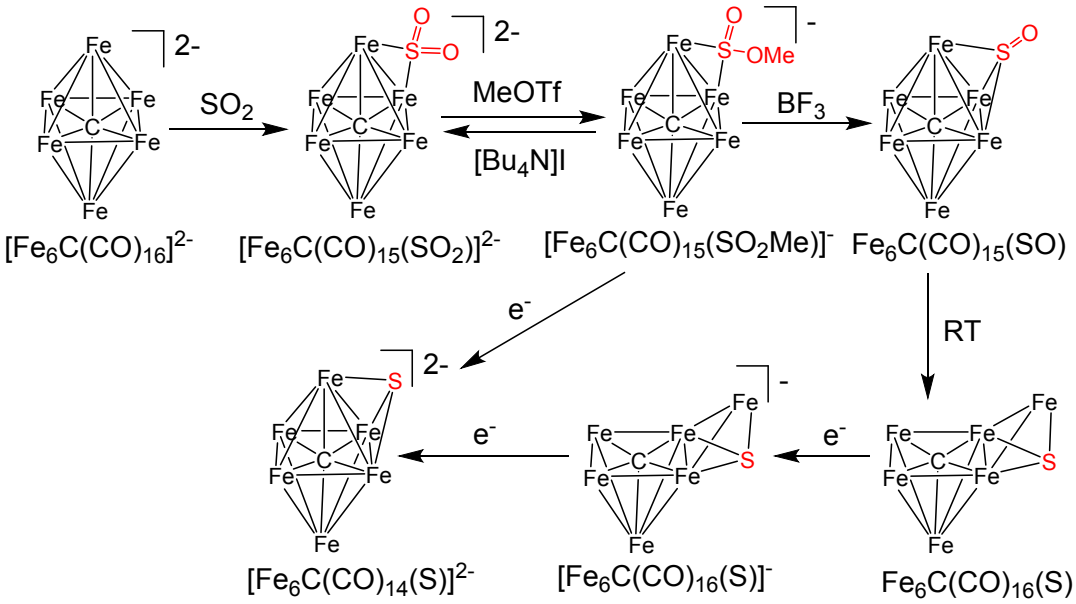

Scheme 9. Synthesis of $Fe_6C(CO)_{16}(S)$ and $[Fe_6C(CO)_{14}(S)]^{2-}$.$[Fe_6C(CO)_{16}]^{2-}$ is transformed into $[Fe_6C(CO)_{15}(SO_2)]^{2-}$ by CO substitution with SO_2. Further reactions with MeOTf, BF_3 and reduction with Na/naphthalene result in the target compounds.[78] CO ligands have been omitted for clarity.

Iron carbonyl clusters containing other main-group elements. Nitride atoms can be introduced into Fe carbonyl clusters by the reduction of NO^+ ions (see ESI: Scheme S3).[3] The thermal reaction of $[NO][BF_4]$ and $[Fe_2(CO)_8]^{2-}$ in diglyme is highly dependent on the temperature;

it affords $[Fe_4N(CO)_{12}]^-$ at 130 °C, whereas it produces $[Fe_5N(CO)_{14}]^-$ at 145 °C. $[Fe_4N(CO)_{12}]^-$ can be alternatively obtained from the redox condensation of $Fe_3(CO)_{12}$ and $[Fe(CO)_3(NO)]^-$. Both $[Fe_4N(CO)_{12}]^-$ and $[Fe_5N(CO)_{14}]^-$ are protonated by strong acids, forming the related neutral mono-hydrides $HFe_4N(CO)_{12}$ and $HFe_5N(CO)_{14}$. The redox condensation of $[Fe_4N(CO)_{12}]^-$ with $[Fe_2(CO)_8]^{2-}$ results in the fully interstitial nitride cluster $[Fe_6N(CO)_{15}]^{3-}$, from which an Fe atom can be removed by oxidation, affording $[Fe_5N(CO)_{14}]^-$.

Oxygen is by far one of the most difficult main-group elements to incorporate into low-valent metal carbonyl clusters because of its oxidising power, hard base nature, and higher affinity for high-valent metals (see ESI: Table S2). One of the most significant exceptions is represented by the μ_3-oxo carbonyl cluster $[Fe_3(\mu_3\text{-}O)(CO)_9]^{2-}$, which is obtained from the reaction of $[Fe_3(CO)_{11}]^{2-}$ with dry air.[79] Indeed, this is a rare case in which letting (dry) air into a Schlenk tube containing an anionic metal carbonyl cluster results in the selective synthesis of a new species. It is noteworthy that protonation of $[Fe_3(\mu_3\text{-}O)(CO)_9]^{2-}$ occurs on the O atom affording the μ_3-hydroxo cluster $[Fe_3(\mu_3\text{-}OH)(CO)_9]^-$, whereas $[AuPPh_3]^+$ adds to the Fe_3 metal cage affording $[Fe_3(\mu_3\text{-}O)(\mu_3\text{-}AuPPh_3)(CO)_9]^-$ (Scheme 10).[8081] This is due to the fact that the hard H^+ acid prefers to add to the hard oxo base, whereas the soft $[AuPPh_3]^+$ acid prefers to interact with the softer base site of the metal cage of the cluster. The coordination of the oxo ligand can be further expanded by reacting $[Fe_3(\mu_3\text{-}O)(CO)_9]^{2-}$ with metal fragments, such as $[Mn(CO)_3(MeCN)_3]^+$ and $Ru_3(CO)_{10}(MeCN)_2$, which results in $[Fe_3Mn(\mu_4\text{-}O)(CO)_{12}]^-$[82] and $[Fe_2Ru_3(\mu_4\text{-}O)(CO)_{14}]^{2-}$.[83]

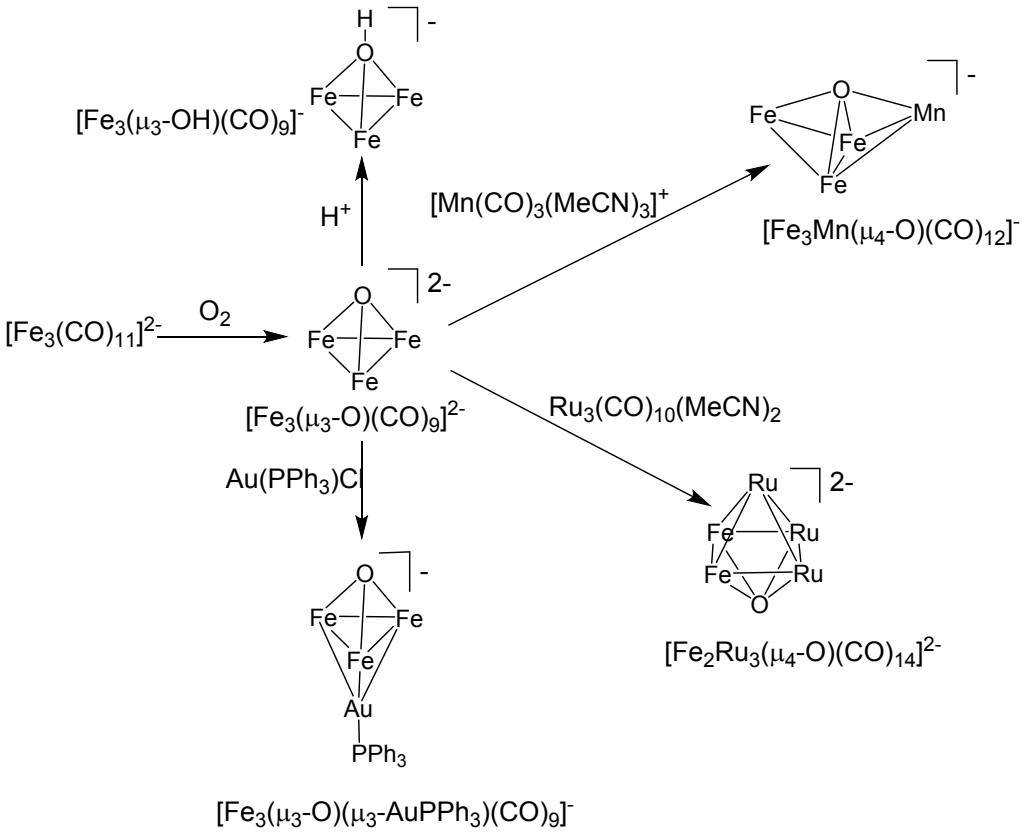

Scheme 10. Reactivity of $[Fe_3(\mu_3\text{-}O)(CO)_9]^{2-}$. This compound is obtained from the reaction of $[Fe_3(CO)_{11}]^{2-}$ with dry air,[79] and is protonated on the oxo ligand resulting in $[Fe_3(\mu_3\text{-}OH)(CO)_9]^{-}$.[80] The metal cage can be expanded by condensation with metal fragments such as $Au(PPh_3)Cl$, $[Mn(CO)_3(MeCN)_3]^{+}$ and $Ru_3(CO)_{10}(MeCN)_2$.[81-83] CO ligands have been omitted for clarity.

Other chalcogen atoms (S, Se, Te) can be introduced into Fe carbonyl clusters by various routes:[8485]

(1) Reacting Fe carbonyl anions with reagents containing the chalcogen in a positive oxidation state, such as EO_3^{2-}, EO_2, and SCl_2;

(2) Reacting neutral Fe carbonyls—usually $Fe(CO)_5$ or $Fe_3(CO)_{12}$—with E_n^{2-} polychalcogenide anions;

(3) Reaction of $Fe(CO)_5$ with the elemental chalcogen in the presence of a base.

Iron carbonyl clusters containing other main-group elements (*e.g.*, As, Bi, Sb, Pb, Tl, Sn) can be generally obtained from the reaction of iron carbonyl anions with main-group halides or oxides (see ESI: Scheme S4).[86]

Heterometallic Fe-based carbonyl clusters. Heterometallic Fe–M carbonyl clusters can be prepared by the reactions of Fe carbonyl anions with metal salts and complexes.[8788] For instance, reactions of the Collman's reagent $Na_2[Fe(CO)_4]\cdot 2THF$ with M(NHC)Cl, where M are Cu, Ag, or

Au and NHC is IMes ($C_3N_2H_2(C_6H_2Me_3)_2$) or IPr ($C_3N_2H_2(C_6H_3{}^iPr_2)_2$), afford the anionic $[Fe(CO)_4\{M(NHC)\}]^-$ and the neutral $Fe(CO)_4\{M(NHC)\}_2$ and $Fe(CO)_4\{M(NHC)\}\{M'(NHC)\}$ complexes (Scheme 11).[89,90,91] These, in turn, may be transformed into larger clusters by means of thermal or chemical reactions. Such Fe–M complexes may be viewed as transition-metal Lewis acid–base pairs[92] with potential applications in bimetallic catalysis.[93] For instance, $Fe(CO)_4\{Cu(IPr)\}_2$ was found to be useful in the bifunctional activation of N_2O.[94]

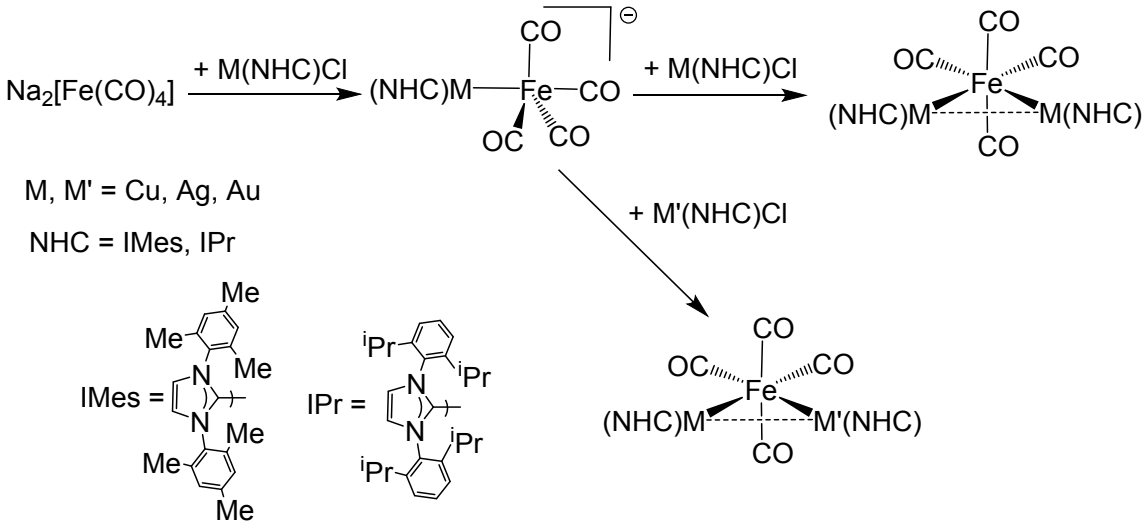

Scheme 11. Reactions of $Na_2[Fe(CO)_4]$ with M(NHC)Cl (M = Cu, Ag, Au; NHC = IMes, IPr; IMes = $C_3N_2H_2(C_6H_2Me_3)_2$; IPr = $C_3N_2H_2(C_6H_3{}^iPr_2)_2$). One or two $[M(NHC)]^+$ fragments as well as two different $[M(NHC)]^+$ and $[M'(NHC)]^+$ fragments can be added, resulting in $[Fe(CO)_4\{M(NHC)\}]^-$, $Fe(CO)_4\{M(NHC)\}_2$ and $Fe(CO)_4\{M(NHC)\}\{M'(NHC)\}$, respectively.[89-91]

Molecular gold nanoclusters protected by Fe–CO fragments have been prepared by redox condensation of $[Fe_3(CO)_{11}]^{2-}$ with $[AuCl_4]^-$. The resulting $[Au_{22}\{Fe(CO)_4\}_{12}]^{6-}$, $[Au_{21}\{Fe(CO)_4\}_{10}]^{5-}$, $[Au_{28}\{Fe(CO)_3\}_4\{Fe(CO)_4\}_{10}]^{8-}$, and $[Au_{34}\{Fe(CO)_3\}_6\{Fe(CO)_4\}_8]^{10-}$ clusters are reminiscent of thiolate-protected Au nanoclusters, comprising Au cores protected by organometallic staple motifs (Figure 2).[95]

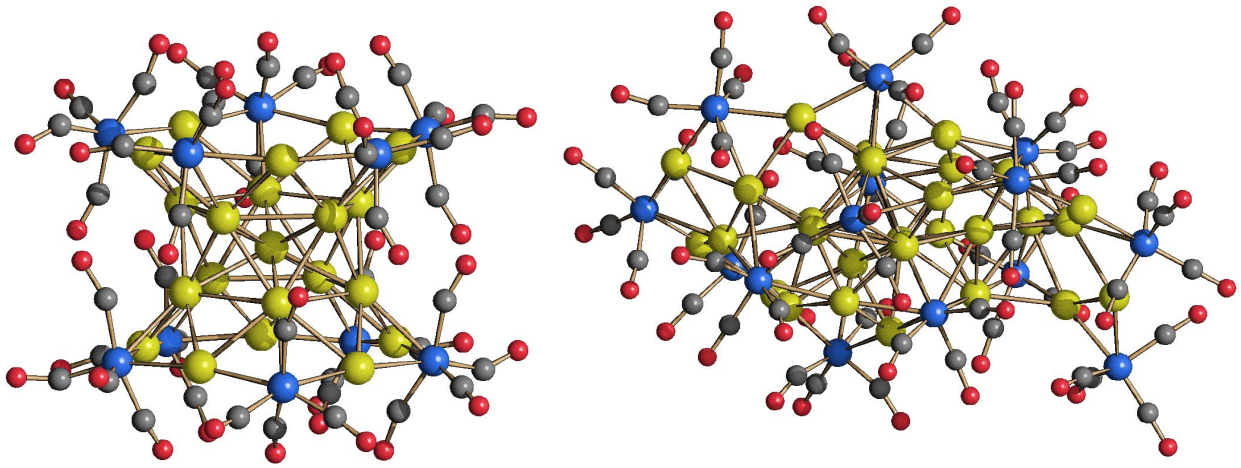

Figure 2. Molecular structures of $[Au_{21}\{Fe(CO)_4\}_{10}]^{5-}$ (left) and $[Au_{28}\{Fe(CO)_3\}_4\{Fe(CO)_4\}_{10}]^{8-}$ (right). Spheres represent atoms as follows: yellow, Au; blue, Fe; red, O; grey, C. Both these molecular nanoclusters can be obtained from the reaction of $[Fe_3(CO)_{11}]^{2-}$ with $[AuCl_4]^-$ under different experimental conditions.[95]

2.3 Ruthenium and Osmium Carbonyl Clusters

$Ru_3(CO)_{12}$ and $Os_3(CO)_{12}$ can be obtained by reductive carbonylation of $RuCl_3$ and OsO_4, respectively, at high temperature and pressure.[36,96] An atmospheric-pressure synthesis of $Ru_3(CO)_{12}$ is also available.[35] The monometallic $M(CO)_5$ carbonyls are obtained at very high CO pressures (180–200 atm), but $Ru(CO)_5$ can also be prepared by photolysis of $Ru_3(CO)_{12}$ under CO at atmospheric pressure.[97] Interestingly, treatment of OsO_4 with a 3:1 combined pressure (180 atm) of CO/H_2 at 160 °C in THF results in the dihydride $H_2Os(CO)_4$, which can be deprotonated to $[HOs(CO)_4]^-$ by Na.

Homometallic Ru and Os carbonyl clusters. Pyrolysis and thermolysis of $M_3(CO)_{12}$ have been thoroughly investigated by Lewis and Johnson,[96,97, 98,99] whose work greatly contributed to the development of the chemistry of high-nuclearity MCCs (see ESI: Tables S3 and S4). The outcome of these thermal reactions largely depends on temperature, time, atmosphere, and solvent (Scheme 12).[98] Their main drawback is that they often lead to product mixtures, which must be separated by chromatography. In contrast, the reaction of $Ru_3(CO)_{12}$ with H_2 (1 atm) in octane at 120 °C selectively affords $H_4Ru_4(CO)_{12}$. Under analogous conditions, $Os_3(CO)_{12}$ is transformed into the unsaturated $H_2Os_3(CO)_{10}$ cluster, whereas higher pressure (60 atm) affords $H_4Os_4(CO)_{12}$.[99]

$H_4M_4(CO)_{12}$ and $H_2Os_3(CO)_{10}$ are very versatile species for the synthesis of other Ru and Os clusters.[100] The reaction of $Os_3(CO)_{12}$ with stoichiometric amounts of Me_3NO in MeCN results in $Os_3(CO)_{12-x}(MeCN)_x$ (x = 1, 2).[101] The lability of MeCN may be exploited for further functionalisation[102] and applications in biology and medicine.[103] Interestingly, pyrolysis of

$Os_3(CO)_{10}(MeCN)_2$ affords different clusters than reactions using $Os_3(CO)_{12}$ (see ESI; Scheme S5). Moreover, reaction of $Os_3(CO)_{10}(MeCN)_2$ with the triosmiumfuryne complex $Os_3(CO)_9(\mu_3\text{-}\eta^2\text{-}C_4H_2O)(\mu\text{-}H)_2$, which contains a bridging furanyl ligand, produces the bis-triosmium complex $Os_3(CO)_9(\mu\text{-}H)_2(\mu_3\text{-}\eta^2\text{-}2,3\text{-}\mu\text{-}\eta^2\text{-}4,5\text{-}C_4HO)Os_3(CO)_{10}(\mu\text{-}H)_2$; CH activation occurs at the uncoordinated C=C double bond of the furanyl (Scheme 13).[104] Further Ru and Os carbonyl clusters can be obtained by reduction of $M_3(CO)_{12}$, as well as by redox reactions on various preformed clusters.

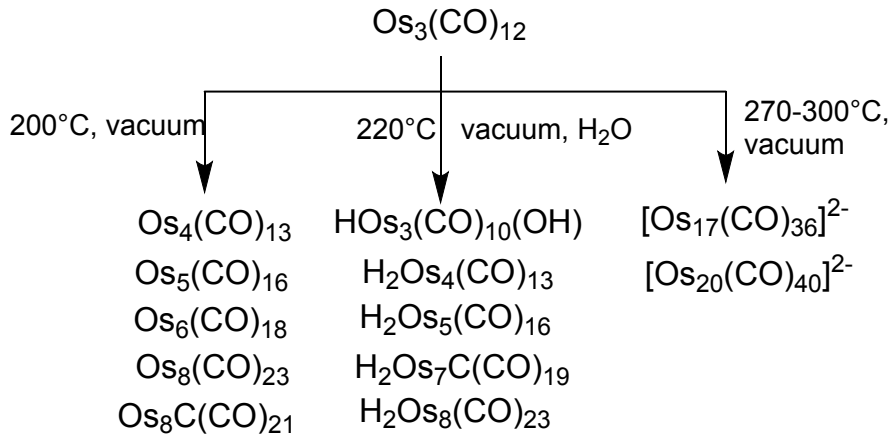

Scheme 12. Synthesis of Os carbonyl clusters by pyrolysis of $Os_3(CO)_{12}$. The obtained products depend on temperature and/or the addition of some water to solid $Os_3(CO)_{12}$ during the pyrolysis. When obtained in mixture, different products can be separated by chromatography.[98]

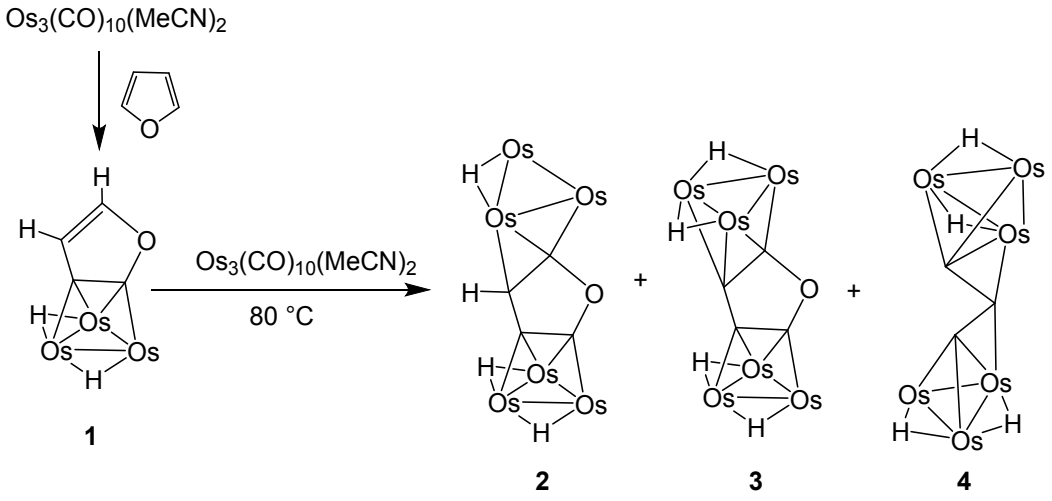

Scheme 13. The reaction of $Os_3(CO)_{10}(MeCN)_2$ with the triosmiumfuryne complex $Os_3(CO)_9(\mu_3\text{-}\eta^2\text{-}C_4H_2O)(\mu\text{-}H)_2$. $Os_3(CO)_9(\mu_3\text{-}\eta^2\text{-}C_4H_2O)(\mu\text{-}H)_2$ (**1**); $Os_3(CO)_9(\mu\text{-}H)_2(\mu_3\text{-}\eta^2\text{-}2,3\text{-}\mu\text{-}\eta^2\text{-}4,5\text{-}C_4HO)Os_3(CO)_{10}(\mu\text{-}H)_2$ (**2**); $Os_3(CO)_9(\mu\text{-}H)_2(\mu_3\text{-}\eta^2\text{-}2,3\text{-}\mu_3\text{-}\eta^2\text{-}4,5\text{-}C_4O)Os_3(CO)_9(\mu\text{-}H)_2$ (**3**); $Os_3(CO)_9(\mu\text{-}H)_2(\mu_3\text{-}\eta^2\text{-}\mu_3\text{-}\eta^2\text{-}C\text{-}C\text{-}C)Os_3(CO)_9(\mu\text{-}H)_2$ (**4**).[104] The products can be separated by chromatography. CO ligands have been omitted for clarity.

Ru and Os carbide carbonyl clusters. Ru and Os carbide carbonyl clusters can be obtained through CO disproportionation at high temperature.[105106107] In particular, $Ru_6C(CO)_{17}$ is conveniently prepared from the thermal treatment of $Ru_3(CO)_{12}$ at 165 °C under 30 atm of C_2H_4. $Ru_6C(CO)_{17}$ is quantitatively transformed into $Ru_5C(CO)_{15}$ after exposure to CO (80 atm). $Ru_6C(CO)_{17}$ and $Ru_5C(CO)_{15}$ are transformed into $[Ru_6C(CO)_{16}]^{2-}$ and $[Ru_5C(CO)_{14}]^{2-}$, respectively, by Na_2CO_3 in MeOH. The reaction of $Ru_3(CO)_{12}$ with CaC_2 affords the dicarbide $[Ru_{10}(C)_2(CO)_{24}]^{2-}$,[108] whereas the monocarbide $[Ru_{10}C(CO)_{24}]^{2-}$ is obtained from the redox condensation of $[Ru_6C(CO)_{16}]^{2-}$ and $Ru_3(CO)_{12}$.[109] In general, Ru carbide clusters may be further transformed by CO substitution and by the addition of neutral or cationic fragments.[110111]

Ru and Os carbonyl clusters containing other main-group elements. The preparation of Ru nitride carbonyl clusters relies on the addition of N_3^- or NO^+ to preformed Ru carbonyls. The stepwise addition of $Ru(CO)_2$ fragments to $[Ru_4N(CO)_{12}]^-$ affords the larger $[Ru_5N(CO)_{14}]^-$, $[Ru_6N(CO)_{16}]^-$, and $[Ru_{10}N(CO)_{24}]^-$ clusters. $[Ru_6N(CO)_{16}]^-$ is readily prepared from $Ru_3(CO)_{12}$ and N_3^- at 80 °C. Reactions of $[H_3M_4(CO)_{12}]^-$ with $NOBF_4$ afford $H_3Ru_4N(CO)_{11}$ and $[Os_4N(CO)_{12}]^-$.[3]

Ru and Os carbonyl clusters containing S, Se, and Te may be prepared by various methods employing the elemental chalcogen, organic chalcogen compounds, or EO_3^{2-} as sources (Scheme 14).[112] The reaction of $Ru_3(CO)_{12}$ with Na_2Te_2 in water at 110 °C in the presence of $[PPh_4]Cl$ affords the Te-rich $[Ru_6(Te_2)_7(CO)_{12}]^{2-}$ cluster (see ESI: Scheme S6).[113] Moreover, reactions of $Ru_3(CO)_{12}$ with K_2TeO_3 in the presence of Cu(I) salts under a variety of experimental conditions result in Te–Ru–Cu carbonyl clusters, which have been recently reviewed.[59,60,114]

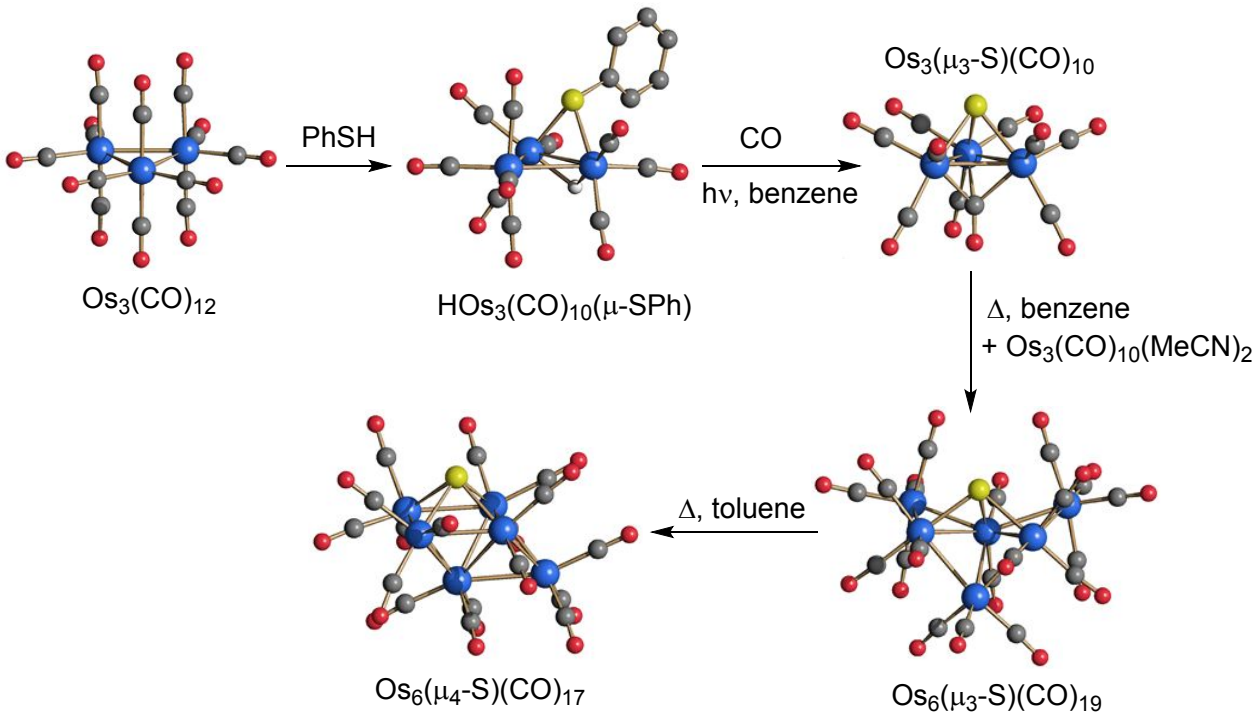

Scheme 14. The reaction of $Os_3(CO)_{12}$ with PhSH (blue, Os; yellow, S; red, O; grey, C; white, H).[112] Hydrogens on organic groups have been omitted for clarity. Light or thermal treatment are indicated by hν and Δ, respectively.

Similar procedures may be applied to other main-group elements.[115] For instance, Ru–Bi and Os–Bi carbonyl clusters may be obtained by reacting $M_3(CO)_{12}$, as well as other Ru and Os carbonyls, with $NaBiO_3$. Using THF as solvent, the reaction of $[HRu_3(CO)_{11}]^-$ with $SbPh_2Cl$ affords $Ru_3(CO)_{10}(\mu\text{-}H)(\mu\text{-}SbPh_2)$, whereas using CH_2Cl_2 results in $Ru_6(CO)_{20}(\mu\text{-}H)_2(\mu\text{-}SbPh_2)_2$ (see ESI: Scheme S7).[116]

Six different Ru–Ge carbonyl clusters have been obtained by heating $Ru_3(CO)_{12}$ and $^tBuGeH_3$ in heptane (Scheme 15): $Ru_3(CO)_9(\mu_3\text{-}Ge^tBu)_2$, $Ru_2(CO)_6(\mu\text{-}Ge^tBuH)_3$, $Ru_4(CO)_{10}(\mu_4\text{-}Ge_2{}^tBu_2)(\mu\text{-}Ge^tBuH)_2$, $Ru_4(CO)_8(\mu_4\text{-}Ge_2{}^tBu_2)(\mu\text{-}Ge^tBuH)_2(\mu_3\text{-}Ge^tBu)(H)$, $Ru_5(CO)_{12}(\mu_3\text{-}Ge^tBu)_2(\mu_4\text{-}Ge^tBu)(H)$, and $Ru_6(CO)_{12}(\mu_3\text{-}Ge^tBu)_4(H)_2$.[117] Additionally, using different experimental conditions, $Os_3(CO)_{10}(\mu_3\text{-}C_6H_4)$, $Os_3(CO)_{10}Ph(\mu\text{-}\eta^2\text{-}O{=}CPh)$, $HOs_6(CO)_{20}(\mu\text{-}\eta^2\text{-}C_6H_4)(\mu_4\text{-}Bi)$, $Os_2(CO)_8(\mu\text{-}BiPh)$, and $HOs_5(CO)_{18}(\mu\text{-}\eta^2\text{-}C_6H_4)(\mu_4\text{-}Bi)$ have been obtained from $Os_3(CO)_{10}(MeCN)_2$ and $BiPh_3$.[102]

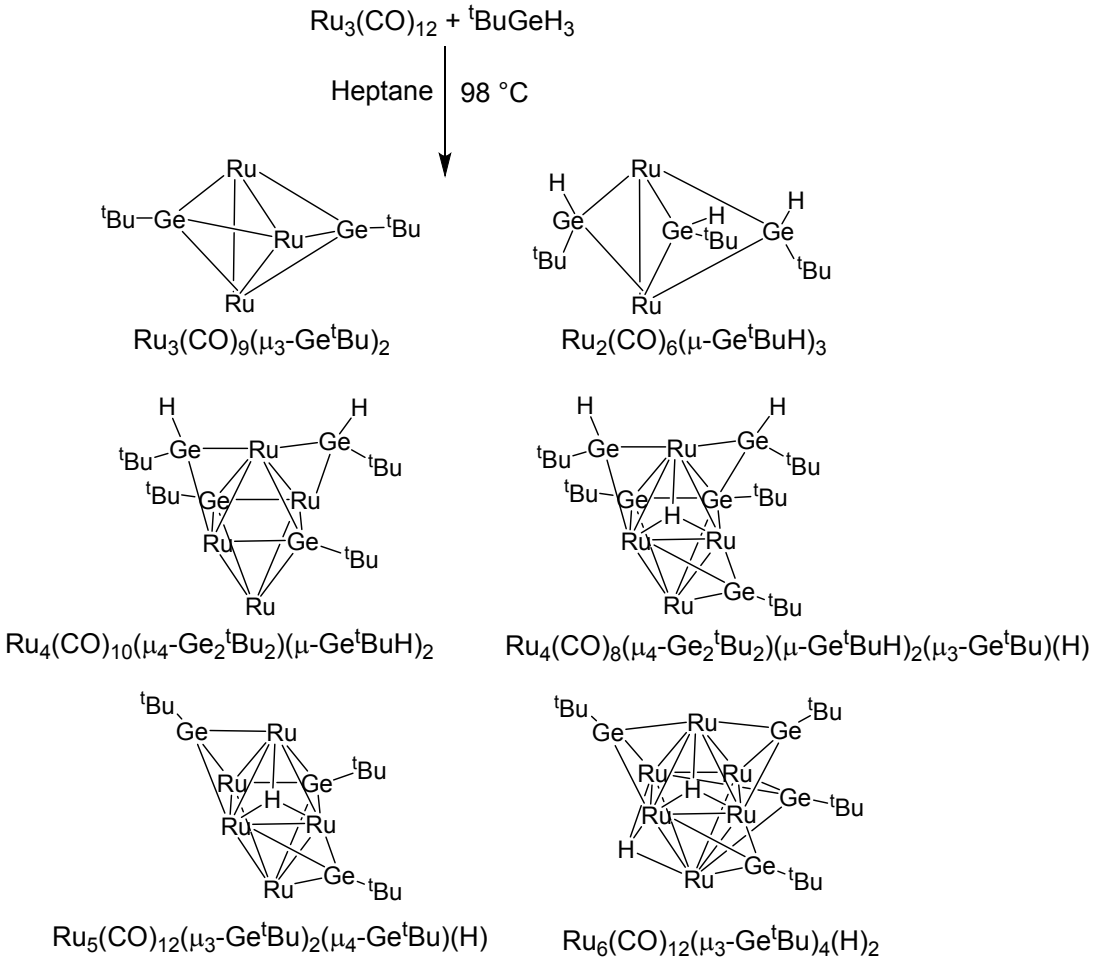

Scheme 15. The products of the thermal reaction of $Ru_3(CO)_{12}$ and $^tBuGeH_3$. The different products have been separated by thin layer chromatography (TLC).[117] CO ligands have been omitted for clarity.

By reacting carbonyls with boranes, boron may be incorporated into Ru and Os carbonyl clusters. Heating $Ru_3(CO)_{12}$ in toluene at 75 °C with $THF{\cdot}BH_3$ affords the octahedral $HRu_6B(CO)_{17}$, whereas the redox condensation of $Ru_3(CO)_{10}(MeCN)_2$ and $[Ru_3(CO)_9(B_2H_5)]^-$ yields the trigonal prismatic cluster $[H_2Ru_6B(CO)_{18}]^-$.[118] The reaction of $H_2Os_3(CO)_{10}$ with B_2H_6 produces the carbonylborylidyne cluster $H_3Os_3(CO)_9(BCO)$, which is transformed into a mixture of $HOs_4(CO)_{12}(BH_2)$ and $HOs_5B(CO)_{12}$ after heating in toluene at 110 °C.[119] The cluster $Os_3(CO)_{10}(MeCN)_2$ may be used for the cage opening of carboranes; its reaction with *closo-o*-$C_2B_{10}H_{10}$ yields two interconvertible isomers: $Os_3(CO)_9(\mu_3\text{-}4,5,9\text{-}C_2B_{10}H_8)(\mu\text{-}H)_2$ and $Os_3(CO)_9(\mu_3\text{-}3,4,8\text{-}C_2B_{10}H_8)(\mu\text{-}H)_2$ (Figure 3).[120]

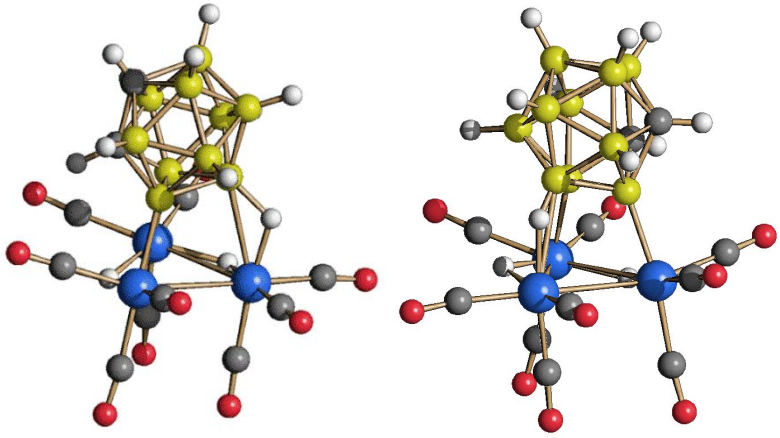

Figure 3. Molecular structures of $Os_3(CO)_9(\mu_3\text{-}4,5,9\text{-}C_2B_{10}H_8)(\mu\text{-}H)_2$ and $Os_3(CO)_9(\mu_3\text{-}3,4,8\text{-}C_2B_{10}H_8)(\mu\text{-}H)_2$ (blue, Os; yellow, B; red, O; grey, C; white, H). These two interconvertible isomers have been obtained from the reaction of $Os_3(CO)_{10}(MeCN)_2$ with *closo-o*-$C_2B_{10}H_{10}$.[120]

Heterometallic Ru- and Os-based carbonyl clusters. Heterometallic Ru–M and Os–M carbonyl clusters can be obtained by redox condensation of preformed Ru and Os carbonyls with metal salts, complexes, and carbonyls. For instance, the reaction of $[Ir(CO)_4]^-$ with 1 equiv. (equivalent(s)) of $Ru_3(CO)_{12}$ yields the tetrahedral cluster $[IrRu_3(CO)_{13}]^-$, whereas employing 2 equiv. of $Ru_3(CO)_{12}$ results in $[IrRu_6(CO)_{23}]^-$ (Scheme 16).[121] Moreover, the redox condensation of $[Os_{10}C(CO)_{24}]^{2-}$ with an excess of $[Pd(MeCN)_4][BF_4]_2$ results in the large cluster, $[Os_{18}Pd_3C_2(CO)_{42}]^{2-}$ (see ESI: Figure S3).[122]

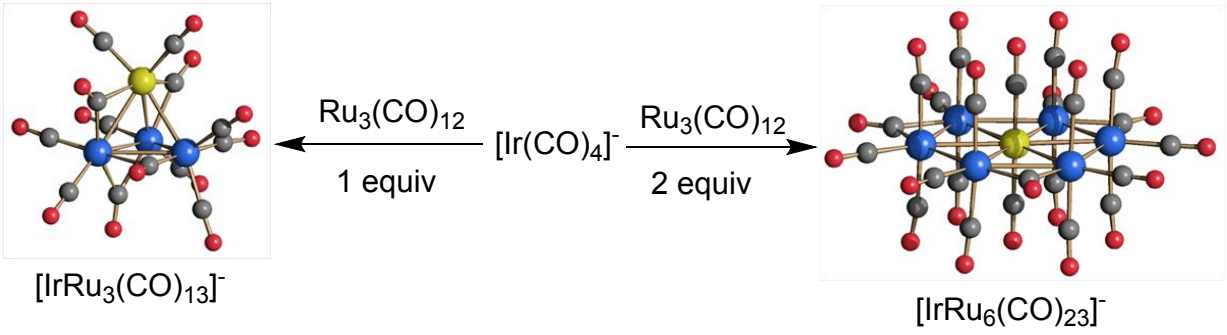

Scheme 16. The reactions of $Ru_3(CO)_{12}$ and $[Ir(CO)_4]^-$ (yellow, Ir; blue, Ru; red, O; grey, C). Depending on the stoichiometry of the reaction, $[IrRu_3(CO)_{13}]^-$ or $[IrRu_6(CO)_{23}]^-$ are formed.[121]

2.4 Cobalt Carbonyl Clusters

The commercially available $Co_2(CO)_8$ is the best starting material for the preparation of cobalt carbonyl clusters (see ESI: Table S5). In the solid state, it adopts the bridged $Co_2(\mu\text{-}CO)_2(CO)_6$ structure with C_{2v} symmetry, whereas in solution there is spectroscopic evidence of two additional

unbridged isomers with D_{3d} and D_{2d} symmetry. Co-crystallization with C_{60} traps the unbridged D_{3d} isomer in the $Co_2(CO)_8 \cdot C_{60}$ adduct.[123]

Homometallic cobalt carbonyl clusters. The tetrahedral $Co_4(CO)_{12}$ cluster is obtained after heating $Co_2(CO)_8$ in low-polarity solvents such THF, dioxane, or ^{i}PrOH. The reaction of $Co_4(CO)_{12}$ with halides or pseudo-halides results in the $[Co_4(CO)_{11}X]^-$ mono-anions (X = Br, I, SCN). Octahedral $Co_6(CO)_{16}$ can be prepared by oxidation of $[Co_6(CO)_{15}]^{2-}$ under a CO atmosphere.

$Co_2(CO)_8$ is quantitatively reduced by Na/naphthalene or Na/Hg to $Na[Co(CO)_4]$, which contains the very versatile cobaltate carbonyl anion. Alternatively, $[Co(CO)_4]^-$ can be obtained as the $[Co(MeOH)_6]^{2+}$ salt by disproportionation of $Co_2(CO)_8$ in methanol at 50 °C. In both cases, a variety of quaternary ammonium or phosphonium salts of $[Co(CO)_4]^-$ are readily prepared by metathesis of the Na^+ or $[Co(MeOH)_6]^{2+}$ cations.

$[Co(CO)_4]^-$ may be considered a pseudo-halide and forms the $HCo(CO)_4$ hydride, which possesses acidic character. Well-defined isocyano analogues of $HCo(CO)_4$ have been recently investigated.[124] The reaction of $[Co(CO)_4]^-$ with M^+ (M = Cu, Ag, Au) or Hg^{2+} in a 2:1 stoichiometric ratio affords the linear $[M\{Co(CO)_4\}_2]^-$ and $Hg\{Co(CO)_4\}_2$ complexes reminiscent of $[MX_2]^-$ and HgX_2 (X = Cl, Br, I, CN).[125] Transmetalation reactions involving 1:2 molar ratio of Ln metal (Ln = Yb, Eu) and $Hg\{Co(CO)_4\}_2$ in Et_2O afford the isocarbonyl polymeric arrays, $[\{(Et_2O)_3Ln[Co_4(CO)_{11}]\}_\infty$, which contain the reduced $[Co_4(CO)_{11}]^{2-}$ anion (see ESI: Figure S4).[126]

$Co_2(CO)_8$ undergoes different disproportionation/condensation equilibria depending on the polarity of the solvent, the presence of base, and the application of vacuum. In very polar solvents under nitrogen, only disproportionation to Co^{2+} and $[Co(CO)_4]^-$ is observed (see ESI: Scheme S8). In contrast, heating $Co_2(CO)_8$ in dry ethanol at 60 °C under vacuum affords the octahedral $[Co_6(CO)_{15}]^{2-}$ cluster as the result of the partial condensation between Co^{2+} and $[Co(CO)_4]^-$. The stoichiometric reaction between $Co_2(CO)_8$ and pyridine in hexane results in the triangular $[Co_3(CO)_{10}]^-$ anion.[127]

$[Co_6(CO)_{15}]^{2-}$ is protonated by strong acids to $[HCo_6(CO)_{15}]^-$, which contains a fully interstitial hydride at the centre of the octahedral cage of the cluster. Reduction of $[Co_6(CO)_{15}]^{2-}$ with alkali metals affords the $[Co_6(CO)_{14}]^{4-}$ tetra-anion (Scheme 17).

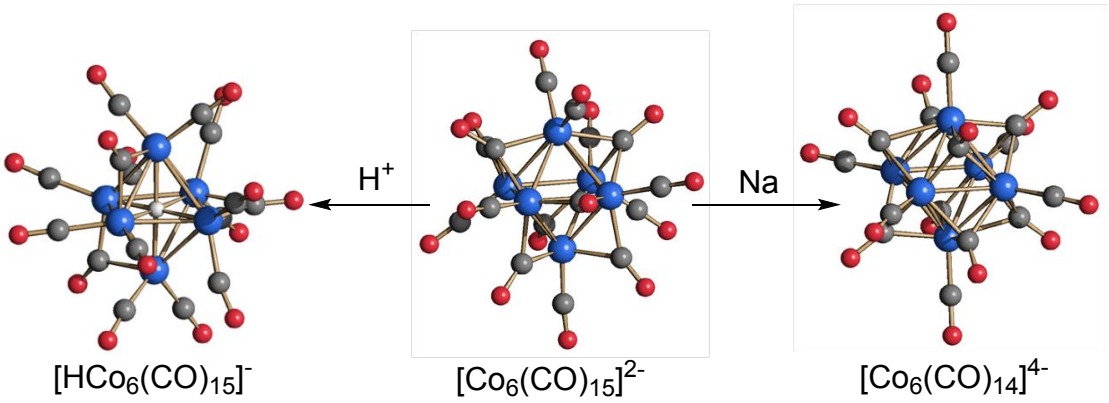

Scheme 17. The reactions of $[Co_6(CO)_{15}]^{2-}$ with acids and Na (blue, Co; red, O; grey, C; white, H). Its protonation results in the fully interstitial hydride $[HCo_6(CO)_{15}]^{-}$, whereas the addition of two electrons promotes the elimination of one CO ligand and affords the $[Co_6(CO)_{14}]^{4-}$ tetra-anion. See Table S5 in ESI for details.

Cobalt carbide carbonyl clusters. Several homometallic Co carbide carbonyl clusters are known, and most of them can be prepared starting from the trigonal prismatic $[Co_6C(CO)_{15}]^{2-}$ cluster[128] *via* thermal or redox reactions (Scheme 18).[48] In addition, $Co_3(\mu_3\text{-}CCl)(CO)_9$ is obtained by refluxing $Co_2(CO)_8$ in CCl_4.

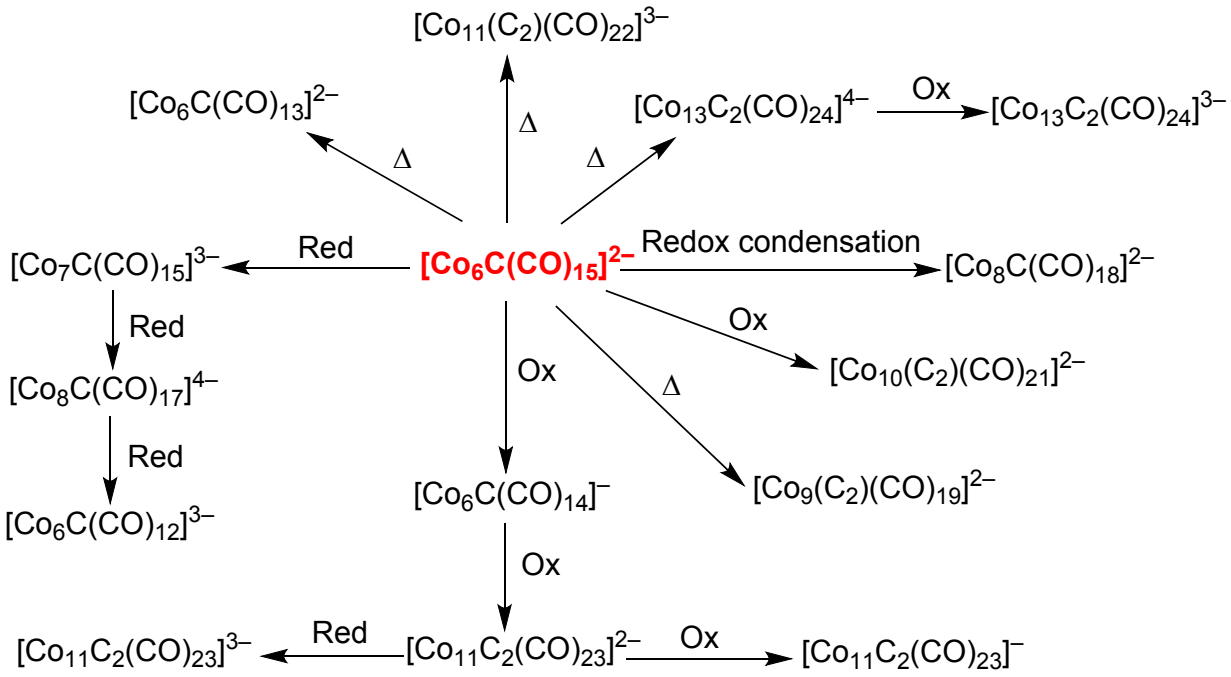

Scheme 18. Synthesis of Co carbide carbonyl clusters (Ox = oxidation; Red = reduction; Δ = thermal reaction). Several homometallic Co carbide carbonyl clusters are prepared by thermal or redox reactions starting from $[Co_6C(CO)_{15}]^{2-}$.[48] See text for details.

$[Co_6C(CO)_{15}]^{2-}$ can be prepared from the reaction of $[Co(CO)_4]^-$ with CCl_4 at a 6:1 molar ratio or from $[Co(CO)_4]^-$ and $Co_3(\mu_3\text{-}CCl)(CO)_9$ at a 3:1 molar ratio. By performing the latter reaction at a 2:1 molar ratio, the paramagnetic $[Co_6C(CO)_{14}]^-$ cluster is obtained. $[Co_6C(CO)_{14}]^-$ can be alternatively obtained by mild oxidation of $[Co_6C(CO)_{15}]^{2-}$ or from the reaction of $[Co_6(CO)_{15}]^{2-}$ with MeCOCl *via* CO scission induced by the addition of $MeCO^+$ to a coordinated CO ligand. In the presence of even weak bases, $[Co_6C(CO)_{14}]^-$ is converted to $[Co_6C(CO)_{15}]^{2-}$.

Gently heating $[Co_6C(CO)_{15}]^{2-}$ in THF results in an intramolecular condensation to yield $[Co_6C(CO)_{13}]^{2-}$ *via* the loss of two CO ligands and the rearrangement of the Co_6 cage from trigonal prismatic to octahedral geometry. Under more severe thermal conditions, larger clusters such as $[Co_{13}C_2(CO)_{24}]^{4-}$ are obtained. The stepwise reduction of $[Co_6C(CO)_{15}]^{2-}$ with Na/naphthalene affords, in sequence, the highly reduced clusters $[Co_7C(CO)_{15}]^{3-}$ and $[Co_8C(CO)_{17}]^{4-}$, and eventually, $[Co_6C(CO)_{12}]^{3-}$.[48]

Several heterometallic Co–M carbide carbonyl clusters have been reported. Although they will not be reviewed in detail, some general strategies for their synthesis, along with pertinent examples, are listed below:

1) *Reaction of $Co_3(\mu_3\text{-}CCl)(CO)_9$ with metal carbonyl complexes or clusters*. $Co_3(\mu_3\text{-}CCl)(CO)_9$ reacts with $[Rh(CO)_4]^-$ yielding $[Co_2Rh_4C(CO)_{13}]^{2-}$,[129] whereas it reacts with $Mo(CO)_3(MeCN)_3$ producing $[Mo_3Co_3C(CO)_{18}]^-$.[130] Interestingly, $[Co_3Ni_9C(CO)_{20}]^{3-}$ results from the addition of $Co_3(\mu_3\text{-}CCl)(CO)_9$ to $[Ni_6(CO)_{12}]^{2-}$,[131] whereas a different product, $[Co_6Ni_2C_2(CO)_{16}]^{2-}$, is obtained by doing the opposite—adding $[Ni_6(CO)_{12}]^{2-}$ to $Co_3(\mu_3\text{-}CCl)(CO)_9$.[132] C-C coupling and redox condensation are observed in the reaction of $Co_3(\mu_3\text{-}CCl)(CO)_9$ with $[Ni_9C(CO)_{17}]^{2-}$, which affords the $[Co_3Ni_7(C_2)(CO)_{15}]^{3-}$ mono-acetylide.[133] The Ni–Co hexacarbide carbonyl cluster $[H_{6-n}Ni_{22}Co_6C_6(CO)_{36}]^{n-}$ (n = 3–6) has been obtained by the redox condensation of $[Ni_{10}(C_2)(CO)_{16}]^{2-}$ and $Co_3(\mu_3\text{-}CCl)(CO)_9$ (Scheme 19). Thermolysis of $[H_2Ni_{22}Co_6C_6(CO)_{36}]^{4-}$ in THF affords the larger octa-carbide $[Ni_{36}Co_8C_8(CO)_{48}]^{6-}$.[39,134]

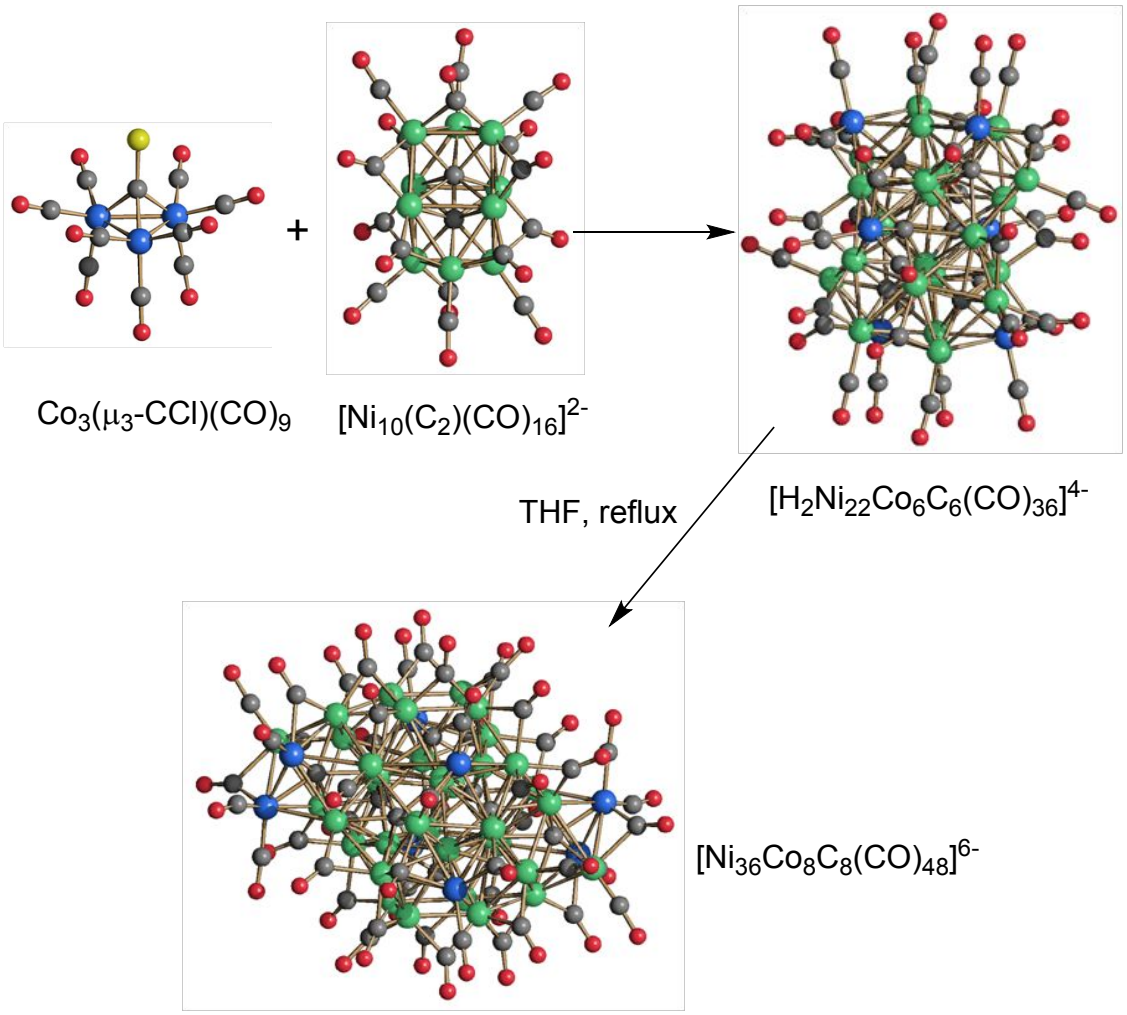

Scheme 19. Synthesis of $[H_2Ni_{22}Co_6C_6(CO)_{36}]^{4-}$ and $[Ni_{36}Co_8C_8(CO)_{48}]^{6-}$ (green, Ni; blue, Co; yellow, Cl; red, O; grey, C). Redox condensation of $[Ni_{10}(C_2)(CO)_{16}]^{2-}$ and $Co_3(\mu_3\text{-}CCl)(CO)_9$ affords $[H_2Ni_{22}Co_6C_6(CO)_{36}]^{4-}$, which is thermally converted into $[Ni_{36}Co_8C_8(CO)_{48}]^{6-}$.[39,134]

2) *Redox condensation involving a Co carbide carbonyl cluster and a metal complex, salt or cluster*. Some recent examples are represented by the reactions of $[Co_6C(CO)_{15}]^{2-}$ with $Pt(Et_2S)_2Cl_2$ and with $Pd(Et_2S)_2Cl_2$, which result in the formation of $[Co_8Pt_4C_2(CO)_{24}]^{2-}$ [135] and $[H_{6-n}Co_{20}Pd_{16}C_4(CO)_{48}]^{n-}$ (n = 3–6), respectively (Scheme 20).[50-52]

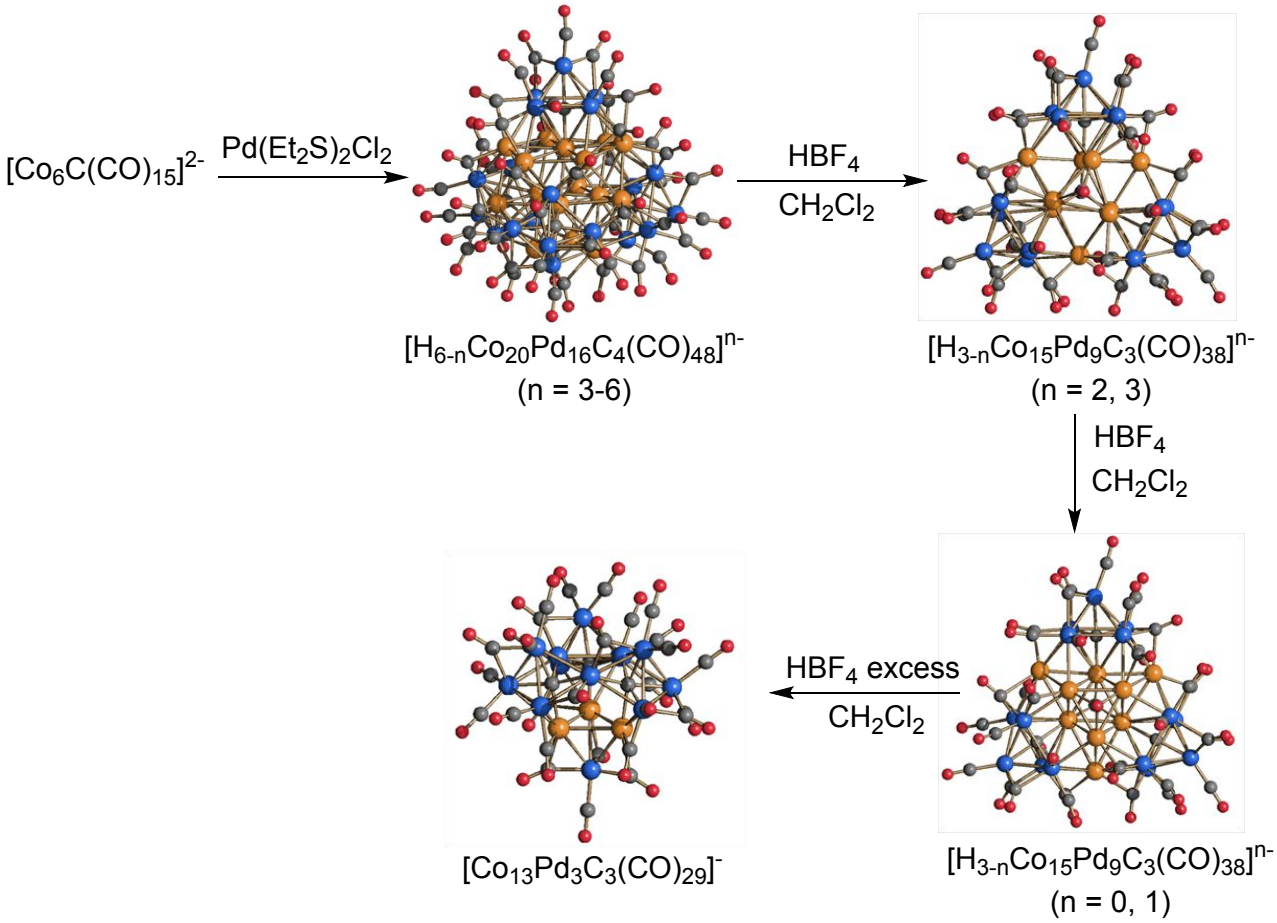

Scheme 20. Synthesis and reactivity of $[H_{6-n}Co_{20}Pd_{16}C_4(CO)_{48}]^{n-}$ (n = 3–6) (orange, Pd; blue, Co; red, O, grey, C). This compound is obtained from the redox condensation of $[Co_6C(CO)_{15}]^{2-}$ and $Pd(Et_2S)_2Cl_2$. $[H_{6-n}Co_{20}Pd_{16}C_4(CO)_{48}]^{n-}$ (n = 3–6) is transformed into $[H_{3-n}Co_{15}Pd_{96}C_3(CO)_{38}]^{n-}$ (n = 0–3) and, eventually, $[Co_{13}Pd_3C_3(CO)_{29}]^-$ upon reaction with increasing amounts of strong acids.[50-52]

3) *Addition of cationic metal fragments to an anionic Co carbide carbonyl cluster anion with the formation of a Lewis-type acid–base adduct*. This method is represented well by the reaction of $Au(PPh_3)Cl$ with $[Co_6C(CO)_{15}]^{2-}$, which affords several Co carbide carbonyl clusters decorated by $AuPPh_3$ fragments, depending on the experimental conditions (see ESI: Scheme S9).[136]

Cobalt carbonyl clusters containing other main-group elements. The $[Co_6N(CO)_{15}]^-$ nitride, which is isostructural to $[Co_6C(CO)_{15}]^{2-}$, can be obtained from $[Co_6(CO)_{15}]^{2-}$ and $[NO][BF_4]$. Removal of two CO ligands from the trigonal prismatic $[Co_6N(CO)_{15}]^-$ by means of Me_3NO affords the octahedral nitride $[Co_6N(CO)_{13}]^-$. Redox condensation between $[Co_6N(CO)_{15}]^-$ and $[Co(CO)_4]^-$ results in $[Co_7N(CO)_{15}]^{2-}$, whereas the treatment of $[Co_6N(CO)_{15}]^-$ with OH^- ions

leads to the formation of the di-nitride $[Co_{10}N_2(CO)_{19}]^{4-}$. Thermal treatment of $[Co_6N(CO)_{15}]^-$ in diglyme at 140–150 °C results in the tri-nitride $[Co_{14}N_3(CO)_{26}]^{3-}$, which can be transformed into $[Co_{13}N_2(CO)_{24}]^{3-}$ by heating at 100 °C in a water solution buffered at pH 11.[137]

The incorporation of other main-group elements into Co carbonyl clusters usually involves starting with suitable anions, such as $[Co(CO)_4]^-$, $[Co_6(CO)_{15}]^{2-}$, and even the neutral $Co_2(CO)_8$, in the presence of a main-group compound, which is often a halide, EX_n. This method is exemplified well by the synthesis Co phosphide carbonyl clusters (Figure 4), which strongly depends on the precursors and experimental conditions. The reaction of $[Co(CO)_4]^-$ with PCl_3 affords $[Co_6P(CO)_{16}]^-$, whereas using PCl_5 results in $[Co_9P(CO)_{21}]^{2-}$. The triangular $Co_3P(CO)_9$ cluster can be prepared from $[Co_6(CO)_{15}]^{2-}$ and PBr_3, whereas $[HCo_{10}P_2(CO)_{23}]^-$ has been isolated mixing $[Co(CO)_4]^-$, $[Co_6(CO)_{15}]^{2-}$, and PBr_3 at a 4:1:2 molar ratio.[138] Cluster expansion may be achieved by redox condensation, as exemplified by the synthesis of $[Co_{10}P(CO)_{22}]^{3-}$ from $[Co_9P(CO)_{21}]^{2-}$ and $[Co(CO)_4]^-$.[139] Alternatively, P-atoms may be directly introduced as in the reaction between $Co_2(CO)_8$ and $W(CO)_4(PH_3)_2$, which results in the formation of $Co_8P_2(CO)_{19}$ or $Co_{10}P_2(CO)_{24}$ in a mixture with $[\{Co_3(CO)_8\{\mu_4\text{-}PW(CO)_5\}\}\{(\mu_4\text{-}P)Co_3(CO)_9\}]$, depending on the stoichiometric ratio.[140]

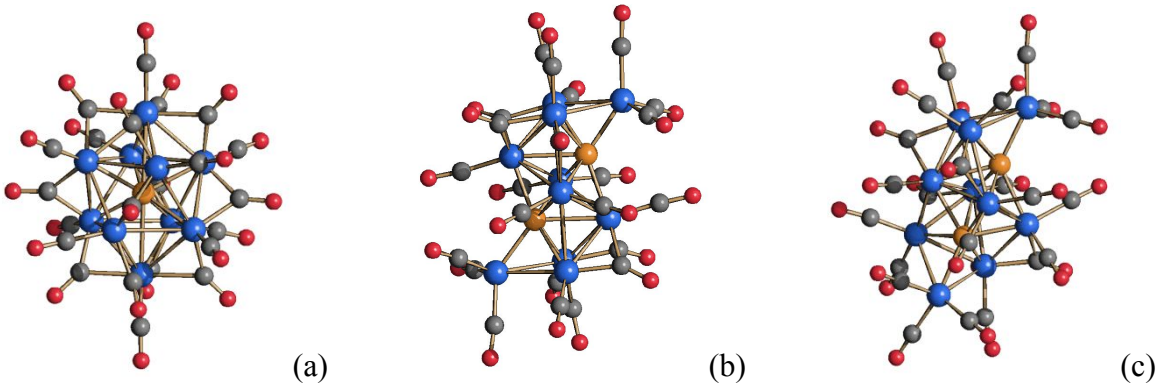

Figure 4. Molecular structures of (a) $[Co_{10}P(CO)_{22}]^{3-}$, (b) $[HCo_{10}P_2(CO)_{23}]^-$ (the hydride ligand has not been located by X-ray crystallography and, thus, is not represented in the figure), and (c) $Co_{10}P_2(CO)_{24}$ (blue, Co; orange, P; red, O; grey, C).[138-140]

2.5 Rhodium and Iridium Carbonyl Clusters

$Rh_4(CO)_{12}$ and $Ir_4(CO)_{12}$ are the major carbonyl species isolated following the reductive carbonylation of Rh and Ir salts at atmospheric pressure.[31-33] The dinuclear species $M_2(CO)_8$ (M = Rh, Ir) have been observed only by spectroscopic methods at very high CO pressures or in matrix experiments at low temperatures.[141] $Rh_4(CO)_{12}$ spontaneously loses CO under N_2 atmosphere

affording $Rh_6(CO)_{16}$. Meanwhile, the analogous $Ir_6(CO)_{16}$ is conveniently obtained from the oxidation of $[Ir_6(CO)_{15}]^{2-}$.[142]

Homometallic Rh and Ir carbonyl clusters. Neutral Rh and Ir carbonyls are suitable precursors for the synthesis of larger clusters (see ESI: Tables S6 and S7). Moreover, CO ligands can be replaced by phosphines or other soft nucleophiles, resulting in heteroleptic clusters. $Rh_4(CO)_{12}$ and $Rh_6(CO)_{16}$ disproportionate in the presence of bases, such as amines. For instance, the ionic couple $[Rh(CO)_2(py)]^+[Rh_5(CO)_{13}(py)_2]^-$ is formed in pyridine.[143] The most powerful technique for obtaining anionic Rh and Ir carbonyl clusters involves the reduction of $M_4(CO)_{12}$ (M = Rh, Ir).[144] Several different species may be obtained, depending on the nature (alkali metals or alkali hydroxides) and amount of reducing agent, the temperature, and the reaction atmosphere (N_2, CO, H_2, vacuum).

The reduction of $Rh_4(CO)_{12}$ with increasing amounts of NaOH or KOH under CO at atmospheric pressure affords $[Rh_{12}(CO)_{30}]^{2-}$, $[Rh_6(CO)_{15}]^{2-}$, $[Rh_7(CO)_{16}]^{3-}$, $[Rh_4(CO)_{11}]^{2-}$, and $[Rh(CO)_4]^-$. Again with increasing base, the reduction of the analogous $Ir_4(CO)_{12}$ produces $[HIr_4(CO)_{11}]^-$, $[Ir_4(CO)_{11}]^{2-}$, $[HIr_4(CO)_{10}]^{3-}$, $[Ir_4(CO)_{10}]^{4-}$, and $[Ir(CO)_4]^-$ (see ESI: Scheme S10).[33] Careful dosage of NaOH during thermolysis of $Rh_4(CO)_{12}$ under different atmospheres enables the more or less selective preparation of several high-nuclearity Rh carbonyl clusters (see ESI: Scheme S11), including $[H_{5-n}Rh_{13}(CO)_{25}]^{n-}$ (n = 2, 3), $[Rh_{22}(CO)_{37}]^{4-}$, $[H_{8-n}Rh_{22}(CO)_{35}]^{n-}$ (n = 4, 5), $[Rh_{19}(CO)_{31}]^{5-}$, and $[Rh_{33}(CO)_{47}]^{5-}$ (Figure 5).[145146] Similarly, the base-induced condensation of $Ir_4(CO)_{12}$ may lead to products such as $[Ir_8(CO)_{22}]^{2-}$, $[Ir_9(CO)_{20}]^{3-}$, $[HIr_9(CO)_{19}]^{4-}$, and $[Ir_{10}(CO)_{21}]^{2-}$, depending on the solvent and reaction conditions.[147] Moreover, $[Ir_6(CO)_{15}]^{2-}$ may be obtained from the reductive carbonylation of K_2IrCl_6 in 2-methoxy-ethanol/water or the redox condensation of $Ir_4(CO)_{12}$ and $[Ir(CO)_4]^-$; this is a valuable precursor for the preparation of larger Ir clusters. For instance, oxidation of $[Ir_6(CO)_{15}]^{2-}$ with $[Cp_2Fe]^+$ (Cp = cyclopentadienyl) affords $[Ir_{14}(CO)_{27}]^-$ (Figure 5), which is the largest homometallic Ir carbonyl cluster reported to date.[148]

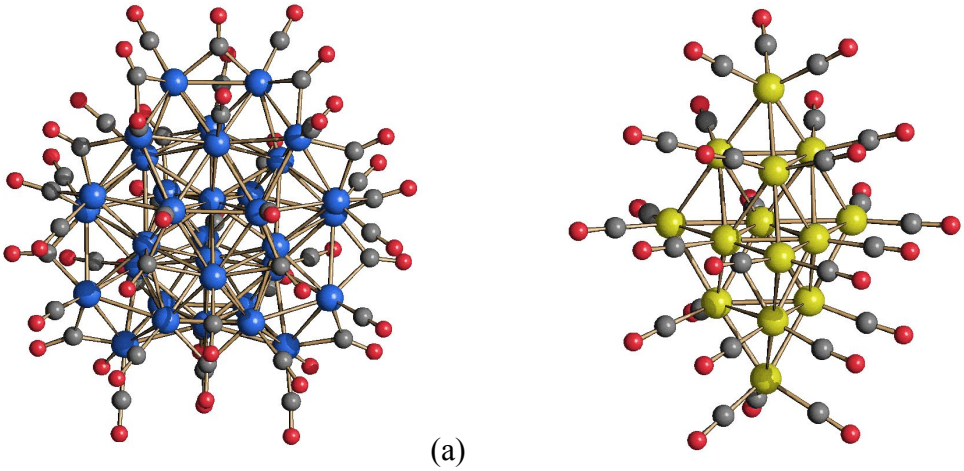

Figure 5. Molecular structures of (a) $[Rh_{33}(CO)_{47}]^{5-}$ and (b) $[Ir_{14}(CO)_{27}]^{-}$, the largest homometallic homoleptic Rh and Ir carbonyl clusters (yellow, Ir; blue, Rh; red, O; grey, C).[145-147]

The robustness of the Rh–Rh and Ir–Ir bonds also allows the isolation of unusual species, such as the μ-η^1-η^1-peroxo $Ir_4(CO)_5(PR_3)_3(O_2)_2$ [149] and the $Rh_6(CO)_{12}(\mu_3\text{-GaCp*})_4$ and $Rh_6(CO)_{16-x}(\mu_3\text{-InCp*})_x$ (x = 1, 2) derivatives containing ECp* ligands (E = Ga, In; Cp* = pentamethylcyclopentadienyl) (Figure 6).[150]

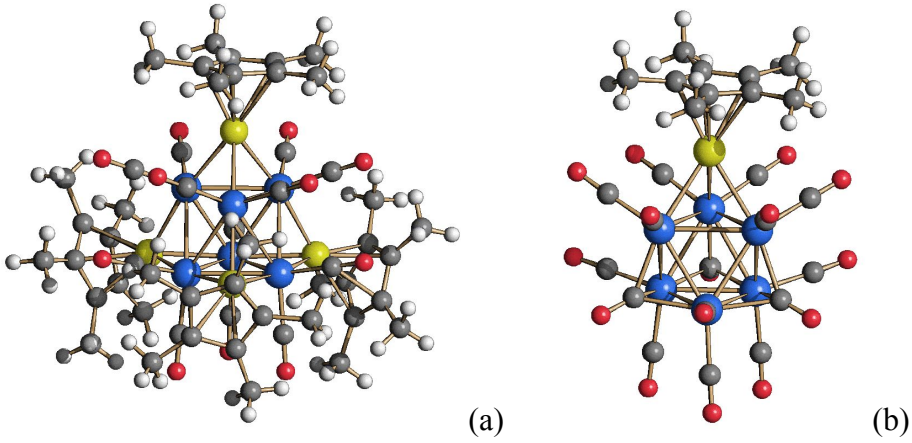

Figure 6. Molecular structures of (a) $Rh_6(CO)_{12}(\mu_3\text{-GaCp*})_4$ and (b) $Rh_6(CO)_{15}(\mu_3\text{-InCp*})$ (blue, Rh; yellow, Ga (a) or In (b); red, O; grey, C; white, H).[150] These compounds have been obtained upon reactions of $Rh_6(CO)_{16}$ with GaCp* and $Rh_6(CO)_{15}(MeCN)$ with InCp*, respectively (Cp* = pentamethylcyclopentadienyl).

Rhodium carbonyl clusters containing main-group elements. Rh forms several carbonyl clusters containing interstitial heteroatoms (E = C, N, P, S, Ge, As, Sn, Sb, Bi), whereas the analogous interstitial heteronuclear Ir carbonyl clusters are not known. This is due to the fact that Ir–Ir bonds are stronger than Rh–Rh bonds. Consequently, Ir clusters prefer to maximise Ir–Ir

contacts, rather than allowing interstitial heteroatoms to replace them with Ir–E bonds. Indeed, as also observed for Pt, a few heteronuclear Ir carbonyl clusters have been reported, but they contain an iridium core with the heteroatoms on the surface.[151152] An exciting advancement in this field is the recent discovery of the 15-vertex deltahedral cluster $[(\eta^3\text{-}Bi_3)_2(IrCO)_6(\mu_4\text{-}Bi)_3]^{3-}$, which is obtained from $Ir(CO)_2(acac)$ (acac = acetylacetonate) and K_5Bi_4 (Scheme 21).[153]

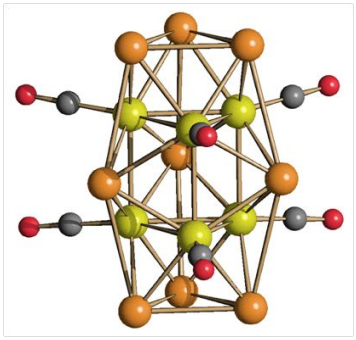

Scheme 21. Synthesis of the 15-vertex deltahedral cluster $[(\eta^3\text{-}Bi_3)_2(IrCO)_6(\mu_4\text{-}Bi)_3]^{3-}$ (yellow, Ir; orange, Bi; red, O; grey, C).[153]

A general strategy for the synthesis of Rh carbonyl clusters containing heavy main-group elements such as Ge, Sn, Sb, and Bi is represented by the reaction of $[Rh_7(CO)_{16}]^{3-}$ with EX_n compounds.[11,38,154155] Conversely, lighter elements, P and As, have been introduced into $[Rh_{10}As(CO)_{22}]^{3-}$,[156] $[Rh_{10}P(CO)_{22}]^{3-}$, and $[Rh_9P(CO)_{21}]^{2-}$[157] by reductive carbonylation of Rh(I) complexes at high pressure and temperature in the presence of EPh_3 (E = P, As). $[Rh_{10}S(CO)_{22}]^{2-}$ was obtained from $Rh_4(CO)_{12}$ and SCN^-.[158]

$[Rh_6C(CO)_{15}]^{2-}$ may be obtained from the reductive carbonylation of $RhCl_3$ at atmospheric pressure and RT in MeOH in the presence of $CHCl_3$, or from the reaction of $[Rh(CO)_4]^-$ and CCl_4.[159] Refluxing the trigonal prismatic $[Rh_6C(CO)_{15}]^{2-}$ in ^{i}PrOH generates the octahedral $[Rh_6C(CO)_{13}]^{2-}$ by the removal of two CO ligands.[41] The self-assembly of $[Rh_6C(CO)_{15}]^{2-}$ with Ag^+ ions affords oligomeric and polymeric species, such as $[Ag\{Rh_6C(CO)_{15}\}_2]^{3-}$ and $[\{AgOC_4H_8\{Rh_6C(CO)_{15}\}AgOC_4H_8\}pyz]_\infty$ (pyz = pyrazine).[160] Oxidation of $[Rh_6C(CO)_{15}]^{2-}$ with Fe^{3+} ions results in $Rh_{12}C_2(CO)_{25}$, whereas heating $[Rh_6C(CO)_{15}]^{2-}$ at 70 °C in the presence of H_2SO_4 produces $[Rh_{12}C_2(CO)_{24}]^{2-}$. This latter cluster may be further transformed into $[Rh_{12}C_2(CO)_{23}]^{4-}$ by treatment with alkali hydroxides or into $[Rh_{12}C_2(CO)_{20}\{Au(PPh_3)\}_4]$ and $[Rh_{12}C_2(CO)_{18}\{Au(PPh_3)\}_4]$ after reaction with $Au(PPh_3)Cl$. In turn, several multivalent clusters based on the $Rh_{10}(C)_2Au_{4\text{-}6}$ framework may be obtained *via* the reduction of $[Rh_{12}C_2(CO)_{20}\{Au(PPh_3)\}_4]$.[161]

The chemistry of Rh nitride carbonyl clusters is quite rich. $[Rh_6N(CO)_{15}]^{3-}$ can be prepared from the reaction of $[Rh_6(CO)_{15}]^{2-}$ with $NOBF_4$, or by treating $[Rh_7CO)_{16}]^{3-}$ with base under NO/CO atmosphere.[3] $[Rh_6N(CO)_{15}]^{3-}$ undergoes nucleophilic attack when reacted with OH^-, affording the hydride $[HRh_6N(CO)_{14}]^{3-}$.[162] Thermal treatment of $[Rh_6N(CO)_{15}]^{3-}$ under different experimental conditions (*e.g.*, temperature, solvent, time, pH) results in larger nitride and polynitride clusters, such as $[HRh_{12}N_2(CO)_{23}]^{3-}$, $[HRh_{12}N_2(CO)_{24}]^{-}$, $[Rh_{12}N_2(CO)_{24}]^{2-}$, $[Rh_{14}N_2(CO)_{25}]^{2-}$, $[Rh_{23}N_4(CO)_{38}]^{3-}$, and $[H_{6-n}Rh_{28}N_4(CO)_{41}]^{n-}$ (n = 4, 5).[163] Redox condensation of $[Rh_6N(CO)_{15}]^{3-}$ with $[PtRh_4(CO)_{14}]^{2-}$ and with $[M(CO)_4]^-$ (M = Co, Ir) results in the heterometallic nitrides $[PtRh_{10}N(CO)_{21}]^{3-}$ and $[MRh_6N(CO)_{15}]^{2-}$, respectively.[164]

Anionic Rh and Ir carbonyl clusters may be used in combination with metal salts and complexes for the preparation of heterometallic clusters *via* redox condensation.

2.6 Nickel Carbonyl Clusters

$Ni(CO)_4$ was the first metal carbonyl to be discovered and is nowadays produced at industrial quantities for the obtainment of ultra-pure Ni metal. Its main drawback is the fact that $Ni(CO)_4$ is highly toxic and carcinogenic; therefore, it must be handled with care.

Homometallic nickel carbonyl clusters. The reduction of $Ni(CO)_4$ with base was investigated first by Hieber,[165] and then, rationalised in the seminal work of Chini and Longoni (see ESI: Table S8).[166167] The most suitable and versatile precursor cluster for Ni carbonyl cluster chemistry is $[Ni_6(CO)_{12}]^{2-}$, which can be prepared by the reduction of $Ni(CO)_4$ using a variety of experimental conditions. The most efficient synthesis for a gram-scale yield is the reaction of $Ni(CO)_4$ with alkali hydroxides (NaOH, KOH) in DMF or DMSO followed by the addition of water (Scheme 22). In this reaction, the main product of the reduction is initially $[Ni_5(CO)_{12}]^{2-}$, and water is required to oxidise it to $[Ni_6(CO)_{12}]^{2-}$. It must be remarked that if aqueous NH_4Cl is present, $[HNi_{12}(CO)_{21}]^{3-}$ is produced rather than the hydrolysis to $[Ni_5(CO)_{12}]^{2-}$; if H_3PO_4 is present, the dihydride $[H_2Ni_{12}(CO)_{21}]^{2-}$ is formed. These hydrides $[HNi_{12}(CO)_{21}]^{3-}$ and $[H_2Ni_{12}(CO)_{21}]^{2-}$ can easily interconvert to one another as simple acid–base reactions. In contrast, their full deprotonation to $[Ni_{12}(CO)_{21}]^{4-}$ occurs only under very drastic basic conditions. $[Ni_5(CO)_{12}]^{2-}$ can be prepared in pure form by treating $[Ni_6(CO)_{12}]^{2-}$ with CO at atmospheric pressure. $[Ni_5(CO)_{12}]^{2-}$ is readily oxidised back to $[Ni_6(CO)_{12}]^{2-}$ simply using water, and thus, it must be handled under very anhydrous conditions.

$[Ni_9(CO)_{18}]^{2-}$ can be obtained by redox condensation of $[Ni_6(CO)_{12}]^{2-}$ with $Ni(CO)_4$, or oxidation of $[Ni_6(CO)_{12}]^{2-}$ with Ni^{2+}, Fe^{3+} or H^+ ions. In the latter case, the reaction must be carefully controlled in order to avoid the formation of $[HNi_{12}(CO)_{21}]^{3-}$ and $[H_2Ni_{12}(CO)_{21}]^{2-}$.

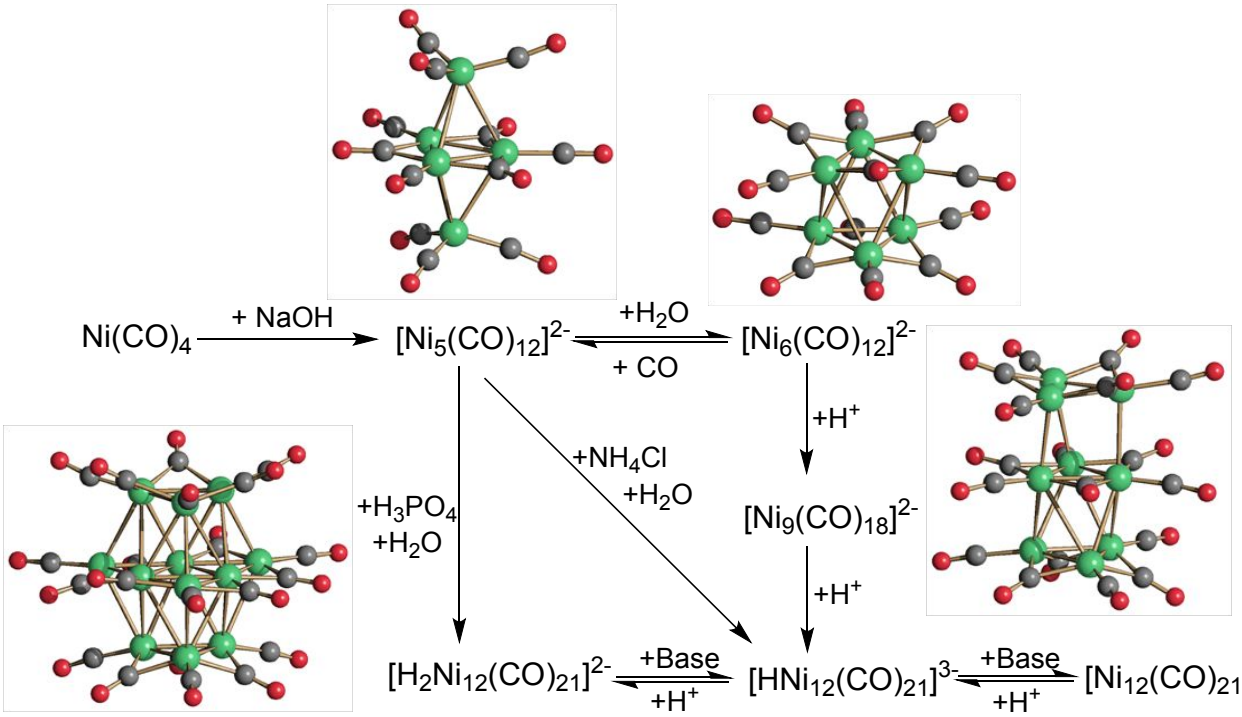

Scheme 22. Synthesis of homoleptic homometallic Ni carbonyl clusters (green, Ni; red, O; grey, C). The reaction of $Ni(CO)_4$ with NaOH in DMF or DMSO affords $[Ni_5(CO)_{12}]^{2-}$, whose hydrolysis results in $[Ni_6(CO)_{12}]^{2-}$, $[HNi_{12}(CO)_{21}]^{3-}$ or $[H_2Ni_{12}(CO)_{21}]^{2-}$ depending on the pH.[166,167]

Heterometallic Ni-based carbonyl clusters. $[Ni_6(CO)_{12}]^{2-}$ can undergo redox condensation with metal salts, metal complexes, MCCs, and main-group compounds in order to obtain a large variety of heterometallic MCCs and MCCs containing main-group elements. The reaction fails only with very electropositive elements, such as alkali and earth alkali metals, Al, Zn, early transition metals, and lanthanides. In these cases, a reaction is not observed for elements that are weak acids. In contrast, oxidation of $[Ni_6(CO)_{12}]^{2-}$ to $[Ni_9(CO)_{18}]^{2-}$ occurs with stronger acids such as Zn^{2+}, due to the hydrolysis of H_2O and the oxidation of the cluster *via* the H^+/H_2 redox couple. When the electropositive metal is a soft Lewis acid, such as Cd(II) and In(III), the formation of Lewis acid–base adducts comprising the cluster anion and the metal salt is observed rather than the redox condensation. As a result, the reaction of $[Ni_6(CO)_{12}]^{2-}$ with $InBr_3$ yields $[Ni_6(CO)_{11}(\mu_3\text{-}InBr_3)(\mu_4\text{-}In_2Br_5)]^{3-}$, $[Ni_6(CO)_{10}(\mu_4\text{-}In_2Br_5)_2]^{4-}$, and $[\{Ni_6(CO)_{11}\}_2(\mu_6\text{-}In)\{\mu_6\text{-}In_2Br_4(OH)\}]^{4-}$, which contain $[Ni_6(CO)_{11}]^{4-}$ and $[Ni_6(CO)_{10}]^{6-}$ cores decorated by $InBr_3$, $[In_2Br_5]^+$, In^{3+}, and $[In_2Br_4(OH)]^+$ fragments.[168] Moreover, the reaction of $[Ni_6(CO)_{12}]^{2-}$ with $CdCl_2$ results in the formation of the Lewis acid–base adduct $\{Cd_2Cl_3[Ni_6(CO)_{12}]_2\}^{3-}$.[169]

In contrast, less electropositive transition metals can be incorporated into heterometallic Ni–M clusters *via* redox condensation. Limiting our scope to homoleptic carbonyls, these include Cr, Mo, W, Fe, Ru, Os, Co, Rh, Ir, Pd, Pt, Cu, Ag, and Au (Figure 7; see also ESI: Table S9).[170171172173]

The highest nuclearities, which are obtained for Ni–Pd and Ni–Pt clusters, can exceed 40 metal atoms.

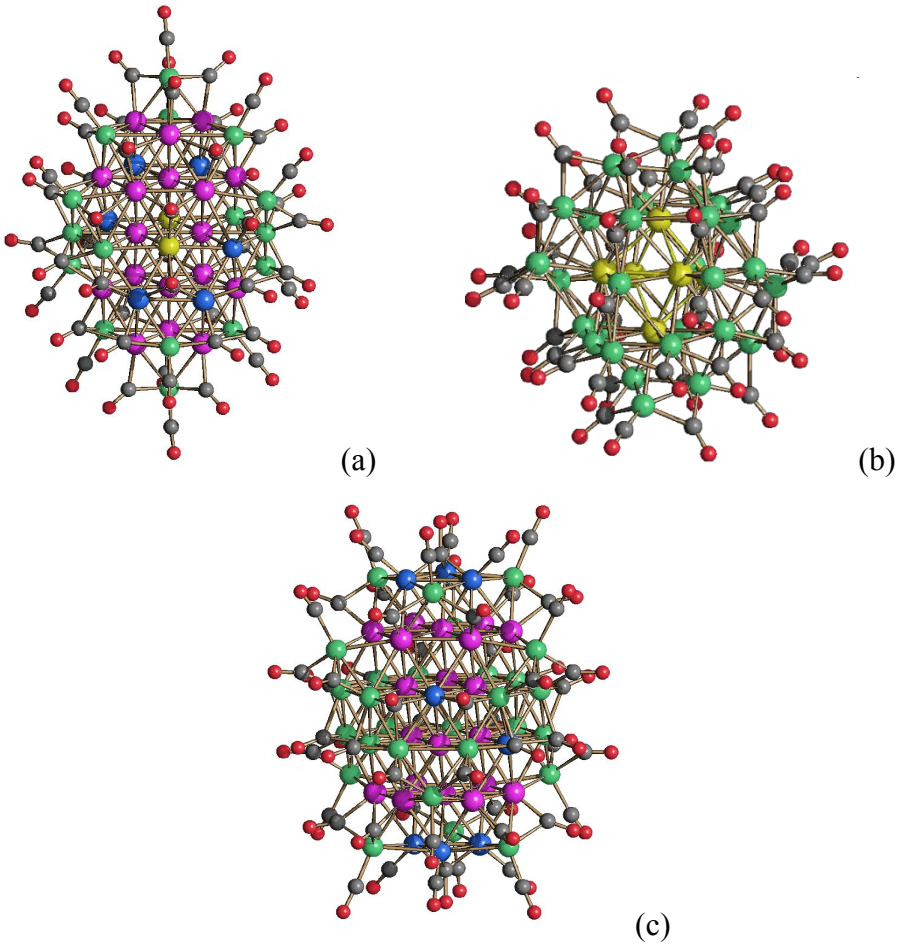

Figure 7. The molecular structures of (a) $[Ni_{22-x}Pd_{20+x}(CO)_{48}]^{6-}$ (x = 0.62) (green, Ni; purple, Pd; yellow, Ni/Pd ≈ 16:84; blue, Ni/Pd ≈ 85:15) (b) $[Ni_{32}Au_6(CO)_{44}]^{6-}$ (green, Ni; yellow, Au), (c) $[Ni_{32}Pt_{24}(CO)_{56}]^{n-}$ (green, Ni; purple, Pt; blue, Ni/Pt ≈ 66:34). In all structures, grey and red represent C and O, respectively. These are representative high nuclearity heterometallic Ni-M carbonyl clusters obtained from redox condensation of $[Ni_6(CO)_{12}]^{2-}$ with metal salts and complexes.[170-173]

Nickel carbonyl clusters containing main-group elements. A similar trend has been observed with post-transition metals; redox condensation yielding heteronuclear Ni–E clusters has been observed with Ga, Ge, Sn, Sb, and Bi, whereas Lewis-type acid–base adducts are found for In, which behaves like Cd. In addition, non-metallic main-group elements, such as C, P, As, Se, and Te, can be included in the metal cage of Ni carbonyl clusters.

Several Ni carbide carbonyl clusters may be obtained from reactions of $[Ni_6(CO)_{12}]^{2-}$ with halocarbons (CCl_4, C_2Cl_4, C_2Cl_6, C_3Cl_6, C_4Cl_6); they contain isolated C atoms or tightly bonded C_2

units (see ESI: Table S10). Ni carbide carbonyl anions can be further reacted with metal salts or complexes, affording heterometallic Ni–M carbide carbonyl clusters.[174175176177178] Alternatively, such compounds can be prepared starting from a preformed M carbide carbonyl and a Ni (carbonyl or non-carbonyl) compound.

The reaction of $[Ni_6(CO)_{12}]^{2-}$ with $GaCl_3$ in CH_2Cl_2 under nitrogen atmosphere results in a mixture of $[Ni_{12+x}Ga(CO)_{22+x}]^{3-}$ (x = 0–3) clusters, which is transformed into $[Ni_{12}Ga(CO)_{22}]^{3-}$ after exposure to CO atmosphere (see ESI: Figure S5).[179] Several Ni–Sb carbonyl clusters can be obtained by the redox condensation of $[Ni_6(CO)_{12}]^{2-}$ with $SbCl_3$ using various experimental conditions (see ESI: Figure S5).[180] Moisture must be avoided in order to prevent hydrolysis of the ECl_3 reactant. Indeed, anhydrous PCl_3 and $POCl_3$ are required for obtaining the Ni–P carbonyl clusters $[Ni_{11}P(CO)_{18}]^{3-}$, $[Ni_{14}P_2(CO)_{22}]^{2-}$, $[Ni_{22-x}P_2(CO)_{29-x}]^{4-}$ (x = 0.84), $[Ni_{22}P_6(CO)_{30}]^{2-}$, $[Ni_{23-x}P_2(CO)_{30-x}]^{4-}$ (x = 0.84), $[H_{6-n}Ni_{31}P_4(CO)_{39}]^{n-}$ (n = 4, 5), and $[Ni_{39}P_3(CO)_{44}]^{6-}$ (Figure 8).[181]

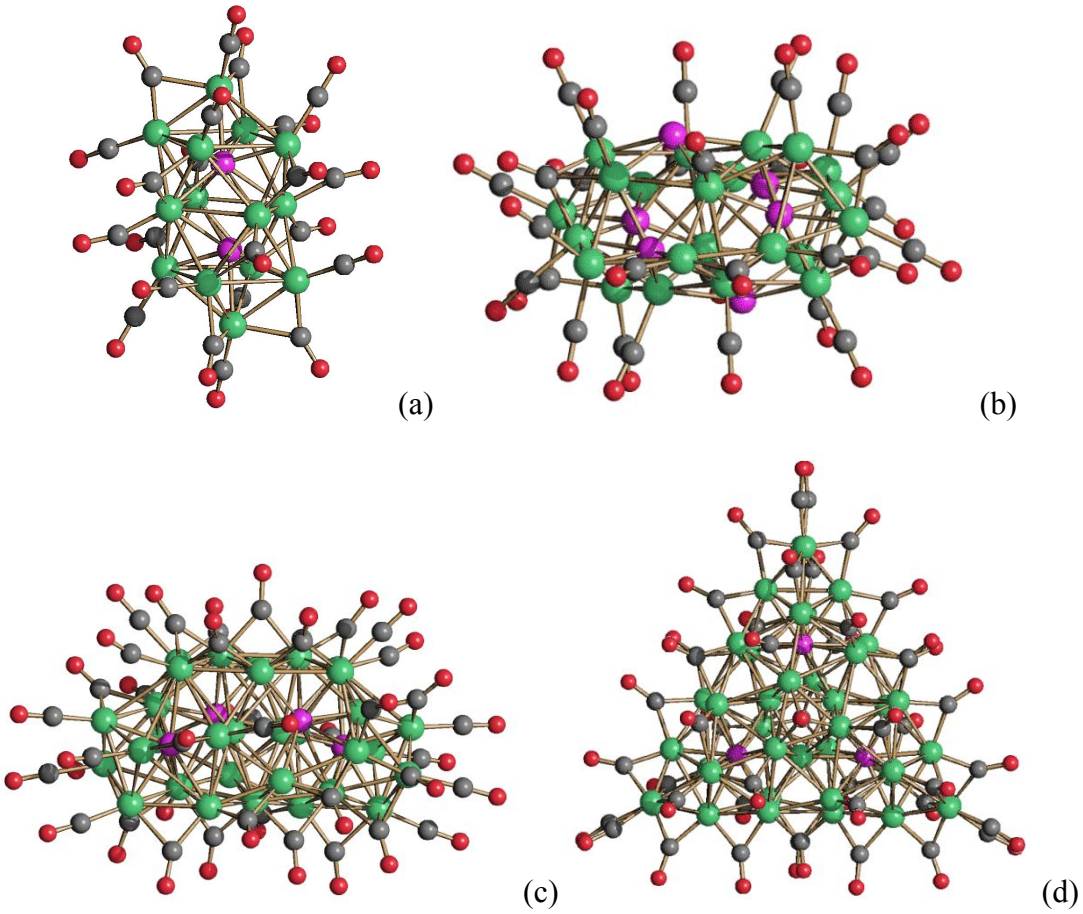

Figure 8. The molecular structures of (a) $[Ni_{14}P_2(CO)_{22}]^{2-}$, (b) $[Ni_{22}P_6(CO)_{30}]^{2-}$, (c) $[H_{6-n}Ni_{31}P_4(CO)_{39}]^{n-}$ (n = 4 and 5), and (d) $[Ni_{39}P_3(CO)_{44}]^{6-}$ (green, Ni; purple, P; grey, C; red, O).[181] These have been obtained from the reactions of $[Ni_6(CO)_{12}]^{2-}$ with PCl_3 or $POCl_3$ under different experimental conditions (e.g., stoichiometry, solvent).

2.7 Platinum Carbonyl Clusters

Platinum carbonyl clusters have been recently reviewed.[8,10] Chini clusters of the general formula $[Pt_{3n}(CO)_{6n}]^{2-}$ (n = 1–10) represent a milestone in inorganic and cluster chemistry.[34] As demonstrated by Chini and Longoni, they can be obtained by reductive carbonylation of Na_2PtCl_6 in MeOH at RT and atmospheric pressure of CO. Modulating the nature and amount of base, it is possible to control the nuclearity of the $[Pt_{3n}(CO)_{6n}]^{2-}$ (n = 1–10) clusters (Figure 9).[182183184] Chini clusters have been used for the preparation of several homoleptic, heteroleptic, and heterometallic carbonyl clusters, as well as for the preparation of metal nanoparticles, nanostructured materials, and heterogeneous catalysts.[8,10]

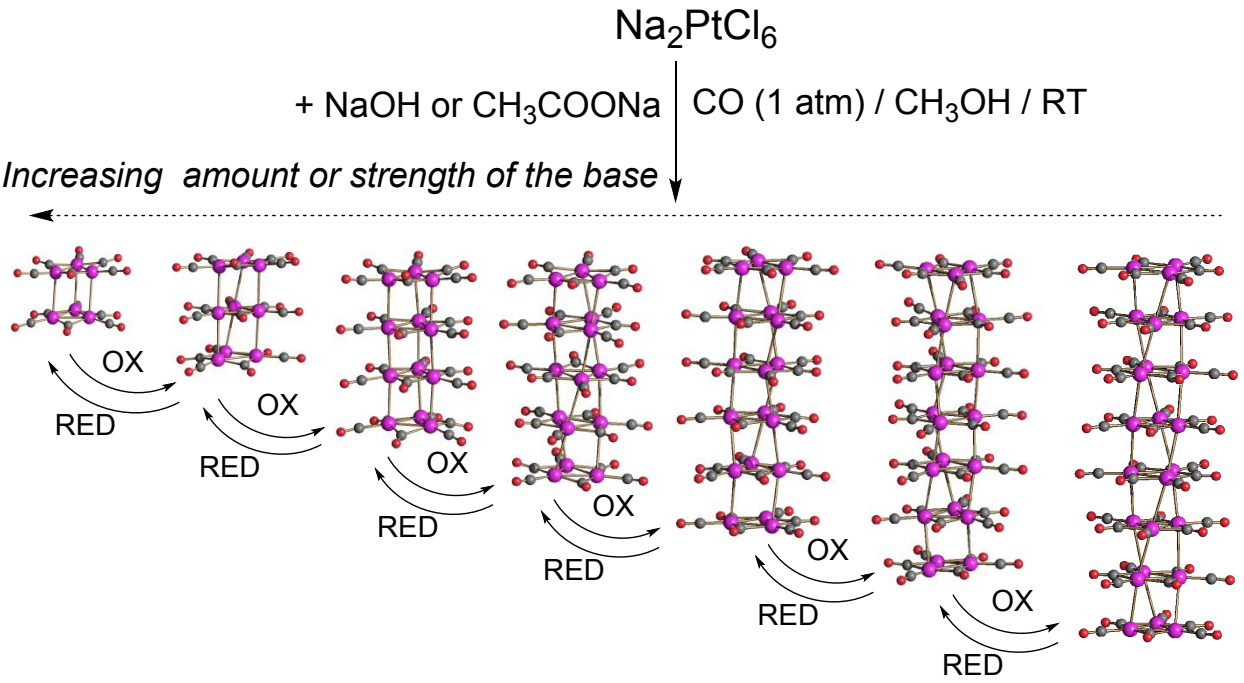

Figure 9. Synthesis of Chini clusters, $[Pt_{3n}(CO)_{6n}]^{2-}$ (n = 2–8), using reductive carbonylation of Na_2PtCl_6 and their redox interconversion (purple, Pt; red, O; grey, C).[8,10,182,183,184] OX and RED represent oxidation and reduction, respectively.

The reactions of Chini clusters may be grouped into two main categories, depending on whether the resulting clusters do (**A**) or do not (**B**) retain the trigonal prismatic structure of the parent species (Table 1 and Figure 10).

Table 1. Categorising the reactions of Chini clusters.

(A) The product retains the trigonal prismatic structure of the Chini Cluster.	**(B) The product does not retain the trigonal prismatic structure of the Chini Cluster.**
(**A-1**) Redox reaction	(**B-1**) Redox fragmentation
(**A-2**) CO/Phosphine substitution	(**B-2**) Thermal reaction
(**A-3**) Lewis acid–base adduct formation	(**B-3**) Formation of surface-decorated clusters
	(**B-4**) Formation of heterometallic clusters

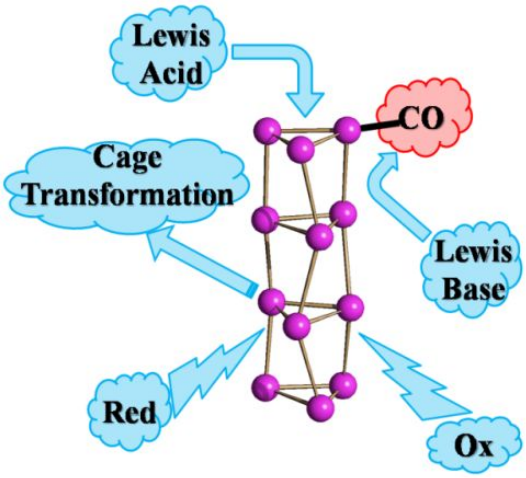

Figure 10. Illustrating the general reaction categories of Chini clusters.

Redox reactions of Chini clusters (A-1). Chini clusters may be easily and reversibly interconverted by means of redox reactions (**A-1**), with full retention of their trigonal prismatic structures. Reduction of $[Pt_{3n}(CO)_{6n}]^{2-}$ under CO atmosphere results in the gradual decrease of cluster nuclearity, whereas oxidation leads to higher nuclearities (Figure 9). The oxidation process eventually results in insoluble, infinite, and conductive molecular Pt carbonyl wires composed of continuous stacks of $Pt_3(\mu\text{-}CO)_3(CO)_3$ units.[182-184]

Reactions of Chini clusters with soft nucleophiles: Non-redox substitution (A-2) and redox fragmentation (B-1). The reactions of Chini clusters with soft nucleophiles may result in heteroleptic Chini clusters *via* non-redox substitution (**A-2**) or in zero-valent neutral Pt–(CO)–L species *via* redox fragmentation (**B-1**), where L is a phosphine-based ligand (Figure 11). The outcome of the reaction depends on the nature of the nucleophile, the nuclearity of the Chini cluster, and the stoichiometry of the reaction. In the case of phosphines, non-redox substitution is favoured by the stoichiometric addition of the phosphine to lower-nuclearity Chini clusters, whereas redox fragmentation is observed for larger clusters and in the presence of excess of ligand.[185186187]

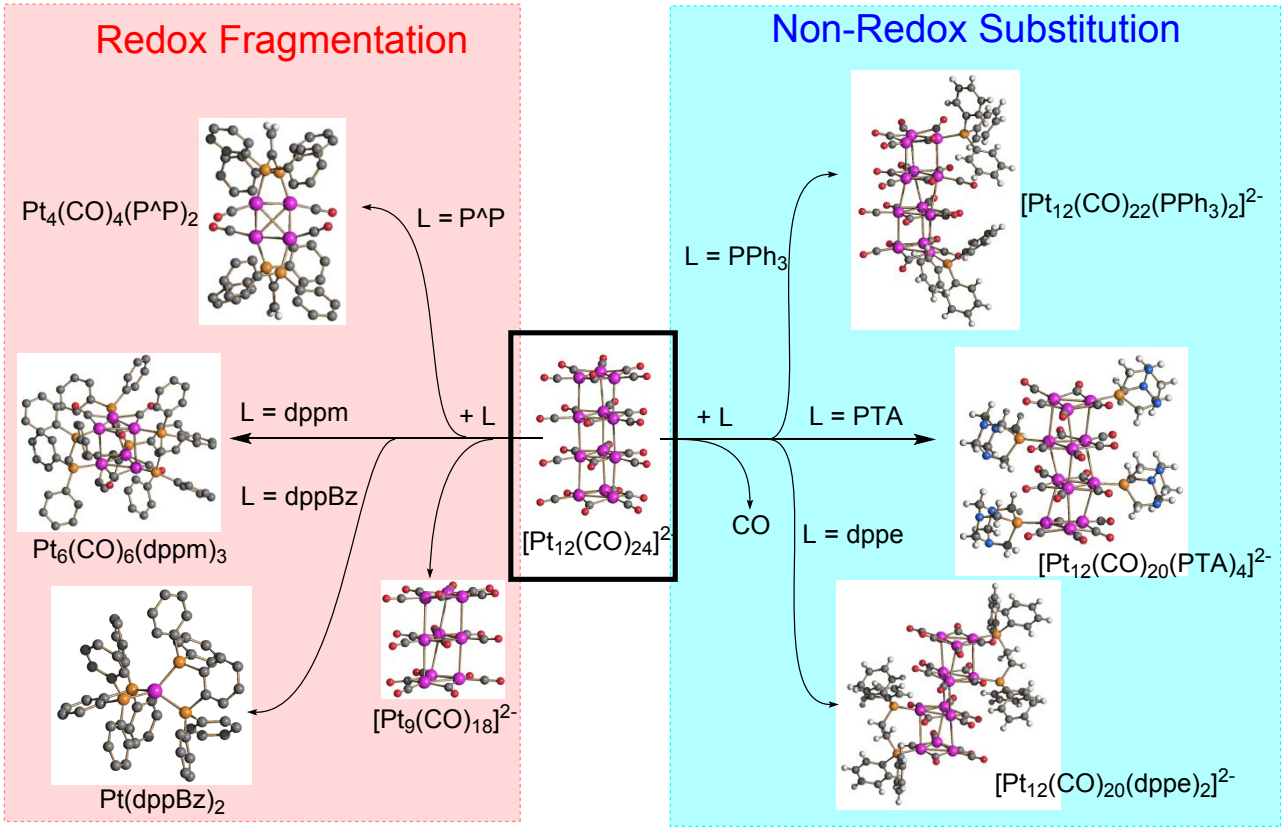

Figure 11. Reactions of Chini clusters with phosphines (L) include redox fragmentation (**B-1**) and non-redox substitution (**A-2**). P^P = $H_2C{=}C(PPh_2)_2$; dppm = $CH_2(PPh_2)_2$; dppBz = 1,2-$C_6H_4(PPh_2)_2$; PTA = $C_6H_{12}N_3P$; dppe = $Ph_2PCH_2CH_2PPh_2$. In the examples reported in this Figure, 1-4 CO ligands of $[Pt_{12}(CO)_{24}]^{2-}$ can be substituted with phosphines leading to heteroleptic Chini-type clusters *via* non-redox substitution.[185-187] Alternatively, redox fragmentation leads to the more reduced homoleptic $[Pt_9(CO)_{18}]^{2-}$ cluster and neutral complexes containing Pt(0).

Formation of Lewis acid–base adducts based on Pt Chini clusters (A-3). The external triangular faces of Chini clusters have been predicted to behave as Lewis bases. Nonetheless, this feature has only been exploited in two cases, both of which produce Lewis acid–base adducts (**A-3**). The reaction of $[Pt_9(CO)_{18}]^{2-}$ with $CdCl_2$ affords 1-D $\{[Pt_9(CO)_{18}(\mu_3\text{-}CdCl_2)_2]^{2-}\}_\infty$ superwires,[188] and the reactions of $[Pt_{3n}(CO)_{6n}]^{2-}$ (n = 2, 3) with Ag(IPr)Cl (IPr = $C_3N_2H_2(C_6H_3{}^iPr_2)_2$) result in the neutral adducts $[Pt_{3n}(CO)_{6n}(AgIPr)_2]$ (see ESI: Figure S6).[189] Otherwise, the reactions of Chini clusters with other Lewis acids proceed *via* oxidation to $[Pt_{3(n+1)}(CO)_{6(n+1)}]^{2-}$ species (**A-1**) or formation of surface-decorated clusters (**B-3**).

Surface-decorated Pt carbonyl clusters (B-3). This reaction path may be considered as an oxidation accompanied by the loss of CO ligands, resulting in the formation of a $Pt_n(CO)_m$ core with MX_x fragments decorating its surface. For instance, $[Pt_{3n}(CO)_{6n}]^{2-}$ (n = 2–5) clusters react with $SnCl_2$ resulting in $[Pt_8(CO)_{10}(SnCl_2)_4]^{2-}$, $[Pt_5(CO)_5\{Cl_2Sn(OR)SnCl_2\}_3]^{3-}$ (R = H, Me, Et, ^{i}Pr),

$[Pt_6(CO)_6(SnCl_2)_2(SnCl_3)_4]^{4-}$, $[Pt_9(CO)_8(SnCl_2)_3(SnCl_3)_2(Cl_2SnOCOSnCl_2)]^{4-}$, and $[Pt_{10}(CO)_{14}\{Cl_2Sn(OH)SnCl_2\}_2]^{2-}$ (Figure 12).[190191192] Moreover, heating $[Pt_{3n}(CO)_{6n}]^{2-}$ (n = 2–10) in the presence of $CdBr_2{\cdot}nH_2O$ affords the larger $[Pt_{13}(CO)_{12}Cd_{10}Br_{14}(DMF)_6]^{2-}$, $[Pt_{19}(CO)_{17}Cd_{10}Br_{14}(DMF)_6]^{2-}$, and $[H_2Pt_{26}(CO)_{20}(CdBr)_{12}]^{8-}$ clusters (Figure 12).[193]

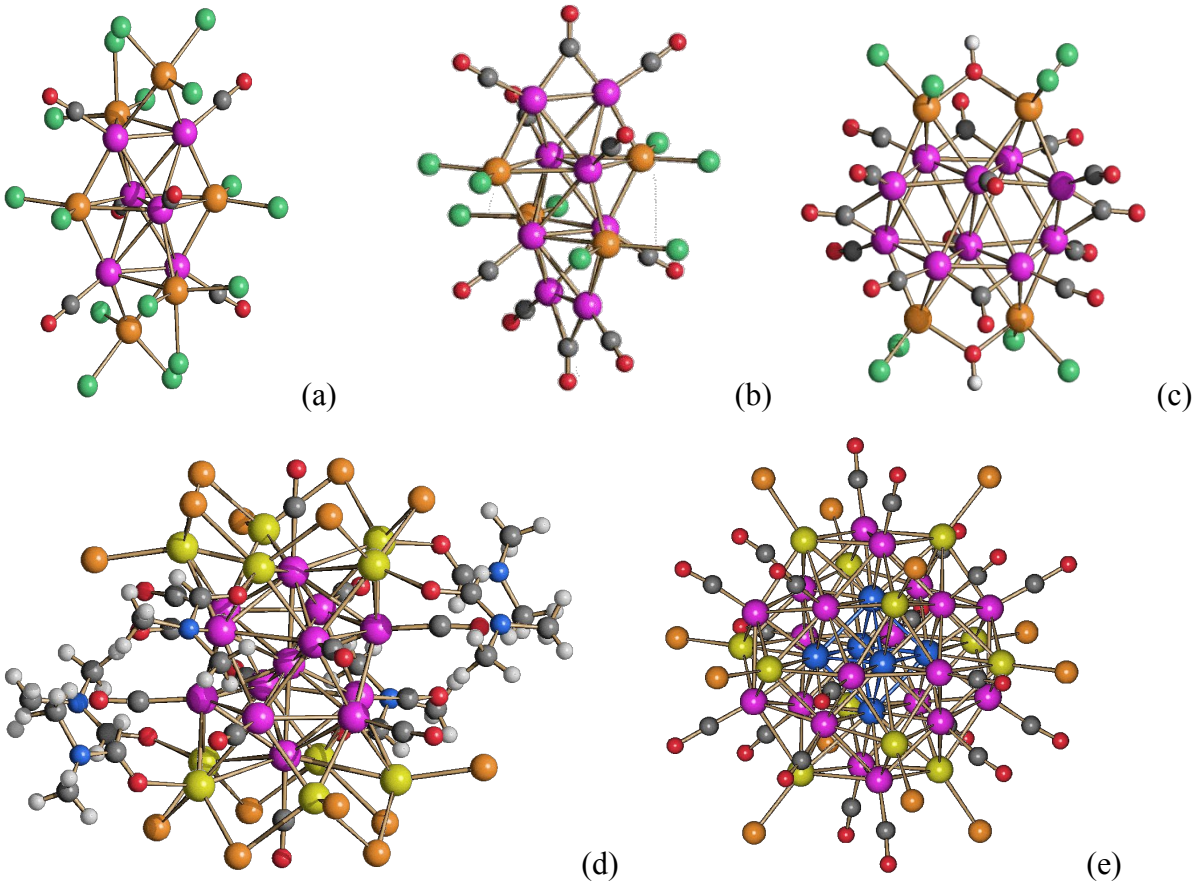

Figure 12. Some examples of surface-decorated Pt carbonyl clusters produced from Chini clusters via reaction pathway **B-3**: (a) $[Pt_6(CO)_6(SnCl_2)_2(SnCl_3)_4]^{4-}$, (b) $[Pt_8(CO)_{10}(SnCl_2)_4]^{2-}$, (c) $[Pt_{10}(CO)_{14}\{Cl_2Sn(OH)SnCl_2\}_2]^{2-}$, (d) $[Pt_{13}(CO)_{12}Cd_{10}Br_{14}(DMF)_6]^{2-}$, (e) $[H_2Pt_{26}(CO)_{20}(CdBr)_{12}]^{8-}$ (purple, Pt; yellow, Cd; orange, (a-c) Sn and (d,e) Br; blue, N; red, O; grey, C; white, H).[190-193]

Thermal reactions of Chini clusters (B-2). Thermal treatment of Chini clusters under controlled conditions causes CO loss and condensation *via* the formation of additional Pt-Pt bonds (**B-2**), eventually leading to Pt–CO globular molecular nanoclusters, often referred to as Pt browns due to their colour in solution.[47194195] The full list of homoleptic homometallic Pt carbonyl clusters (including Pt brown) that are structurally characterised to date is available in the ESI (Table S11); some representative examples are given in Figure 13.

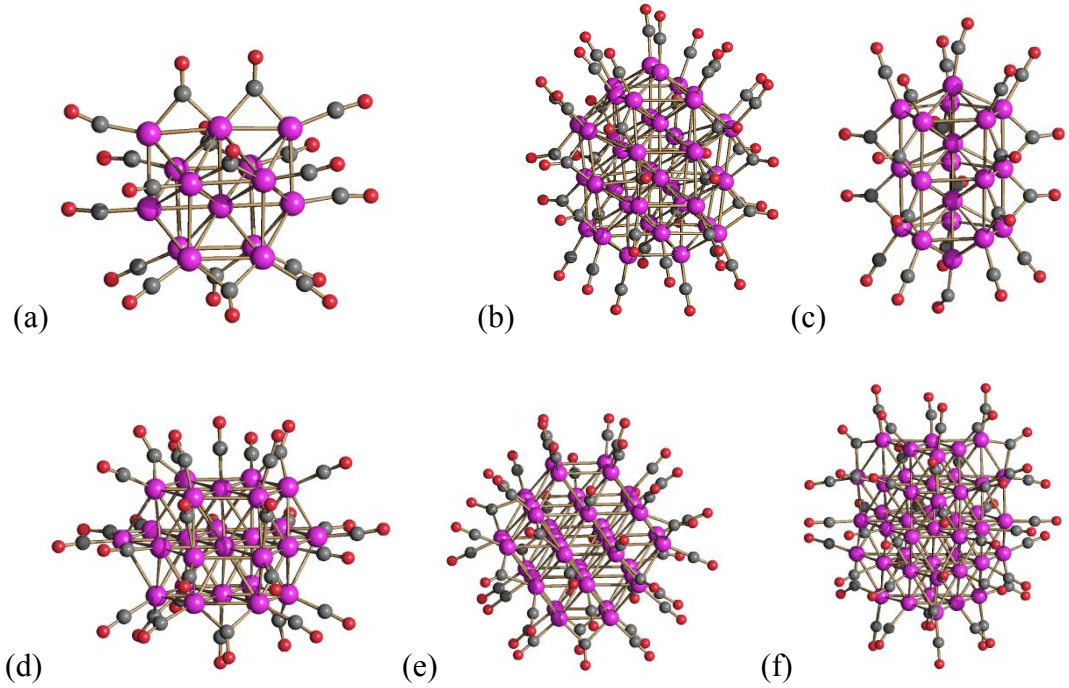

Figure 13. The molecular structures of some platinum browns: (a) $[Pt_{14}(CO)_{18}]^{4-}$ (*bcc*), (b) $[Pt_{40}(CO)_{40}]^{6-}$ (*bcc*), (c) $[Pt_{19}(CO)_{22}]^{4-}$ (*pp*), (d) $[Pt_{26}(CO)_{32}]^{-}$ (*hcp*), (e) $[Pt_{38}(CO)_{44}]^{2-}$ (*ccp*) and (f) $[Pt_{44}(CO)_{45}]^{n-}$ (*ccp/hcp*) (purple, Pt; red, O; grey, C). The structure of the metal core of the cluster is given in parentheses: *bcc*, body-centred cubic; *pp*, pentagonal prismatic; *hcp*, hexagonal close packed; *ccp*, cubic close packed. All these clusters have been obtained from thermal decomposition (**B-2**) of Chini clusters (see ref. 194, 195 and Table S11 in ESI).

Heterometallic clusters (B-4). Heteronuclear Pt–M carbonyl clusters can be prepared by the redox condensation of Chini clusters with metal salts, complexes, or carbonyls (**B-4**). Alternatively, as described in the previous sections, such Pt–M clusters can be obtained from the redox condensation of carbonyl anions of the second metal and Pt salts or complexes. For instance, $[Co_8Pt_4C_2(CO)_{24}]^{2-}$ can be synthesised from $[Co_6C(CO)_{15}]^{2-}$ and $[Pt_6(CO)_{12}]^{2-}$ or more conveniently, from $[Co_6C(CO)_{15}]^{2-}$ and $Pt(Et_2S)_2Cl_2$.[135]

3. Metal Carbonyl Clusters: Catalysis

3.1 General Principles

This Section will discuss catalysis performed by MCCs. We will give an overview of homogeneous catalysts and their proposed mechanisms in Section 3.2 and follow this with a discussion of homogeneous electrocatalysis and electrochemical mechanistic studies in Section 3.3. Most examples of MCCs in catalysis come from Groups 8 – 10. This is most likely because those clusters are the most stable under a variety of reaction conditions. A common mechanistic feature observed

for both the homogeneous catalysis and electrocatalysis promoted by MCCs is the ability of substrates, CO ligands, and hydride ligands or protons to migrate around the metal–metal bonds of the cluster core. In most cases, careful probes for the formation of nanoparticles, using Hg poisoning[196] or measurements of solution dispersivity,[197,198] are required to ensure that nanoparticle side-products are not responsible for observed reactivity.

The geometric and electronic structures of MCCs (Figure 14) fall between those of single-site metal coordination complexes (molecular catalysts) and those of extended solids (heterogeneous catalysts). When discussing heterogeneous materials, we use a band diagram as a model for the energy levels that make up the valence band and conduction band. When we talk about molecular catalysts, we refer to a molecular orbital diagram. However, as molecules become larger as in the case of clusters, their molecular orbitals become closer in energy and approach the band-diagram model. The size and electronic structure of both metal clusters and nanomaterials are found between those of single-site metal coordination complexes and of heterogeneous materials. When MCCs are large enough, it has been demonstrated that their properties—such as diffusion coefficients in solutions and even their size—more closely resemble those of a nanoparticle, quantum dot, or fullerene than that of a molecule. Many of the more convincing links between the structure and reactivity of MCCs with those of nanomaterials have been elucidated from comparisons of their electrochemical properties, *e.g.*, electron-transfer rate constants. Thus, one motivation for studying MCCs in thermally driven catalysis and electrocatalysis is that we can characterise their properties using the tools of molecular chemistry, which include single-crystal X-ray diffraction (SC-XRD), NMR, and IR spectroscopy; these provide atom-level insights into reactivity, which can also inform our understanding of the reactivity and properties of nanomaterials.

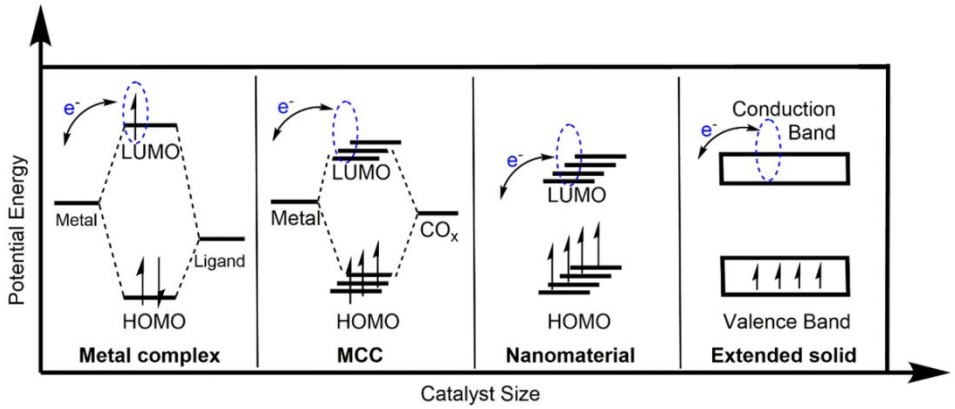

Figure 14. Relative energy spacings in the electronic structures of a single-site metal coordination complex (molecular catalyst), MCC, nanomaterial, and extended solid (heterogeneous material or electrocatalysts). MCC = metal carbonyl cluster. Reproduced with permission from Ref. 238.

Unique to the homogeneous catalysis of MCCs, the MCC in many cases—but not all—serves as a catalyst precursor, and therefore, debates regarding the active catalyst remain in many examples. Fragmentation of the cluster to form a mononuclear complex is one possibility when ligands are added as co-catalyst and when they include protons, phosphine, silane, and MeCN. While this article focuses on carbonyl clusters, clusters where one or two of the carbonyl ligands are replaced by another ligand, such as phosphine or amine, are also discussed. Fragmentation of clusters was well-characterised in some mechanistic proposals for homogeneous catalysis with MCCs,[199] and it is consistent with the fact that most reactions catalysed by MCCs are thermally initiated. In the following discussion of homogeneous catalysis by MCCs, we include clusters of Groups 8, 9, and 10 that are accompanied by various additives used to initiate the catalytic reaction. Many examples of stoichiometric reaction chemistry have been explored on the MCC framework, and a review of that work falls outside the scope of this manuscript.[77,78,200] MCCs have also served as precursors to heterogeneous catalysts, which also falls outside the scope of this review article.

Electrocatalytic reactions using MCCs has seen increased interest since about 2011, and efforts have focused on reduction chemistry—primarily hydride-transfer chemistry—using Fe and Co clusters containing interstitial atoms. These clusters represent some of the most stable known species in the transition series. Consequently, their product profiles and the mechanistic details of their catalysis have been thoroughly characterised, primarily employing the electrochemical technique of cyclic voltammetry (CV). The two-electron reduction of two protons to yield H_2 is the simplest reaction performed by Fe and Co MCCs. This simple reaction has enabled a mechanistic study for understanding hydride formation and hydride-transfer reactivity as mediated by MCCs. The resulting insights have made it possible to tailor hydride transfer to other substrates, such as CO_2 for formate production.

3.2 Homogeneous Catalysis by MCCs

The earliest work on catalysis by MCCs focused on syngas as the substrate. Syngas comprises CO, CO_2, H_2, and H_2O in various ratios, as produced by petroleum refining processes. Due to the abundance of CO in syngas, it serves well as a source of CO during catalytic reactions; the CO can contribute to MCC stability, acting as a substrate for CO insertion reactions and hydroformylation, or it can regenerate the MCC in a catalytic cycle where one of its CO ligands was consumed. CO-

containing headspaces have also been shown to enhance MCC stability in electrocatalytic reactions promoted by MCCs (*vide infra*). Pettit et al. made a comparison of various metal (Fe, Rh, Ru, Os, Ir, and Pt) carbonyl complexes and clusters as catalysts for the hydroformylation reaction and the water-gas shift reaction (Scheme 23). In one of the simpler proposed mechanisms for syngas reactivity, CO is replaced by a hydride to initiate hydride-transfer chemistry. In the foregoing paragraphs, we give more specific details of homogeneous catalysis by MCCs, organizing the reactions by group, *i.e.*, Group 8, 9, and 10.

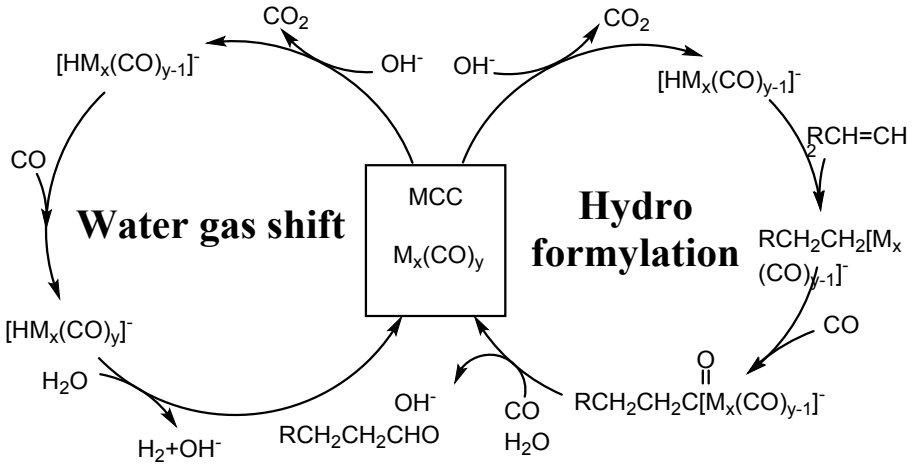

Scheme 23. Mechanisms of CO-driven MCC-mediated catalysis.

Catalysis by MCCs of Group 8 (Fe, Ru, Os). A variety of MCC structure types were explored for catalytic applications in the early development of MCC chemistry, and much of the work focused on Group 8 compounds due to their increased stability relative to MCCs with other transition elements (Chart 1, Table 2).[201,202,203,204,205] Casey and coworkers have shown catalytic performances of the iron cluster $Fe_3(CO)_{12}$ on the isomerization reaction of the alkene in the 1970s; more specifically, $Fe_3(CO)_{12}$ catalysed the isomerization of the ethyl pentene substrates. Deuterium-labeling studies revealed that the olefin isomerization reaction occurs *via* intramolecular hydrogen shift.[206] Geoffroy and coworkers utilised the radical state of the iron cluster, $[Fe_3(CO)_{11}]^{-\bullet}$, to perform the reduction of nitrobenzene to aniline. The Fe radical anion was produced from the disproportionation reaction of the halide anion with $Fe_3(CO)_{12}$. While the reaction is stoichiometric, $PhNO_2$ convert to the azo-azoxybenzene product.[65]

In more recent examples using MCCs as catalysts, additives are often used, and their role in the chemistry varies. Nagashima and coworkers[207] reported hydrosilylation of tertiary amides to amine functional groups with $Fe_3(CO)_{12}$ as the catalyst and with 1,1,3,3-tetramethyl disiloxane (TMDS) or polymethyl-hydro siloxane (PMHS) as the reducing agent. Nearly concurrently, Beller

and coworkers demonstrated the catalytic activity of iron- and ruthenium-based MCCs toward hydrosilylation chemistry.[208,209,210] In a report by Enthaler and coworkers, a combination of $Fe_3(CO)_{12}$ and stoichiometric amounts of silyl reagent results in the activation of a sulfoxide, yielding sulfide product.[211]

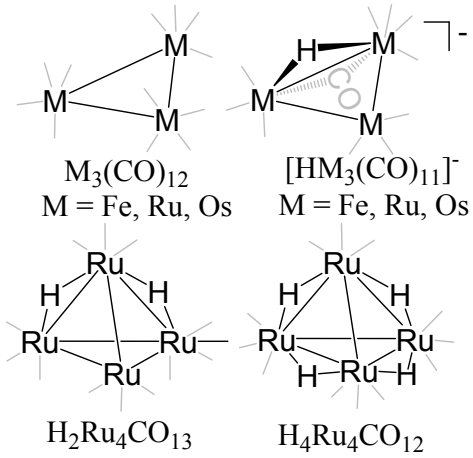

Chart 1. Homogeneous MCC Catalysts from Group 8. Terminal CO ligands have been omitted for clarity.

Table 2. Summary of catalysis by Fe carbonyl clusters.

MCC	Additive, substrate	Reaction	Product (yield [a])	Reference
$Fe_3(CO)_{12}$	3-ethyl-1-pentene	Isomerization of 3-ethyl-1-pentene	3-ethyl-2-pentene (97)	Casey 1973 [206]
$[HFe_3(CO)_{11}]^-$	CO_2, H_2, alcohol	Formate ester formation	Methyl formate (5.8)	Evans 1978 [201]
$[Fe_3(CO)_{11}]^{-\bullet}$		Reduction of $PhNO_2$	Stoichiometric reaction	Geoffroy 1995 [65]
$Fe_3(CO)_{12}$	TMDS, hv, carboxamide substrates	Thermal- or photo-assisted amine reduction	Amine products (21–96, thermal; 73–95, photo)	Nagashima 2009 [207]
$Fe_3(CO)_{12}$	Silane, methyl phenyl sulfoxide	Reduction of methyl phenyl sulfoxide	Methyl phenyl sulfide (99)	Enthaler, 2011 [211]
$Fe_3(CO)_{12}$	Phosphine, ketone substrates	Asymmetric ketone hydrogenation	Alcohol products (66–99)	Gao 2014 [212,213]
$Fe_3(CO)_{12}$	$PhSiH_3$, *N,N*-dimethylbenzamide	Amide to amine	Amine products (99)	Beller 2019 [208]
$[HFe_3(CO)_{11}]^-$	$(EtO)_2MeSiH$, primary amines	Dehydration of amides to nitriles	Nitrile products (52–99)	Beller 2009 [209]
$[HFe_3(CO)_{11}]^-$	P_2N_2 ligand[b], base, iPrOH, *N*-(diphenylphosphinyl)-imines derivatives	Hydrogenation of imine	Amine products (35–95)	Beller 2010 [210]
$[TeFe_3(CO)_9]^{2-}$	Copper catalyst, aryl	Homocoupling	Biphenyl	Shieh

$[SeFe_3(CO)_9]^{2-}$	boronic acid	reaction	products (54–99)	2015 [214]

[a] %yield, [b] *N*,*N*′-bis[*o*-(diphenylphosphino)benzylidene]cyclohexane-1,2-diamine

The transformation of amide functional groups into nitriles has been explored using the hydrogenated iron carbonyl cluster, $[Et_3NH][HFe_3(CO)_{11}]$. Using various silyl additives such as Ph_2SiH_2, $(EtO)_3SiH$, and $(EtO)_2MeSiH$, the amide group is transformed into a nitrile group within 3 h with above 90% yield. The same transformation was achieved in 97% yield using $Fe_2(CO)_9$ although the reaction time was longer (20 h);[213] 83% yield was obtained using $Fe_3(CO)_{12}$ with a 2-h reaction time. In general, the amide substrates employed in this work were primary carboxylic amides, which include alkyl, aromatic, heteroaromatic, and aliphatic amides. Reactions with activated phenyl carboxylic amides achieved completion in 4 h, whereas unactivated substrates took 30 h.

Asymmetric transfer hydrogenation (ATH) converts a ketone or amine into an alcohol or imine, respectively. Various iron-containing catalysts, including mononuclear catalysts and the iron carbonyl clusters $[Et_3NH][HFe_3(CO)_{11}]$ and $Fe_3(CO)_{12}$, show high yields and selectivity in ATH; however, there are significant differences in reaction outcomes depending on the cluster employed, as described below. The hydrogenation of imines was successfully achieved and described by Beller and coworkers using systems with chiral ligands also acting as co-catalysts.[210] The scope of the imine substrates included a ketamine, aromatic imine, and hetero-aromatic imine, while the co-substrates for ATH included iPrOH and chiral P_2N_2 ligands, which are tetradentate ligating at two P and two N centres. Since these observations were made under conditions employing chiral ligand additives, it was initially inferred that the chiral ligand likely promoted the formation of a chiral mono-iron coordination complex, which serves as the active catalyst when used with $Fe_3(CO)_{12}$. However, a recent report by Gao and coworkers has shown that varying the iron carbonyl clusters for ATH does change the reaction outcomes. As an example, $Fe_3(CO)_{12}$ fully converts acetophenone to (*S*)-1-phenylethanol with 97% ee (enantiomeric excess), while $[Et_3NH][HFe_3(CO)_{11}]$ does not activate the substrate. One possible explanation for these different catalytic performances might arise from the varying coordination of the chiral ligands directly onto different Fe_3 cluster cores or perhaps to a fragment of the initial cluster.[213] In another report by Gao and coworkers, the catalytic reaction was monitored by IR spectroscopy, verifying that $[Et_3NH][HFe_3(CO)_{11}]$ stayed intact during the reaction. This may serve as evidence for $[Et_3NH][HFe_3(CO)_{11}]$ playing the role of active catalyst, or it may be that a very small fraction of $[Et_3NH][HFe_3(CO)_{11}]$ is converted to the active catalyst although the event is not detected by IR.[212] Taken together, these studies do not yet define a clear role for $Fe_3(CO)_{12}$ or $[Et_3NH][HFe_3(CO)_{11}]$ in the catalytic ATH conversion of amines to imines. Shieh and coworkers have recently reported

homocoupling reactions where a copper catalyst is coordinated with $[Se/TeFe_3(CO)_9]^{2-}$.[214] Comparing to previous examples, the iron cluster supports the catalysis as a ligand substitute. For both the Se- and Te-containing species, the reaction yield is above 80% for the homocoupling reaction.

The study of catalytic reactions using ruthenium carbonyl clusters started with interest in reactions utilising syngas. Examples reported by Ford and coworkers[215] and Shore and coworkers[216] provided evidence for hydrogen evolution from water and CO gas using various Ru carbonyl clusters (Table 3). Darensbourg and coworkers screened a series of Ru carbonyl clusters and demonstrated C–C bond formation between CO_2 and methanol to afford methyl formate: in the presence of CO and H_2, reactions promoted by $[HRu_3(CO)_{11}]^-$ had a turnover number (TON) of around 4, while those promoted by $[HRCO_2Ru_3(CO)_{10}]^-$ had a TON of 5.7. In this work, it was suggested that the trinuclear Ru cluster is a precursor for the active catalyst, which is formed *via* a fragmentation step to a tetranuclear species. Evidence suggested that a mononuclear Ru species is not the active catalyst. The formation of methyl formate from H_2 and CO_2 is regarded as a water-gas shift reaction that can be used to produce CO. For experiments performed in the absence of H_2 and CO_2, use of CO led to TONs of up to 106. Thus, it is plausible that the formation of methyl formate arises from the insertion of carbon monoxide into methanol.[204]

Table 3. Summary of catalysis by Ru carbonyl clusters.

MCC	Additive, substrate	Reaction	Product [a]	Reference
$Ru_3(CO)_{12}$ $H_4Ru_4(CO)_{12}$	Amine, CO, H_2O, propylene	Hydroformylation Water-gas shift	Aldehydes, alcohol, H_2	Pettit 1977 [202]
$Ru_3(CO)_{12}$ $H_2Ru_4(CO)_{13}$ $H_4Ru_4(CO)_{12}$ $Ru_6C(CO)_{17}$	KOH, H_2O, CO, ethoxyethanol	H_2 evolution	H_2 (Catalyst: 1.5–4.4 [b])	Ford 1978 [215]
$Ru_3(CO)_{12}$	CO_2, H_2, MeOH	Alkyl formate production	Methyl formate (106 [b])	Darensbourg 1983 [204]
$[HRu_3(CO)_{11}]^-$	H_2O, CO	H_2 evolution	H_2 (100)	Shore 1985 [216]
$Ru_3(CO)_{12}$	$(EtO)_3SiH$	Hydrosilylation of olefin, acetophenone	1-octene (70 [c]) acetophenone (220 [c])	Hilal 1993 [217]
$Ru_3(CO)_{12}$	CO, imines	Carbonylative [4+1] cycloaddition	Various lactams product (51–96)	Murai 1999 [218]
$Ru_3(CO)_{12}$	Acenaphthylene, silane	Hydrosilylation of ketone	Silyl ether product (76–99) Alcohol products (72–98)	Nagashima 2000 [219]
$Ru_3(CO)_{12}$	Silane (Et_3SiH), ester	Hydrosilylation of esters to alkyl silyl acetals	Alkyl silyl acetal product (36–94)	Fuchikami 2001 [220]
$Ru_3(CO)_{12}$	CO/C_2H_4	CO insertion	Stoichiometric reaction	Imhof 2005 [221]
$Ru_3(CO)_{12}$	Acenaphthylene, silane, amides	Amide to amine	Amines (34–98)	Nagashima 2009 [207]

[a] % yield, [b] activity (Moles of H_2 per mole of complex per day), [c] turnover number

The second area of interest for Ru carbonyl clusters involves reactions with silane additives. Some of the most successful implementations of this approach include the transformation of esters to alkyl silyl acetals, which are hydrolysed to aldehyde. The proposed mechanism of this reaction involves oxidative addition of silane to a metal in $Ru_3(CO)_{12}$, and mechanistic work suggests that an intermediate silane-ligated Ru cluster is important for Si–H bond activation, which leads to subsequent reaction with olefin.[222] Also using $Ru_3(CO)_{12}$, hydrosilylation of acetophenone has faster turnover than olefin formation for 1-octene using $(EtO)_3SiH$ (TON: 220 and 60, respectively).[217] By replacing the silane with $(EtO)_3Si(CH_2)_3NH_2$, the Ru catalyst becomes more active for the hydrogenation of olefin substrates.[223] Murai and coworkers demonstrated the carbonylative [4+1] cycloaddition of alkyl and aryl α,β-unsaturated imines with CO using $Ru_3(CO)_{12}$. Although they were not able to definitively identify the active species, a mechanism has been proposed (Scheme 24).[216]

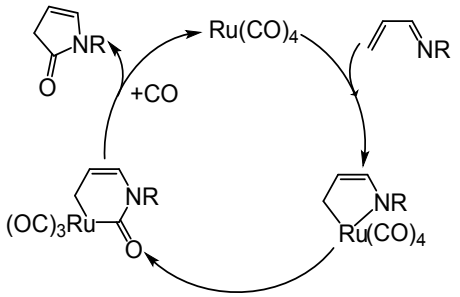

Scheme 24. Proposed mechanism for carbonylative [4+1] cycloaddition using $Ru_3(CO)_{12}$.

Fuchikami and coworkers have reported reduction of an ester to aldehyde *via* a proposed silyl acetal intermediate that is hydrolyzed to afford the aldehyde.[218] The role of the silane addition is different in this example because it reacts with the substrate directly, rather than activating $Ru_3(CO)_{12}$ by direct reaction with a Ru centre.[220] Nagashima has found that coordination between $Ru_3(CO)_{12}$ and acenaphthylene enables catalytic hydrosilylation of ketone and reduction of an amide to an amine group in a presence of silane additive.[219]

Compared with Fe and Ru carbonyl clusters, there are far fewer reports of catalysis using Os carbonyl clusters (Table 4).[205,224] Muetterties and coworkers investigated the reactivity of $Os_3(CO)_{12}$ and $Ir_4(CO)_{12}$ towards hydrocarbons, which led to the discovery that $Os_3(CO)_{12}$ can effect hydrogen–deuterium exchange. Years later, Adams proposed multiple molecular structures of intermediates to better understand the catalytic reaction of $Os_3(CO)_{12}$ with isocyanides and related functional groups, using a series of stoichiometric reactions where activation of the nitrile CN bond was observed.[225]

Table 4. Summary of catalysis by Os carbonyl clusters.

MCC	Additive, substrate	Reaction	Product [a]	Reference
$Os_3(CO)_{12}$	CO, H_2	CO reduction to methane	Alkane (not mentioned)	Muetterties 1976 [205]
$Os_3(CO)_{12}$		H–D exchange	Deuterated benzene (not mentioned)	Muetterties 1976 [224]
$Os_3(CO)_{12}$ $H_4Os_4(CO)_{12}$	Amine, CO, propylene	Hydroformylation Water-gas shift	C4 aldehyde (13 [b]) H_2 (270 [b])	Pettit 1977 [202]
$Os_3(CO)_{12}$	CO, H_2O, trimethylamine, nitrobenzene	Reduction of nitrobenzene	Aniline (100)	Pettit 1978 [203]
$Os_3(CO)_{12}$		Reactivity with isocyanides and nitrile group	Stoichiometric reaction	Adams 1982 [225]

[a] % yield, [b] activity (Moles of H_2 per mole of complex per day)

Catalysis by MCCs of Group 9 (Co, Rh, Ir). Pittman and coworkers studied phosphine-substituted Co carbonyl clusters, $Co_3(CO)_9CPh$ and $Co_4(CO)_{10}(PPh)_2$.[226] These clusters promote the hydroformylation reaction of pentene, which was the first example of homogeneous catalysis with Co clusters (Chart 2, Table 5). Both catalysts completely converted 1- or 2-pentene to three different types of formylated products within 24 h. A discussion of possible fragmentation pathways to afford the active catalyst was presented, but no definitive active catalyst could be identified in this work.

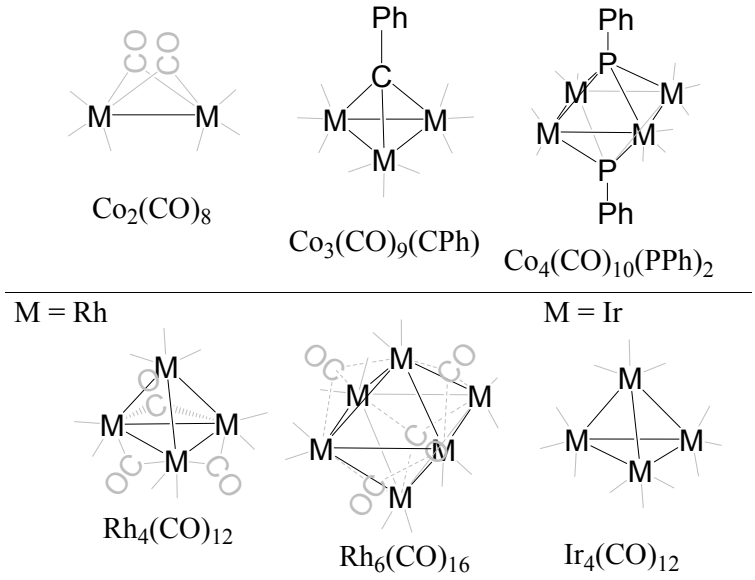

Chart 2. Homogeneous MCC Catalysts from Group 9. Terminal CO ligands have been omitted for clarity.

Table 5. Summary of catalysis by Co carbonyl clusters.

MCC	Additive, substrate	Reaction	Product (yield [a])	Reference
$Co_3(CO)_9CPh$ $Co_4(CO)_{10}(PPh)_2$	CO, H_2, 1-pentene, 2- pentene	Hydroformylation	Aldehydes (99.7–100)	Pittman 1977 [226]
$Co_2(CO)_8$	Me_3SiH, benzonitrile	Hydrosilylation of benzonitrile	Disilyl amines (11–91)	Murai 1989 [227]
$Co_2(CO)_8$ $Co_2Rh_2(CO)_{12}$ $Co_3Rh(CO)_{12}$	$HSiMe_2Ph$, isoprene	Hydrosilylation of isoprene	Silane product (40–100)	Ojima 1991 [228]
$Co_3(CO)_9CCl$	Amine–phosphine ligand, KOH, propiophenone	Asymmetric ketone hydrogenation	Alcohol product (75)	Gao 2014 [212]

[a] % yield

Homoleptic Co carbonyl clusters have also be used as homogeneous catalysts. Using a silane additive, Murai and coworkers performed a hydrosilylation reaction of benzonitrile.[227] Ojima

and coworkers explored cobalt–rhodium carbonyl clusters for hydrosilylation of isoprene, cyclohexanone, and cyclohexanone derivatives.[228] Although $Rh_4(CO)_{12}$ and Co–Rh carbonyl clusters show higher conversion rates, $Co_2(CO)_8$ can also perform the catalytic hydrosilylation of isoprene.[229] In recent work by Gao and coworkers, an additional example of asymmetric hydrogenation of ketone was presented; that was described above in the discussion of Fe carbonyl cluster catalysts.[212]

In the catalysis of rhodium carbonyl clusters, $Rh_4(CO)_{12}$ and $Rh_6(CO)_{16}$ are popular (Chart 2, Table 6). Pettit and coworkers used $Rh_6(CO)_{16}$ clusters and CO gas to perform hydroformylation [202] and nitrobenzene reduction.[203] Yamazaki and coworkers demonstrated synthetic pathways with $Rh_4(CO)_{12}$ and $Rh_6(CO)_{16}$, where they focused on C–H activation of an arene followed by the addition of substrates, including benzene, *N*-methylpyrrole, thiophene, and furan. They also introduced hydrocarbonylation of acetylene and olefins in the presence of CO to afford furanone derivatives.[230] Using silane additives, Ojima and coworkers activated $Rh_4(CO)_{12}$, to convert unsaturated hydrocarbon substrates—such as 1-hexyne, isoprene, and cyclohexenone—into highly regioselective and stereoselective silylated product.[228]

Table 6. Summary of catalysis by Rh carbonyl clusters.

MCC	Additive, substrate	Reaction	Product [a]	Reference
$Rh_6(CO)_{16}$	Amine, CO, H_2O, propylene	Hydroformylation	C4 aldehyde (300 [b]) H_2 (1700 [b])	Pettit 1977 [202]
$Rh_6(CO)_{16}$	CO, H_2O, nitrobenzene	Reduction of nitrobenzene	Aniline (100)	Pettit 1978 [203]
$Rh_4(CO)_{12}$ $Rh_6(CO)_{16}$	CO, ethanol diphenylacetylene	Carbonylation of dipheylactylene	Furanone (59–67)	Yamazaki 1983 [230]
$Rh_4(CO)_{12}$ $Co_2Rh_2(CO)_{12}$ $Co_3Rh(CO)_{12}$	$HSiMe_2Ph$, isoprene	Hydrosilylation of isoprene	Silane product (40–100)	Ojima 1991 [228]
$Rh_4(CO)_{12}$ $Co_2Rh_2(CO)_{12}$	$HSiMe_2R$, 1-hexyne	Silylformylation of 1-hexyne	Silane product (63–95)	Ojima 1991 [229]
$Rh_6(CO)_{16}$	CO, H_2O, amine	Reduction of nitro groups	Amines (74–95)	Kaneda 1994 [231]

[a] % yield, [b] turnover number

In our earlier discussion of Os-carbonyl-mediated catalysis, we mentioned the application of $Ir_4(CO)_{12}$ in the hydrogen–deuterium exchange reactions of hydrocarbons (Table 7).[202,205,224] In addition, applications of supported Ir carbonyl clusters have been reported by Gates and coworkers. For example, MgO-supported $[HIr_4(CO)_{11}]^-$ enables propane hydrogenolysis to yield methane and ethane when the reaction is carried out at 200 °C and 1 atm of H_2. Using $Ir_6(CO)_{16}$ encapsulated by

NaY zeolite, catalytic CO hydrogenation yields a C_2–C_4 carbon product. Gates and coworkers have also investigated catalytic performances of various other MCCs supported by MgO or zeolite.[232,233] The encapsulated Ir cluster was prepared by the adsorption of $[Ir(CO)_2(acac)]$ into the cage of NaY zeolite and thermal treatment. IR and extended X-ray absorption fine structure (EXAFS) techniques were adopted to verify the structure of the final catalyst because $Ir_6(CO)_{16}$ has a distinct signature at 1730 cm^{-1}. Using a feedstock of CO and H_2, zeolite-encaged Ir cluster yields various hydrogenated products, which were detected by gas chromatography (GC). The continuous reaction time of up to 8 days reveals high stability for $Ir_6(CO)_{16}$ within the zeolite cage. In the reactions starting with MgO-supported $Ir_6(CO)_{16}$, IR spectroscopy detected the structure of $Ir_4(CO)_{12}$, and it is believed that this cluster forms on the MgO surface. In each of these reports, it is believed that the supporting substrate enhances the stability of the MCCs.

Table 7. Summary of catalysis by Ir carbonyl clusters.

MCC	Additive, substrate	Catalysis	Product [a]	Reference
$Ir_4(CO)_{12}$	CO, H_2	CO reduction to methane	Alkane (not mentioned)	Muetterties 1976 [205]
$Ir_4(CO)_{12}$		H–D exchange	Deuterated benzene (not mentioned)	Muetterties 1976 [224]
$Ir_4(CO)_{12}$	Amine, CO, H_2O	Hydroformylation Water-gas shift	C4 aldehyde (250 [b]) H_2 (300 [b])	Pettit 1977 [202]
$Ir_4(CO)_{12}$	KOH, H_2O, CO	Water-gas shift (H_2 evolution)	H_2 (5.3 [c])	Ford 1978 [215]
$Ir_6(CO)_{16}$	Zeolite encapsulated	Hydrogenation of CO Decarbonylation	Propane (not mentioned)	Gates 1993 [232]
$HIr_4(CO)_{11}^-$	Supported on MgO surface	Propane hydrogenolysis	H_2 (not mentioned)	Gates 1993 [233]

[a] % yield, [b] turnover number, [c] activity

Catalysis by MCCs of Group 10 (Pd and Pt). Likely due to their limited stability, the carbonyl clusters of Ni are not represented in the literature for catalysis. As for Pt carbonyl clusters (Chart 3, Table 8), the first catalytic reaction was reported by Pettit and coworkers in 1977, and that report described hydroformylation and water-gas shift reactions.[202] The next known catalytic reaction was reported in the late 1990s. It is challenging to stabilise the MCCs of Group 10 under ambient conditions, especially under catalytic conditions; for this reason, all the examples involve catalysts supported on mesoporous silica or zeolite. Various evidence for the identity of the active catalyst in each of these cases is obtained from *in-situ* IR spectroscopy and EXAFS. In an alternative mechanism for catalysis in Group 10, Bhaduri and coworkers have employed redox

pathways where a reduced form of $Pt_9(CO)_{18}$ is used as a reductant to reduce nicotinamide adenine dinucleotide (NAD^+). In this reaction, the platinum cluster takes the role of electron transporter from the sacrificial electron-donor molecules, which are hydroxide ions (OH^-) recovered from ferric cyanide. In an alternative redox reaction, methylene blue, Safranine O, and methyl viologen were used as sacrificial electron acceptors, which were then reduced by the Pt cluster.[235]

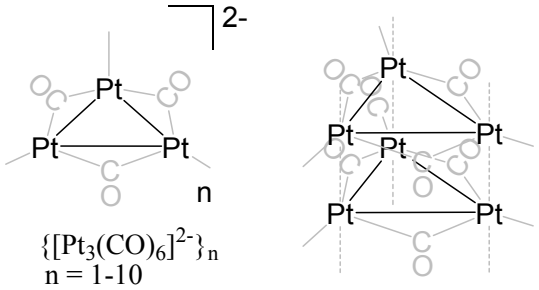

Chart 3. Homogeneous MCC Catalysts from Group 10. Terminal CO ligands have been omitted for clarity.

Table 8. Summary of catalysis by Pt carbonyl clusters.

MCC	Additive, substrate	Reaction	Product [a]	Reference
$[Pt_3(CO)_6]_5^-$	Amine, CO, H_2O, propylene	Hydroformylation Water-gas shift	C4 aldehyde (0.5 [b]) H_2 (700 [b])	Pettit 1977 [202]
$[Pt_3(CO)_6]_5^{2-}$	Zeolite-encapsulation, ethene, 1,3-butadiene	Hydrogenation of ethene, 1,3-butadiene	Alkyl product (<0.1 [c])	Ichikawa 1998 [234]
$[Pt_9(CO)_{18}]^{2-}$	Sacrificial electron-donor/-acceptor	Electron-transfer mediator	Not mentioned	Bhaduri 2000 [235]
$[Pt_{12}(CO)_{24}]^{2-}$	Mesoporous silica, MCM-41 support, methyl pyruvate, acetophenone	Hydrogenation of methyl pyruvate or acetophenone	Not verified (10□–40)	Bhaduri 2005 [236]
$Pd_{13}(CO)_x$	Zeolite Y, CO, H_2	CO hydrogenation	Hydrocarbon (1.8–2.3)	Sachtler 1992 [237]

[a] % yield, [b] turnover number, [c] turnover frequency (s^{-1})

3.3 Electrocatalysis by MCCs

In an electrocatalytic reaction, an external applied potential is used to initiate the reaction of an electron-transfer event with the redox-active catalyst, which may be homogeneous or heterogeneous, depending on whether it can be in solution with the substrate. Homogeneous electrocatalysts are metal-based coordination complexes or clusters, which will exist in solution with the other reagents; heterogeneous electrocatalysts may be extended solids or other insoluble

materials that are commonly deposited on the electrode. We will focus only on homogeneous electrocatalysis, where the most basic requirements for the electrocatalyst include stability in a polar solvent system and a redox potential that is accessible without oxidising or reducing the solvent. These criteria alone limit the number of MCCs that might be suitable electrocatalysts, but those MCCs that do meet these criteria have many advantages over single-metal-ion homogeneous electrocatalysts, as described below. Considered from another angle, there are advantages for using electrocatalysis instead of thermal activation as a means to control the reactivity of MCCs. One big advantage of electrochemical catalysis is that energy can be added to the system at RT and with very mild conditions; as a result, the stability of MCCs can be maintained throughout the catalytic reaction and for many turnovers. In most instances, it is also possible to include a partial atmosphere of CO (if it is needed), imparting even greater stability to the MCC; the mole-fraction of CO in the headspace can be tuned at will.

The advantages of using suitable MCCs as homogeneous electrocatalysts, rather than using single-site metal–ligand catalysts or heterogeneous electrocatalysts, have come to light in recent years. Suitable MCCs and their reduced forms are readily protonated, allowing the formation of hydride intermediates at low applied potential; in one instance, catalysis was promoted at a rate of 10^9 s^{-1} with an applied potential as low as –0.86 V vs. SCE (versus the saturated calomel electrode).[238] Multiple sites for protonation on the clusters lead to very fast rates of proton transfer (PT), facilitating diffusion-limited PT chemistry, which can be applied to hydride-transfer reactions. It is thought that the fast rates arise from a statistical effect of having so many possible protonation sites and hydride migration sites. Another advantage of MCCs as electrocatalysts involve the easy substitution reactions at the cluster surface, where CO ligands can be replaced by phosphines containing an array of functional groups. Those substitutions can be used to tune the secondary coordination sphere of a catalyst or to tune the reactivity properties by changing the electronic properties of the cluster core. Substitutions of metal ions within the MCC core or of an interstitial atom within the cluster core can also change the electronic and reactivity properties. A more detailed discussion of synthetic modifications to MCCs and their effect on catalysis is included below.

Electrocatalytic reactions where MCCs have been employed are all reduction reactions; low-valent clusters can stabilise additional electron density with their delocalised electronic structures and multiple π-acceptor CO ligands. Electrons added to the molecular-orbital manifold of MCCs often strengthen the bonding between the metal and carbon atoms of the M–CO moiety. In a typical electrocatalytic reduction reaction—including those mediated by MCCs, catalysis is initiated by electron transfer (ET) to the MCC as potential is applied; this electrochemical elementary step is

abbreviated as "E" in the standard nomenclature of the field. After the initiation step, if the intermediate has enough energy to react with the substrate, it will react chemically, and that chemical reaction is abbreviated as "C" (Scheme 25). Alternatively, the initial E event can be followed by a second E event before any chemical steps proceed. Thus, a series of elementary steps in an electrocatalytic reaction will be described as a series of E or C steps. The most common reaction mechanisms are ECEC and EECC. The latter is considered equivalent to the ECCE mechanism; while they differ in their starting points in the catalytic cycle, they have identical electrochemical responses when CV is used to monitor their reactions.[239]

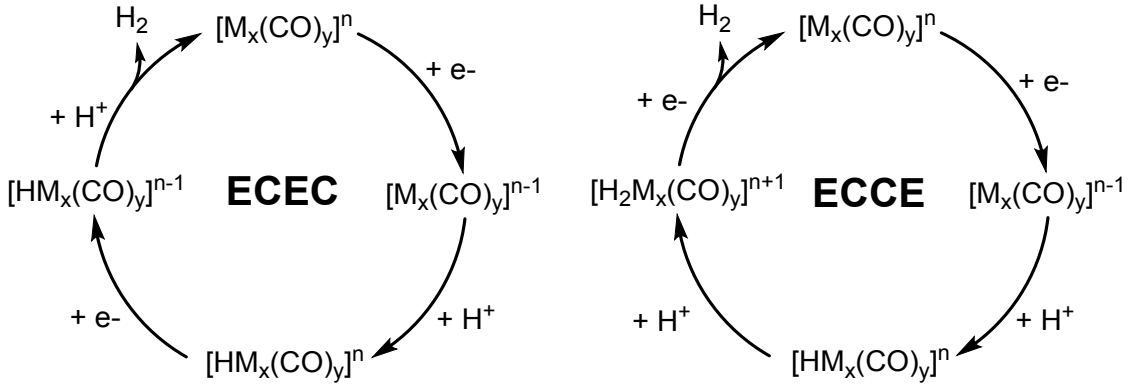

Scheme 25. Examples of electrocatalytic hydrogen-evolution pathways by MCCs.

In any electrochemical reaction, the energy difference between the electron-donor and -acceptor is an important parameter, and this difference is expressed by their redox potentials with respect to a reference electrode. The IUPAC (International Union of Pure and Applied Chemistry) recommends use of the ferrocene/ferrocenium couple as a reference in organic solvent;[240] other commonly employed references include the SCE and the natural hydrogen electrode (NHE). Provided that the experimental conditions are clearly described, conversion between the different referencing schemes is generally trivial, allowing catalysts to be compared.[241] In this review, we use SCE referencing throughout. Metrics used to assess the utility of electrocatalytic reactions include the Faradaic efficiency (FE) and the turnover frequency (TOF). The FE is the percentage of the charge that is converted into product in a preparative-scale experiment. The TOF is equivalent to k_{obs}, the observed rate constant, and it is reported in units of s^{-1}; as long as factors such as the applied potential or the overpotential (η) are accounted for, it can be used to compare the rates of reactions.

Two electrochemical reactions have been studied using MCCs as the electrocatalyst:

(a) the two-electron reduction of two protons to H_2, and

(b) the two-electron reduction of protons and CO_2 into formate.

These transformations share the same two initial steps in the catalyst cycle, where ET is followed by PT to generate a reduced hydride intermediate (Scheme 26). Reaction of the hydride with protons generates H_2, and reaction of the hydride with CO_2 generates formate in the third step. The fourth step is another ET, so the overall mechanism in either case is ECCE. Even from this simple overview, it is clear that controlling the reaction chemistry of the intermediate hydride can lead to many applications for hydride-transfer chemistry using MCCs and potentially many substrates.

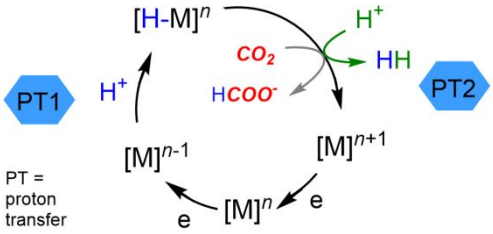

Scheme 26. Schematic showing the two possible reaction pathways for a metal hydride – which can (a) react with protons to form H_2 or (b) react with CO_2 to form formate.

Electrocatalysis by MCCs of Group 8 (Fe). It was first reported in 2011 that $[Fe_4N(CO)_{12}]^-$ can cause the evolution of H_2 from protons or the evolution of formate from CO_2, depending on the reaction conditions [244] (Chart 4, Table 9). The first attempt for the electrocatalytic hydrogen-evolution reaction (HER) and CO_2-reduction reaction (CO_2RR) was carried out under 1 atm of N_2 or CO_2, respectively, using organic acids as the proton source. In the proposed mechanism, $[Fe_4N(CO)_{12}]^-$ is first reduced at −1.23 V (vs. SCE), and then PT affords $[HFe_4N(CO)_{12}]^-$, which can go on to react with either H^+ or CO_2 following an ECCE mechanism. There are very few molecular electrocatalysts that produce formate selectively,[242] and $[Fe_4N(CO)_{12}]^-$ performs this reaction at modest rates and a low applied potential. In subsequent work reported in 2013, replacement of organic acids with water buffered at pH 7 afforded formate with 97% FE at –1.23 V of applied potential.[246] The solvent-dependence reflects a lowering of the activation barrier for hydride transfer due to solvation effects,[243] which will not be discussed in detail here. In addition to the ability of $[Fe_4N(CO)_{12}]^-$ to perform catalytic small-molecule reduction chemistry effectively, these reports have demonstrated that it is stable in water and that it is stable under an applied potential over reaction times of up to 24 h, although longer reactions were not investigated.

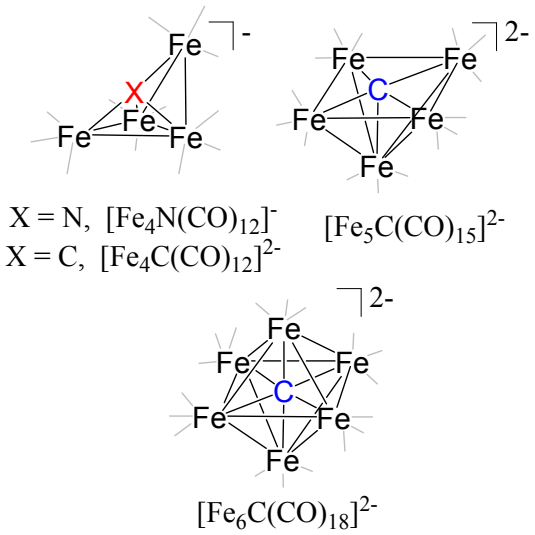

Chart 4. Drawings of homometallic Fe carbonyl clusters used as electrocatalysts. CO ligands have been omitted for clarity.

Table 9. Homometallic clusters of Fe and Co and their reactivity for HER and CO_2RR.

MCC	Additive	Potential (V vs. SCE)	η (mV)	Reaction	FE (%) [a]	k_{obs} (s^{-1})	Reference
$[Fe_4N(CO)_{12}]^-$	Benzoic acid	−1.23	280	HER	Quant.	1.0	Berben 2011 [244]
$[Fe_4N(CO)_{12}]^-$	Benzoic acid, CO_2	−1.25	300	formate	nr	nr	Berben 2011
$[Fe_4N(CO)_{12}]^-$	MeCN/H_2O (95:5)	−1.25	440	HER	Quant.	nr	Berben 2015 [245]
$[Fe_4N(CO)_{12}]^-$	MeCN/H_2O (95:5), CO_2	−1.2	440	formate	95	10	Berben 2015
$[Fe_4N(CO)_{12}]^-$	$KHCO_3$/KCO_3 pH 6.5	−1.2		formate	95		Berben 2015
$[Fe_4C(CO)_{12}]^{2-}$ $[Fe_5C(CO)_{15}]^{2-}$ $[Fe_6C(CO)_{18}]^{2-}$	Acetate buffer pH 5	−1.25	714	HER	83 72 64	368 nr nr	Berben 2013 [246]
$[Co_{13}C_2(CO)_{24}]^{4-}$	Anilinium tetrafluoroborate	−0.86	760	HER	78	10^8	Berben 2020

[a] quant. = Quantitative yield, and nr = not reported

In 2013, the electrochemical reduction of protons to H_2 was reported using a series of carbide-centred clusters, $[Fe_4C(CO)_{12}]^{2-}$, $[Fe_5C(CO)_{14}]^{2-}$, and $[Fe_6C(CO)_{17}]^{2-}$ (Chart 4).[246] Each of these clusters quickly catalyses H_2 evolution from water, and $[Fe_4C(CO)_{12}]^{2-}$ was observed to be particularly stable. Over time, $[Fe_5C(CO)_{14}]^{2-}$ and $[Fe_6C(CO)_{17}]^{2-}$ converted into $[Fe_4C(CO)_{12}]^{2-}$, which illustrates a feature of MCC chemistry. One particular structure for a combination of atoms is often a thermodynamic sink; whereas other analogous clusters are isolable and quite stable, they are

not a long-term thermodynamic product. This study also enabled a comparison of the nitride-centred $[Fe_4X(CO)_{12}]^-$ and carbide-centred $[Fe_4C(CO)_{12}]^{2-}$ clusters. Protonation of $[Fe_4C(CO)_{12}]^{2-}$ is concerted with ET and is therefore pH-dependent; meanwhile, $[Fe_4N(CO)_{12}]^-$ undergoes sequential ET and PT reactions. The difference in reactivity is attributed to the varied charges on the clusters. For both $[Fe_4N(CO)_{12}]^-$ and $[Fe_4C(CO)_{12}]^{2-}$, the protonation site is located along the bridge of two iron atoms, and the interstitial atom does not get protonated. Another effect of the increased charge on $[Fe_4C(CO)_{12}]^{2-}$ is that PT rates are significantly higher, so H_2 evolution is faster.

Electrocatalysis by MCCs of Group 9 (Co). A cobalt carbonyl cluster has recently been reported as an electrocatalyst for fast H_2 evolution; this cluster has 13 Co atoms, $[Co_{13}C_2(CO)_{24}]^{4-}$.[238] Many of its properties, including its ET and PT rate constants and diffusion coefficient, are very similar to those of nanoparticles or quantum dots, illustrating the ability of MCCs to behave like nanoparticles and like heterogeneous electrocatalysts. The larger size of $[Co_{13}C_2(CO)_{24}]^{4-}$, its multiple Co–Co bonding motifs, and its many electron-withdrawing CO ligands are just some of the structural features that result in its observed physical properties. When studying the reduction of protons to hydrogen or the transfer of hydride to CO_2 to form formate, the ability to detect and monitor reaction intermediates is very important: Co carbonyl clusters offer a unique system for probing protonation chemistry using IR spectra, as was first described by Zacchini and coworkers.[48] When plotting the CO absorption band energy, ν_{CO}, obtained from IR data against the x/z values (where x is the number of Co atoms and z is the cluster charge), a linear relationship is observed for a wide range of clusters—specifically, from 6 to 20 Co atoms. The charge on the clusters, z, can be varied either by redox events or by protonation of a Co cluster. For a given cluster charge, protonation events can be monitored accurately using IR spectroscopy, providing a powerful tool for determining the reaction mechanisms of hydride formation and hydride transfer to substrates.

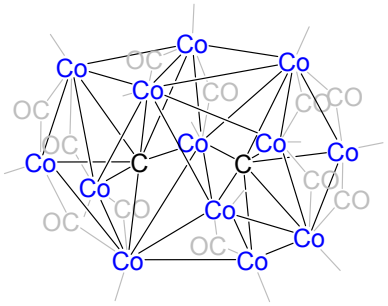

Chart 5. Co carbonyl cluster, $[Co_{13}C_2(CO)_{24}]^{3-}$ used as an electrocatalyst. Terminal CO ligands have been omitted for clarity.

Using $[Co_{13}C_2(CO)_{24}]^{3-}$, the reduction of protons to hydrogen was studied using an applied potential as the source of electrons (Scheme 26). PT rates were measured at 10^9 $M^{-1}s^{-1}$ for the chemical reaction where electrochemically generated $[Co_{13}C_2(CO)_{24}]^{5-}$ reacts with one proton. The fast PT chemistry supported the HER with an observed rate of 2.3×10^9 $M^{-1}s^{-1}$. These PT rates appear to be limited only by diffusion or the mass transport of protons in solution. The ability of $[Co_{13}C_2(CO)_{24}]^{5-}$ to mediate fast rates of PT was attributed to a statistical effect, which arises from the multiple Co–Co bonds available for protonation; in heterogeneous catalysis, a similar effect arises from the multiple PT sites on the electrode surface. Statistical effects that enhance the rates of PT have also been observed in older work for single-site metal catalysts, *i.e.*, mononuclear coordination complexes that can act as homogeneous catalysts. In these cases, PT-rate enhancement is derived from the addition of Lewis bases to the supporting ligands; the multiple Lewis-base sites deliver protons to the catalytic active site on the metal centre.[247] Studies were performed to elucidate the mechanism for HER using $[Co_{13}C_2(CO)_{24}]^{4-}$. When either H_2O or D_2O was added to the CV experiment of $[Co_{13}C_2(CO)_{24}]^{3-}$, an electrochemical kinetic-isotope effect was observed. The shift in peak potential for the reduction of $[Co_{13}C_2(CO)_{24}]^{4-}$ to $[Co_{13}C_2(CO)_{24}]^{5-}$ when D_2O was used is indicative of a PT event that occurs in a concerted process with an ET event. Based on the currently available information, the observed Co–H bond making/breaking process could be either a protonation of the cluster that is concerted with ET or an intracluster proton migration that is concerted with ET; the electrochemical data cannot distinguish between these two possibilities. Both scenarios reflect the ability of large MCCs to interact effectively with protons and to facilitate proton mobility on the surface of the cluster.

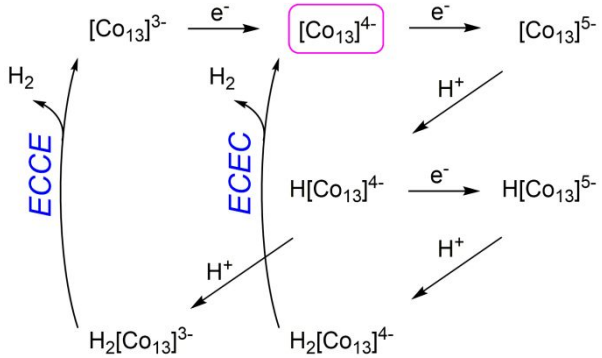

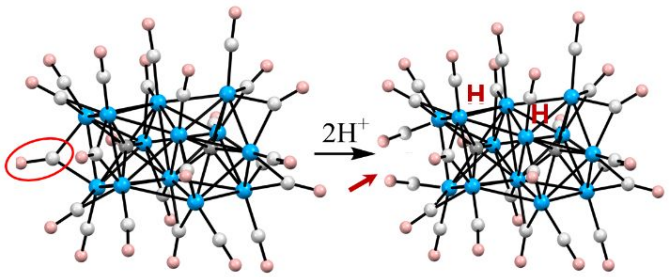

Scheme 26. Top: Proposed mechanism for proton reduction to H_2 in $[Co_{13}C_2(CO)_{24}]^{3-}$; the C and CO ligands are not shown to simplify the mechanistic scheme. Reproduced with permission from ref. 238. Bottom: Protonation of $[Co_{13}C_2(CO)_{24}]^{3-}$ and migration of CO around the cluster core (blue, Co; grey, C; red, O).

Atom substitution in the MCC Core: Effects on electrocatalysis. Starting in 2017, Hogarth and coworkers published several studies on tri-iron carbonyl clusters (Chart 6, Table 10), which were functionalised by replacing CO ligands or by adding capping ligands to the three-iron cluster.[248,249] Ruthenium clusters were also studied in some cases. For each cluster, two one-electron reduction events were observed, and H_2 evolution was observed at the most negative potential. Hydride equivalents generated at the first reduction event were not hydridic enough to transfer hydride to protons, which would have liberated H_2. Thiol-capped $[Fe_3(CO)_9(\mu\text{-SR})(\mu\text{-H})]$ (where R = ^{i}Pr, ^{t}Bu) was investigated using organic acids, CF_3CO_2H or $HBF_4{\cdot}Et_2O$; H_2 evolution was observed at –0.84 (R = ^{i}Pr) or –1.0 (R = ^{t}Bu) V vs. SCE, respectively, with the mechanism assigned as ECEC.[249] Although they are less electron-rich, telluride-capped tri-iron clusters also reduce protons to H_2, but with at slower HER rates. Following phosphine substitution, Te-substituted clusters showed enhanced reactivity. Their proposed mechanism shows that it is possible to evolve hydrogen with a pathway that starts from the cluster's first or second reduced state.[237]

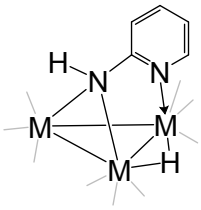

$[Fe_3(CO)_9(\mu_3\text{-pyNPh})(\mu\text{-H})]$
(M = Fe, Ru)

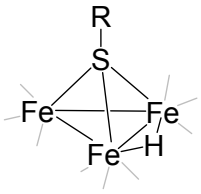

$[Fe_3(CO)_9(\mu_3\text{-SR})(\mu\text{-H})]$
(R = ^{i}Pr, ^{t}Bu)

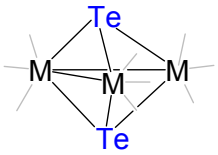

$M_3(CO)_9(\mu_3\text{-Te})_2$
(M = Fe, Ru)

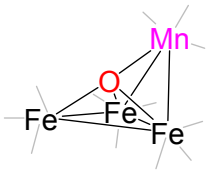

$[Fe_3MnO(CO)_{12}]^-$

Chart 6. Heterometallic and capped Fe carbonyl clusters used as electrocatalysts. CO ligands have been omitted for clarity.

Table 10. Heterometallic and ligand-capped Fe and Ru clusters and their reactivity for HER.

MCC	Additive	Potential V vs. SCE	η (mV)	Reaction	FE (%)	k_{obs} (s^{-1})	Reference
$[Fe_3(CO)_9(\mu^3\text{-pyNH})(\mu\text{-H})]$	TsOH $HBF_4{\cdot}Et_2O$	−1.21	nr	HER	nr	nr	Hogarth 2017 [248]
$[Ru_3(CO)_9(\mu^3\text{-pyNH})(\mu\text{-H})]$	TsOH $HBF_4{\cdot}Et_2O$	−1.61	nr		nr	nr	Hogarth 2017
$[Fe_3(CO)_9(\mu\text{-SR})(\mu\text{-H})]$ R=iPr, tBu	CF_3CO_2H $HBF_4{\cdot}Et_2O$	−0.84 −1.0	nr	HER	nr	nr	Hogarth 2018 [249]
$[Fe(CO)_3]_3(\mu^3\text{-Te})_2$	CF_3CO_2H	nr	nr	HER	nr	nr	Hogarth 2020 [250]
$[Fe_3MnO(CO)_{12}]^-$	MeCN/H_2O (95:5)	−1.3	540	HER	50	nr	Berben 2020 [252]
$[Fe_3MnO(CO)_{12}]^-$	$CClH_2CO_2H$	−1.3	650		nr		Berben 2020

Ts = *p*-toluenesulfonyl; nr = not reported.

Work published in 2020 discussed the effect of Mn substitution in the $[Fe_4N(CO)_{12}]^-$ cluster core where the interstitial nitride atom was also replaced by an oxo atom; the subsequent $[Fe_3MnO(CO)_{12}]^-$ cluster is therefore isoelectronic to $[Fe_4N(CO)_{12}]^-$.[251,252] The two clusters, $[Fe_3MnO(CO)_{12}]^-$ and $[Fe_4N(CO)_{12}]^-$ also have similar reduction potentials of –1.3 and –1.2 V vs. SCE, respectively. Sequential reduction and protonation of $[Fe_3MnO(CO)_{12}]^-$ produced a hydride intermediate, $[H\text{-}Fe_3MnO(CO)_{12}]^-$, which is equivalent to the hydride intermediate observed for $[Fe_4N(CO)_{12}]^-$ (Scheme 26); however, it is at this point that the chemistries of $[Fe_3MnO(CO)_{12}]^-$ and $[Fe_4N(CO)_{12}]^-$ begin to differ. Hydride transfer from $[H\text{-}Fe_3MnO(CO)_{12}]^-$ to CO_2 was not

observed due to its reduced ability for hydride donation, which was determined independently using IR spectroelectrochemical studies.

Ligand substitution on the MCC Core: Effects on electrocatalysis. Ligand substitution on $[Fe_4N(CO)_{12}]^-$, where CO ligands are replaced by phosphine ligands, has been used to study the mechanism of H_2 and formate evolution. Ligand substitution has also been used to modify the reactivity of $[Fe_4N(CO)_{12}]^-$. For these studies, the control compound is $[Fe_4N(CO)_{11}(PPh_3)]^-$, which contains a phosphine ligand but does not contain a reactive functional group.[253] The phosphine-substituted compounds (including the control $[Fe_4N(CO)_{11}(PPh_3)]^-$) have a reduction potential of around –1.45 V, while that of $[Fe_4N(CO)_{12}]^-$ is –1.2 V. Phosphine ligands with hydroxyl, methoxyphenyl, pyridyl, and *N*,*N*-dimethylaniline groups have been used to afford $[Fe_4N(CO)_{11}(PPh_2(CH_2)_2OH)]^-$, $[Fe_4N(CO)_{11}(PPh_2(MeOPh))]^-$, $[Fe_4N(CO)_{11}(PPh_2py)]^-$, and $[Fe_4N(CO)_{11}(PPh_2(N,N\text{-}Me_2NPh))]^-$, respectively (Chart 6). For each of these examples (Table 11), MeCN/H_2O (95:5) was used for the mechanistic or other electrochemical studies because it provided adequate solubility; MeCN has a large electrochemical window, and the small amount of H_2O serves as a proton source and as a source of stabilization for the transition state during hydride transfer. Using multiple approaches, electrochemical mechanistic studies have shown that water stabilises a charge-separated transition state and enhances the rates of hydride transfer from $[H\text{-}Fe_4N(CO)_{12}]^-$ to CO_2 by five orders of magnitude relative to the rates of hydride transfer observed in the absence of water. Other research groups working with single-site hydride-transfer catalysts have also shown using density functional theory (DFT) studies that water may play a role in the stabilization of the hydride-transfer transition state *via* a hydrogen-bonding network.[242]

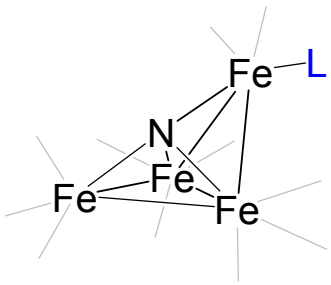

L = CO
PPh_3
$PPh_2(CH_2)_2OH$
$PPh_2(2\text{-}Me_2NPh)$
$PPh_2(2\text{-}MeOPh)$
PPh_2py

Chart 7. Schematic of the phosphine-substituted derivatives of $[Fe_4N(CO)_{12}]^-$. CO ligands have been omitted for clarity.

Table 11. Summary of electrocatalysis by phosphine-substituted derivatives of $[Fe_4N(CO)_{12}]^-$. All reactions were performed in MeCN/H_2O (95:5) and under 1 atm of CO_2 with an applied potential of –1.47 V vs. SCE.

MCC	Reaction	Reference
$[Fe_4N(CO)_{11}(PPh_3)]^-$	CO_2RR	Berben 2016 [253]
$[Fe_4N(CO)_{11}(PPh_2(CH_2)_2OH)]^-$	HER	Berben 2016
$[Fe_4N(CO)_{11}(PPh_2(N,N\text{-}Me_2NPh))]^-$	CO_2RR	Berben 2020 [254]
$[Fe_4N(CO)_{11}(PPh_2(MeOPh))]^-$	HER	Berben 2020
$[Fe_4N(CO)_{11}(PPh_2py)]^-$	HER	Berben 2020

When a CO ligand of $[Fe_4N(CO)_{12}]^-$ is replaced with a phosphine containing a protic functional group, *e.g.*, $[Fe_4N(CO)_{11}(PPh_2(CH_2)_2OH)]^-$, the protic functional group behaves like a proton relay during eletrocatalysis; the catalysts will only make H_2, even under conditions that are otherwise ideal for the reaction of $[Fe_4N(CO)_{12}]^-$ with CO_2.[253] Work using the parent cluster, $[Fe_4N(CO)_{12}]^-$, revealed the possibility of a hydride intermediate in the catalytic cycle, and evidence for the hydride intermediate was first seen in the cyclic voltammetry data, where the hydride was shown to be oxidised. Studies on $[Fe_4N(CO)_{11}(PPh_2(CH_2)_2OH)]^-$, where H_2 evolution is switched on by the proton relay, provide additional evidence for the hydride intermediate.

In other investigations, the functionalised phosphine ligands added to $[Fe_4N(CO)_{12}]^-$ were used to add steric bulk to the secondary coordination sphere. These large functional groups can also facilitate proton relays, spanning the range of pK_a = –0.5 up to 11.2. With bulky functional groups however, clusters of protonated water cannot approach the active site to produce H_2, resulting in the exclusive production of formate, as is observed in $[Fe_4N(CO)_{11}(PPh_2(N,N\text{-}Me_2NPh))]^-$.[254] The hypothesis that steric effects are important was proposed based on measurements of PT rate constants performed under N_2 and CO_2 atmospheres, where the source of protons differ; under N_2, water–MeCN clusters dominate as the proton source, while under CO_2, carbonic acid clusters dominate. The carbonic acid clusters are smaller than the water–MeCN clusters, making PT faster under CO_2 than under N_2. The selectivity of catalysts such as $[Fe_4N(CO)_{11}(PPh_2(N,N\text{-}Me_2NPh))]^-$ for formate formation over H_2 evolution is consistent with the small carbonic acid clusters having easy access to the active site when there are large functional groups present in the secondary coordination sphere.

4. Summary and Outlook

Outlook for the Synthesis of MCCs: From a synthetic point of view, the preparation and molecular-level characterization of larger and larger MCCs remains an ongoing challenge. The total structural determination of the Au_{102}-thiolate nanocluster in 2007[255] by SC-XRD generated a renewed interest in molecular nanoclusters. It also clearly pointed out that SC-XRD is currently the only analytical technique available for structural determination with an atomic precision for the metal core, metal atom surface, and ligand shell of molecular nanoclusters and chemical species in general. Despite the recent advancements in SC-XRD instrumentation, this poses a serious analytical limitation to molecular nanochemistry. Consequently, structure–property–reactivity relationships should be established to provide additional insights for nanoclusters and ultra-small metal nanoparticles; to achieve this, more and more molecular clusters of increasing size should be synthesised, structurally characterised, and chemically and physically analysed. Establishing these relationships may help resolve the persistent open question of how many metal centres are needed to produce metallic properties.[5] The answer depends not only on the dimensions, but also on the nature of the metal (or metals, for alloys), the type of ligands present, and the property of interest.

Another target of synthetic chemists is to better understand which MCCs will be stable enough to use in materials and catalysis applications. Work in electrocatalysis has shown that structures like $[Fe_4N(CO)_{12}]^-$ are incredibly stable—in water, in air, and over multiple days under catalytic conditions. But how do we predict this without having to screen many MCCs? The stability of $[Fe_4N(CO)_{12}]^-$ was determined empirically, just as experimental work determined that many clusters in the iron-carbide series, such as $[Fe_5C(CO)_{14}]^-$ and $[Fe_6C(CO)_{17}]^-$, are not stable, decomposing into $[Fe_4C(CO)_{12}]^-$ and Fe metal over time. Rules for electron-counting may aide with predictions, but their validation must be achieved experimentally. Additionally, a role for theoretical methods in predicting the stability of MCCs is envisioned.

As the applications of MCCs expand further into catalysis, electrocatalysis, and materials chemistry, advancements in their synthetic chemistry would be beneficial, especially with respect to the control of ligand substitution on the cluster cores. Replacement of the CO ligands with other ligands causes many changes in the electronic structure, solubility, and reactivity properties of the MCC. Almost all ligands available for substitution are less efficient π-acceptors than CO, and thus, the cluster core becomes more electron-rich as more ligand substitutions are made; the remaining C–O bonds are weakened, and the remaining M–C(O) bonds are strengthened. This latter effect makes it difficult to substitute multiple CO ligands. Small-cone-angle phosphines and isonitriles have been substituted on $[Fe_4N(CO)_{12}]^-$ up to four times, and greater control and tailoring of these syntheses are needed.[256,257] With ligand substitution enabling changes to MCC properties, it can

also be used to modify the overall charge of a cluster or its solubility, making a cluster more suitable for catalytic applications. Another challenge facing the chemistry of ligand-substituted MCCs is how to better predict which cluster–ligand combinations will afford stable ensembles.

***Outlook for Tuning the Material Properties of MCCs*:** Another area needing further development is the synthesis and characterization of heterometallic and alloy molecular nanoclusters. Mixing different metals with atomic control may lead to nanomaterials with new physical or chemical properties. Alloying and metal-doping of molecular nanoclusters is gaining more and more interest,[258,259] and heterometallic MCCs may contribute to our understanding of the synergetic effects induced by alloying with atomic precision.[87] This might also be of some significance in interpreting the metal migration, chemiadsorption, and catalytic behaviour of alloy nanoparticles.

The electronic properties of molecular nanoclusters can be experimentally investigated using spectroscopic and electrochemical techniques as well as magnetic measurements. For additional insights, they can also be compared to theoretical models. As the size of the cluster increases, an incipient metallisation of its metal core should be observed.[6] Indeed, CV measurements indicate a decrease of the energy gap (ΔE) between consecutive redox couples in multivalent MCCs as their size increases. At a certain size, ΔE should be comparable to the thermal energy at RT, leading to auto-disproportionation and equilibria among isostructural MCCs with different charges. This new electronic status should also influence the magnetic properties of larger MCCs and nanoclusters in general. Paramagnetism of even-electron MCCs has been debated for a long time, but recently it has been clearly demonstrated that they can have unpaired electrons in both the ground and excited electronic configurations.[135] Magnetic measurements of molecular nanoclusters require ultra-pure samples in order to rule out the presence of paramagnetic impurities, but they can add significant information to our knowledge of nanomaterials. In addition, by understanding and learning to tune the electronic and magnetic properties of MCCs, it will be possible to produce suitable candidates for molecular nanocapacitors, superparamagnetic quantum dots, and nanomagnets.

Outlook for Catalysis with MCCs: From a structural point of view, a regular and simple structure–size relationship has not been established in the case of MCCs and molecular nanoclusters. This is likely due to the fact that at these length scales, M–ligand and M–M interactions contribute similarly to the overall energetic properties. Thus, we can expect that introducing defects in the metal cages should lead to rearrangements, as shown in the case of some Pt MCCs. Indeed, there is evidence that the metal cages of some MCCs are fluxional, and generally speaking, they are soft and deformable. A deeper knowledge of the dynamic behaviour of the metal cage and ligand shell of molecular clusters is required, and this might have some relevance also to

heterogeneous catalysis with ultra-dispersed metals. The size, structure, and composition of molecular nanoclusters strongly affect their catalytic behaviour.

There are still significant opportunities for studying MCCs of different sizes and compositions in the activation of small molecules, in homogeneous catalysis, as precursors of heterogeneous nanostructured catalysts, and in homogeneous electrocatalysis. An overview of homogeneous catalysis and homogeneous electrocatalysis by MCCs has been given in this review, and other recent reviews have touched on related aspects of catalysis with MCCs.[23, 260, 261] General ideas that can be drawn from these examples include the knowledge that thermal activation of catalytic cycles often results in MCC decomposition and that many of the most effective thermal catalytic reactions are those that occur under a MCC-stabilising CO atmosphere. Moving forward, it is essential that we develop better predictive methods for knowing which MCCs will be stable to various reaction conditions.

Electrocatalysis has recently provided a method where energy, in the form of the applied potential, can be added to the system without raising the temperature. This has enabled RT catalytic reactions, including reactions proceeding *via* a hydride intermediate. As an example, the reduction of CO_2 into formate can proceed in water for over 24 h when $[Fe_4N(CO)_{12}]^-$ is electrolyzed at –1.2 V vs. SCE.[245] Future work in electrocatalysis with MCCs should take advantage of the tunable surface of MCCs, where CO ligands can be replaced with phosphine ligands. Inclusion of functionalised phosphine ligands has the potential to modulate reaction rates by orders of magnitude and to modulate product selectivity when the correct functional groups are included in the secondary coordination sphere and installed in appropriate locations. Another frontier in electrocatalysis using MCCs is the study of larger and larger clusters. Recent work has shown that larger MCCs, containing 13 cobalt atoms, enhance the rates of proton transfer by many orders of magnitude compared to the four-iron cluster, $[Fe_4N(CO)_{12}]^-$, until they resemble those observed for heterogeneous electrocatalysts. Proton- and hydride-migration chemistry on these tridecanuclear cobalt clusters also resembles the behaviour of hydrogen atoms on a surface where hydrogen atoms are not localised at one place.[238] The combination of these nearly diffusion-limited reaction rates with the ability to use molecular chemistry techniques to characterise structure, reactivity, and reaction kinetics and mechanism in precise detail is a powerful driving force for the future development of electrocatalytic reactions promoted by MCCs.

5. Conclusions

The ongoing, new insights into the electronic properties, structural dynamics, and catalytic mechanisms of MCCs show no sign of abating. Nowadays, we possess a solid and broad knowledge

of the synthesis of MCCs, which can be exploited for future developments and applications as outlined in the Summary and Outlook. The relevance of electrocatalysis to fundamental chemistry and industrial applications is growing; and electrochemical techniques have provided a much-needed RT approach, enabling MCCs to be stable throughout chemical and catalytic transformations. Molecular nanoclusters, in general, and MCCs, in particular, can add new perspectives to electrocatalysis. Being at the cusp of the nanodomain, they can contribute to our knowledge of nanochemistry and solid-state materials.

6. Acknowledgement

L.A.B.'s work on MCCs has been supported by the Department of Energy, Office of Science, Basic Energy Sciences with award number DE-SC0016395. S.Z. thanks the University of Bologna for financial support.

References

[1] E. L. Muetterties, T. N. Rhodin, E. BAND, C.F. Brucker, and W. R. Pretzer, *Chem. Rev.* 1979, **79**, 91-137.
[2] G. Schmid (Ed.), Clusters and Colloids, Wiley-VCH, New York, 1994.
[3] P. Braunstein, L. A. Oro and P. R. Raithby (Eds.), Metal Clusters in Chemistry, Wiley-VCH, New York, 1999.
[4] G. Schmid and D. Fenske, *Phil. Trans. R. Soc. A*, 2010, **368**, 1207-1210.
[5] S. Zacchini, *Eur. J. Inorg. Chem.*, 2011, 4125-4145.
[6] C. Femoni, F. Kaswalder, M. C. Iapalucci, G. Longoni and S. Zacchini, *Coord. Chem. Rev.*, 2006, **250**, 1580-1604
[7] B. F. G. Johnson and J. S. McIndoe, *Coord. Chem. Rev*., 2000, **200-202**, 901-932.
[8] I. Ciabatti, C. Femoni, M. C. Iapalucci, G. Longoni and S. Zacchini, *J. Clust. Sci.*, 2014, **25**, 115-146.
[9] I. Ciabatti, C. Femoni, M. C. Iapalucci, S. Ruggieri and S. Zacchini, *Coord. Chem. Rev.*, 2018, **355**, 27-38.
[10] B. Berti, C. Femoni, M. C. Iapalucci, S. Ruggieri and S. Zacchini, *Eur. J. Inorg. Chem.*, 2018, 3285-3296.
[11] C. Femoni, M. C. Iapalucci, S. Ruggieri and S. Zacchini, *Acc. Chem. Res.*, 2018, **51**, 2748-2755.
[12] K. H. Whitmire, *Coord. Chem. Rev*., 2018, **376**, 114-195.
[13] E. G. Mednikov and L. F. Dahl, *Phil. Trans. R. Soc. A*, 2010, **368**, 1301-1322.
[14] J. A. Cabeza and P. García-Álvarez, *Chem. Soc. Rev*., 2011, **40**, 5389-5405.
[15] W. Hieber, F. Leutert, *Die Naturwissenschaften*. 19, **1931**, 360–361.
[16] G. Hogarth, S. E. Kabir and E. Nordlander, *Dalton Trans.*, 2010, **39**, 6153-5174.
[17] R. Jin, C. Zeng, M. Zhou and Y. Chen, *Chem. Rev.,* 2016, **116**, 10346-10413.
[18] I. Chakraborty and T. Pradeep, *Chem. Rev.,* 2017, **117**, 8208-8271.
[19] X. Kang, Y. Li, M.Zhu and R. Jin, *Chem. Soc. Rev.,* 2020, **49**, 6443-6514.
[20] X. Du and R. Jin, *Dalton Trans.,* 2020, **49**, 10701-10707.
[21] (a) Q. Yao, T. Chen, X. Yuan and J. Xie, *Acc. Chem. Res.,* 2018, **51**, 1338-1348; (b) S. Takano, S. Hasegawa, M. Suyama and T. Tsukuda, *Acc. Chem. Res.,* 2018, **51**, 3074-3083.
[22] (a) Z. Lei, X. -K. Wan, S. -F. Yuan, Z. -J. Guan and Q.- M. Wang, *Acc. Chem. Res.,* 2018, **51**, 2465-2474; (b) K. Konishi, M. Iwasaki and Y. Shichibu, *Acc. Chem. Res.,* 2018, **51**, 3125-3133.
[23] P. Buchwalter, J. Rosé and P. Braunstein, *Chem. Rev.*, 2015, **115**, 28-126.
[24] R. D. Adams and F. A. Cotton (Eds.), Catalysis by Di- and Polynuclear Metal Cluster Complexes, Wiley-VCH, New York, 1998
[25] R. D. Adams and B. Captain, *J. Organomet. Chem.*, 2004, **689**, 4521-4529.
[26] B. C. Gates, *Chem. Rev.,* **1995**, *95*, 511-522.

[27] J. M. Thomas, B. F. G. Johnson, R. Raja, G. Sankar and P. A. Midgley, *Acc. Chem. Res*., **2003**, *36*, 20-30
[28] (a) T. Imoaka, H. Kitazawa, W.-J. Chun, S. Omura, K. Albrecht and K. Yamamoto, *J. Am. Chem. Soc.*, 2013, **135**, 13089-13095; (b) T. Imaoka, H. Kitazawa, W.-J. Chun and K. Yamamoto, *Angew. Chem. Int. Ed.*, 2015, **54**, 9810-9815.
[29] K. Kratzl, T. Kratky, S. Günther, O. Tomanec, R. Zbořil, J. Michalička, J. M. Macak, M. Cokoja and R. A. Fischer, *J. Am. Chem. Soc.,* 2019, **35**, 13962-13969.
[30] P. R. Raithby, *Platinum Metals Rev.*, 1998, **42**, 146-157.
[31] S. Martinengo, G. Giordano and P. Chini, *Inorg. Synth.*, 1980, **20**, 209-212.
[32] L. Malatesta, G. Caglio and M. Angoletta, *Inorg. Synth.*, 1972, **13**, 95-99.
[33] L. Garlaschelli and P. Chini, *Gazz. Chim. Ital.*, 1982, **112**, 285-288.
[34] (a) G. Longoni and P. Chini, *J. Am. Chem. Soc.*, 1976, **98**, 7225-7231; (b) J. C. Calabrese, L. F. Dahl, P. Chini, G. Longoni and S. Martinengo, *J. Am. Chem. Soc.*, 1974, **96**, 2614-2616.
[35] M. Fauré, C. Saccavini and G. Lavigne, *Chem. Commun.*, 2003, 1578-1579.
[36] M. I. Bruce, C. M. Jensen and N. L. Jones, *Inorg. Synth.*, 1990, **28**, 216-218.
[37] (a) M. Ichikawa, *Platinum Met. Rev.*, 2000, **44**, 3-14; (b) A. Fukuoka, N. Higashimoto, Y. Sakamoto, M. Sasaki, N. Sugimoto, S. Inagaki, Y. Fukushima and M. Ichikawa, *Catal. Today*, 2001, **66**, 23-31.
[38] (a) C. Femoni, M. C. Iapalucci, G. Longoni, C. Tiozzo, S. Zacchini, B. T. Heaton and J. A. Iggo, *Dalton Trans.*, 2007, 3914-3923; (b) C. Femoni, M. C. Iapalucci, G. Longoni, C. Tiozzo, S. Zacchini, B. T. Heaton, J. A. Iggo, P. Zanello, S. Fedi, M. V. Garland and C. Li, *Dalton Trans.* 2009, 2217-2223.
[39] I. Ciabatti, C. Femoni, M. C. Iapalucci, G. Longoni and S. Zacchini, *Organometallics*, 2012, **31**, 4593-4600.
[40] A. Fumagalli, S. Martinengo, P. Chini, D. Galli, B. T. Heaton and R. Della Pergola, *Inorg. Chem.*, 1984, **23**, 2947-2954.
[41] (a) V. G. Albano, D. Braga and S. Martinengo, *J. Chem. Soc., Dalton Trans.*, 1986, 981-984; (b) V. G. Albano, D. Braga and S. Martinengo, *J. Chem. Soc., Dalton Trans.*, 1981, 717-720; (c) G. Ciani and S. Martinengo, *J. Organomet. Chem.*, 1986, **306**, C49-C52.
[42] P. Chini, *J. Organomet. Chem.*, 1980, **200**, 37-61.
[43] B. Berti, C. Cesari, C. Femoni, T. Funaioli, M. C. Iapalucci and S. Zacchini, *Dalton Trans.*, 2020, **49**, 5513-5522.
[44] E. Cattabriga, I. Ciabatti, C. Femoni, T. Funaioli, M. C. Iapalucci and S. Zacchini, *Inorg. Chem.*, 2016, **55**, 6068-6079.
[45] J. J. Brunet, *Chem. Rev.*, 1990, **90**, 1041-1059.
[46] R. Della Pergola, F. Demartin, L. Garlaschelli, M. Manassero, S. Martinengo and M. Sansoni, *Inorg. Chem.*, 1987, **26**, 3487-3491.
[47] A. Ceriotti, N. Masciocchi, P. Macchi and G. Longoni, *Angew. Chem. Int. Ed.*, 1999, **38**, 3724-3727.
[48] I. Ciabatti, C. Femoni, M. Hayatifar, M. C. Iapalucci, G. Longoni, C. Pinzino, M. V. Solmi and S. Zacchini, *Inorg. Chem.*, 2014, **53**, 3818-3831.
[49] D. Collini, F. Fabrizi De Biani, S. Fedi, C. Femoni, F. Kaswalder, M. C. Iapalucci, G. Longoni, C. Tiozzo, S. Zacchini and P. Zanello, *Inorg. Chem.*, 2007, **46**, 7971-7981.
[50] I. Ciabatti, F. Fabrizi de Biani, C. Femoni, M. C. Iapalucci, G. Longoni and S. Zacchini, *ChemPlusChem*, 2013, **78**, 1456-1465.
[51] I. Ciabatti, C. Femoni, M. Gaboardi, M. C. Iapalucci, G. Longoni, D. Pontiroli, M. Riccò and S. Zacchini, *Dalton Trans.*, 2014, **43**, 4388-4399.
[52] B. Berti, I. Ciabatti, C. Femoni, M. C. Iapalucci and S. Zacchini, *ACS Omega*, 2018, **3**, 13239-13250.
[53] (a) D. W. Hart, R. G. Teller, C.-Y. Wei, R. Bau, G. Longoni, S. Campanella, P. Chini and T. F. Koetzle, *Angew. Chem. Int. Ed.*, 1979, **18**, 80-81; (b) D. W. Hart, R. G. Teller, C.-Y. Wei, R. Bau, G. Longoni, S. Campanella, P. Chini and T. F. Koetzle, *J. Am. Chem. Soc.*, 1981, **103**, 1458-1466.
[54] P. Chini, *Inorg. Chim. Acta*, 1968, **2**, 31-51.
[55] B. R. Whittlesey, *Coord. Chem. Rev*., 2000, **206-207**, 395-418.
[56] (a) G. Fachinetti, G. Fochi, T. Funaioli and P. F. Zanazzi, *J. Chem. Soc., Chem. Commun.*, 1987, 89-90; (b) C. Mealli, D. M. Proserpio, G. Fachinetti, T. Funaioli, G. Fochi and P. F. Zanazzi, *Inorg. Chem.*, 1989, **28**, 1122-1127.
[57] G. Kong, G. N. Harakas and B. R. Whittlesey, *J. Am. Chem. Soc.*, 1995, **117**, 3502-3509.
[58] C. Femoni, M. C. Iapalucci, G. Longoni and S. Zacchini, *Eur. J. Inorg. Chem.*, 2009, 2487-2495.

[59] M. Shieh and C.-C. Yu, *J. Organomet. Chem*., 2017, **849-850**, 219-227.
[60] M. Shieh, Y.-H. Liu, Y.-H. Li and R. Y. Lin, *CrystEngComm*, 2019, **21**, 7341-7364.
[61] G. Longoni, A. Ceriotti, R. Della Pergola, M. Manassero, M. Perego, G. Piro and M. Sansoni, *Phil. Trans. R. Soc. Lond. A*, 1982, **308**, 47-57.
[62] F. A. Cotton and J. M. Troup, *J. Chem. Soc., Dalton Trans.*, 1974, 800-802.
[63] (a) C. H. Wei and L. F. Dahl, *J. Am. Chem. Soc.*, 1969, **91**, 1351-1361; (b) F. A. Cotton and J. M. Troup, *J. Am. Chem. Soc.,* 1974, **96**, 4155-4159; (c) C. F. Campana, I. A. Guzei, E. G. Mednikov and L. F. Dahl, *J. Clust. Sci*., 2014, **25**, 205-224.
[64] (a) P. J. Krusic, J. R. Morton, K. F. Preston, A. J. Williams and F. L. Lee, *Organometallics*, 1990, **9**, 697-700; (b) P. J. Krusic, J. San Filippo, B. Hutchinson, R. L. Hance and L. M. Daniels, *J. Am. Chem. Soc.*, 1981, **103**, 2129-2131; (c) P. J. Krusic, *J. Am. Chem. Soc.*, 1981, **103**, 2131-2133.
[65] F. Ragaini, J.-S. Song, D. L. Ramage, G. L. Geoffroy, G. A. P. Yap and A. L. Rheingold, *Organometallics*, 1995, **14**, 387-400.
[66] (a) H. A. Hodali, D. F. Shriver and C. A. Ammlung, *J. Am. Chem. Soc.*, 1978, **100**, 5239-5240; (b) K. H. Whitmire and D. F. Shriver, *J. Am. Chem. Soc.*, 1981 **103**, 6754-6755.
[67] (a) C. Femoni, M. C. Iapalucci, G. Longoni, S. Zacchini and S. Zarra, *Inorg. Chem.*, 2009, **48**, 1599-1605; (b) C. Femoni, M. C. Iapalucci, G. Longoni and S. Zacchini, *Dalton Trans.*, 2011, **40**, 8685-8694.
[68] M. Bortoluzzi, I. Ciabatti, C. Femoni, M. Hayatifar, M. C. Iapalucci, G. Longoni and S. Zacchini, *Angew. Chem. Int. Ed.*, 2014, **53**, 7233-7237.
[69] (a) M. R. Churchill, J. Wormald, J. Knight and M. J. Mays, *J. Am. Chem. Soc.*, 1971, **93**, 3073-3074; (b) M. R. Churchill and J. Wormald, *J. Chem. Soc., Dalton Trans.*, 1974, 2410-2415.
[70] M. Bortoluzzi, I. Ciabatti, C. Cesari, C. Femoni, M. C. Iapalucci and S. Zacchini, *Eur. J. Inorg. Chem.*, 2017, 3135-3143.
[71] A. Gourdon and Y. Jeannin, *J. Organomet. Chem.*, 1985, **290**, 199-211.
[72] (a) J. S. Bradley, G. B. Ansell and E. W. Hill, *J. Am. Chem. Soc.*, 1979, **101**, 7417-7419; (b) J. S. Bradley, S. Harris, J. M. Newsam, E. W. Hill, S. Leta and M. A. Modrick, *Organometallics*, 1987, **6**, 2060-2069.
[73] E. M. Holt, K. H. Whitmire and D. F. Shriver, *J. Organomet. Chem.*, 1981, **213**, 125-137.
[74] S. Kuppuswamy, J. D. Wofford, C. Joseph, Z.-L. Xie, A. K. Ali, V. M. Lynch, P. A. Lindahl and M. J. Rose, *Inorg. Chem.*, 2017, **56**, 5998-6012.
[75] (a) C. Femoni, R. Della Pergola, M. C. Iapalucci, F. Kaswalder, M. Riccò and S. Zacchini, *Dalton Trans.*, 2009, 1509-1511; (b) R. Della Pergola, A. Sironi, L. Garlaschelli, D. Strumolo, C. Manassero, M. Manassero, S. Fedi, P. Zanello, F. Kaswalder and S. Zacchini, *Inorg. Chim. Acta*, 2010, **363**, 586-594; (c) I. Ciabatti, C. Femoni, M. Hayatifar, M. C. Iapalucci, I. Maggiore, S. Stagni and S. Zacchini, *J. Clust. Sci.*, 2016, **27**, 431-456.
[76] (a) M. Tachikawa, R. L. Geerts and E. L. Muetterties, *J. Organomet. Chem.*, 1981, **213**, 11-24; (b) R. Reina, L. Rodríguez, O. Rossell, M. Seco, M. Font-Bardia and X. Solans, *Organometallics*, 2001, **20**, 1575-1579.
[77] (a) C. Joseph, S. Kuppuswamy, V. M. Lynch and M. J. Rose, *Inorg. Chem.*, 2018, **57**, 20-23; (b) J. McGale, G. E. Cutsail III, C. Joseph, M. J. Rose and S. DeBeer, *Inorg. Chem.*, 2019, **58**, 12918-12932.
[78] L. Liu, T. B. Rauchfuss and T. J. Woods, *Inorg. Chem.*, 2019, **58**, 8271-8274.
[79] A. Ceriotti, L. Resconi, F. Demartin, G. Longoni, M. Manassero and M. Sansoni, *J. Organomet. Chem.*, 1983, **249**, C35-C37.
[80] C. Femoni, M. C. Iapalucci, G. Longoni, S. Zacchini and E. Zazzaroni, *Dalton Trans.*, 2007, 2644-2651.
[81] V. G. Albano, C. Castellari, C. Femoni, M. C. Iapalucci, G. Longoni, M. Monari, M. Rauccio and S. Zacchini, *Inorg. Chim. Acta*, 1999, **291**, 372-379.
[82] C. K. Schauer, S. Harris, M. Sabat, E. J. Voss and D. F. Shriver, *Inorg. Chem.*, 1995, **34**, 5017-2028.
[83] C. K. Schauer, S. Harris, M. Sabat and D. F. Shriver, *J. Am. Chem. Soc.*, 1989, **111**, 7662-7664.
[84] M. Shieh, C.-Y. Miu, Y.-Y. Chu, C.-N. Lin, *Coord. Chem. Rev.*, 2012, **256**, 637-694.
[85] J. P. Shupp and M. J. Rose, *Dalton Trans.*, 2020, **49**, 23-26.
[86] (a) D. E. Schipper, B. E. Young and K. H. Whitmire, *Organometallics*, 2016, **35**, 471-483; (b) K. H. Whitmire, M. R. Churchill and J. C. Fettinger, *J. Am. Chem. Soc.,* 1985, **107**, 1056-1057; (c) K. H. Whitmire, C. B. Lagrone, M. R. Churchill, J. C. Fettinger and L. V. Biondi, *Inorg. Chem.*, 1984, **23**, 4227-4232.
[87] M. Ferrer, R, Reina, O. Rossell and M. Seco, *Coord. Chem. Rev.*, 1999, **193-195**, 619-642.

[88] B. Berti, M. Bortoluzzi, C. Cesari, C. Femoni, M. C. Iapalucci, L. Soleri and S. Zacchini, *Inorg. Chem.*, 2020, **59**, 15936-15952.
[89] (a) M. Bortoluzzi, C. Cesari, I. Ciabatti, C. Femoni, M. Hayatifar, M. C. Iapalucci, R. Mazzoni and S. Zacchini, *J. Clust. Sci.*, 2017, **28**, 703-723; (b) B. Berti, M. Bortoluzzi, C. Cesari, C. Femoni, M. C. Iapalucci, R. Mazzoni, F. Vacca and S. Zacchini, *Eur. J. Inorg. Chem.*, 2019, 3084-3093.
[90] B. Berti, M. Bortoluzzi, C. Cesari, C. Femoni, M. C. Iapalucci, R. Mazzoni, F. Vacca and S. Zacchini, *Inorg. Chem.*, 2019, **58**, 2911-2915.
[91] (a) B. Berti, M. Bortoluzzi, C. Cesari, C. Femoni, M. C. Iapalucci, R. Mazzoni and S. Zacchini, *Eur. J. Inorg. Chem.*, 2020, 2191-2202; (b) B. Berti, M. Bortoluzzi, C. Cesari, C. Femoni, M. C. Iapalucci, R. Mazzoni, F. Vacca and S. Zacchini, *Inorg. Chem.*, 2020, **59**, 2228-2240.
[92] N. P. Mankad, *Chem. Commun.*, 2018, **54**, 1291-1302.
[93] N. P. Mankad, *Chem. Eur. J.*, 2016, **22**, 5822-5829.
[94] Y. Lakliang and N. P. Mankad, *Organometallics*, 2020, **39**, 2043-2046.
[95] C. Femoni, M. C. Iapalucci, G. Longoni, C. Tiozzo and S. Zacchini, *Agew. Chem. Int. Ed.* **2008**, *47*, 6666-6669.
[96] B. F. G. Johnson and J. Lewis, *Inorg. Synth.*, 1972, **13**, 92-95.
[97] (a) F. Calderazzo and F. L'Eplattenier, *Inorg. Chem.*, 1967, **6**, 1220- 1224; (b) F. L'Eplattener, *Inorg. Chem.*, 1969, **8**, 965-970; (c) B. F. G. Jonhson, J. Lewis and M. V. Twigg, *J. Organomet. Chem.*, 1974, **67**, C75-C76.
[98] J. Lewis and P. R. Raithby, *J. Organoment, Chem.*, 1995, **500**, 227-237.
[99] (a) C. R. Eady, B. F. G. Johnson and J. Lewis, *J. Chem. Soc., Dalton Trans.*, 1977, 838-844; (b) S. A. R. Knox, J. W. Koepke, M. A. Andrews and H. D. Kaesz, *J. Am. Chem. Soc.*, 1975, **97**, 3942-3947.
[100] M. Yu. Afonin, B. Yu. Savkov, A. V. Virovets, V. S. Korenev, A. V. Golovin and V. A. Maksakov, *Eur. J. Inorg. Chem.*, 2017, 3105-3114.
[101] B. F. G. Johnson, J. Lewis and D. A. Pippard, *J. Chem. Soc., Dalton Trans.*, 1981, 407-412.
[102] (a) S. P. Oh, Y.-Z. Li and W. K. Leong, *J. Organomet. Chem.*, 2015, **783**, 46-48; (b) R. D. Adams, Y. Kan and Q. Zhang, *J. Organomet. Chem.*, 2014, **751**, 475-481.
[103] (a) K. V. Kong, W. K. Leong, S. P. Ng, T. H. Nguyen and L. H. K. Lim, *ChemMedChem*, 2008, **3**, 1269-1275; (b) K, V. Kong, W. K. Leong and L. H. K. Lim, *Chem. Res. Toxicol.*, 2009, **22**, 1116-1122.
[104] R. D. Adams, E. J. Kiprotich and M. D. Smith, *Chem. Commun.*, 2018, **54**, 3464-3467.
[105] P. J. Bailey, B. F. G. Johnson and J. Lewis, *Inorg. Chim. Acta*, 1994, **227**, 197-200.
[106] J. P. Canal, A. A. Bengali, M. C. Jennings and R. K. Pomeroy, *Inorg. Chem. Commun.*, 2014, **43**, 31-34.
[107] S. Takemoto and H. Matsuzaka, *Coord. Chem. Rev.*, 2012, **256**, 574-588.
[108] M. I. Bruce, N. N. Zaitseva, B. W. Skelton and A. H. White, *J. Chem. Soc., Dalton Trans.*, 2002, 3879-3885.
[109] M. P. Cifuentes, M. G. Humphrey, J. E. McGrady, P. J. Smith, R. Stranger, K. S. Murray and B. Moubaraki, *J. Am. Chem. Soc.*, 1997, **119**, 2647-2655.
[110] (a) B. F. G. Johnson, S. Hermans and T. Khimyak, *Eur. J. Inorg. Chem.*, 2003, 1325-1331; (b) R. D. Adams, M. D. Smith, J. D. Tedder and N. D. Wakdikar, *Inorg. Chem.*, 2019, **58**, 8357-8368.
[111] (a) R. D. Adams, B. Captain, W. Fu, P. J. Pellechia and M. D. Smith, *Angew. Chem. Int. Ed.*, 2002, **41**, 1951-1953; (b) S. Saha, L. Zhu and B. Captain, *Inorg. Chem.*, 2013, **52**, 2526-2532.
[112] (a) R. D. Adams, I. T. Horváth and H.-S. Kim, *Organometallics*, 1984, **3**, 548-552; (b) R. D. Adams, I. T. Horváth and P. Mathur, *Organometallics*, 1984, **3**,623-630; (c) R. D. Adams and I. T. Horváth, *Inorg. Chem.*, 1984, **23**, 4718-4722.
[113] S.-P. Huang and M. G. Kanatzidis, *J. Am. Chem. Soc.,* 1992, **114**, 5477-5478.
[114] M. Shieh, M.-H. Hsu, W.-S. Sheu, L.-F. Jang, S.-F. Lin, Y.-Y. Chu, C.-Y. Miu, Y.-W. Lai, H.-L. Liu and J. L. Her, *Chem. Eur. J.*, 2007, **13**, 6605-6616.
[115] (a) H. G. Ang, C. M. Hay, B. F. G. Johnson, J. Lewis, P. R. Raithby and A. J. Whitton, *J. Organomet. Chem.*, 1987, **330**, C5-C11; (b) M. D. Randles, A. C. Willis, M. P. Cifuentes and M. G. Humphrey, *J. Organomet. Chem.*, 2007, **692**, 4467-4472.
[116] Y.-Z. Li, R. Ganguly, W. K. Leong and Y. Liu, *Eur. J. Inorg. Chem.*, 2015, 3861-3872.
[117] S. Saha, D. Isrow and B. Captain, *J. Organomet. Chem.*, 2014, **751**, 815-820.

[118] (a) F.-E. Hong, T. J. Coffy, D. A. McCarthy and S. G. Shore, *Inorg. Chem.*, 1989, **28**, 3284-3285; (b) C. E. Housecroft, D. M. Matthews, A. L. Rheingold and X. Song, *J. Chem. Soc., Chem. Commun.*, 1992, 842-843.
[119] J.-H. Chung, D. Knoeppel, D. McCarthy, A. Columbie and S. G. Shore, *Inorg. Chem.*, 1993, **32**, 3391-3392.
[120] R. D. Adams, J. Kiprotich, D. V. Peryshkov and Y. O. Wong, *Chem. Eur. J.*, 2016, **22**, 6501-6504.
[121] R. D. Adams, Q. Zhang and X. Yang, *J. Am. Chem. Soc.*, 2011, **133**, 15950-15953.
[122] K.-F. Yung and W.-T. Wong, *Angew. Chem. Int. Ed.*, 2003, **42**, 553-555.
[123] T. Y. Garcia, J. C. Fettinger, M. M. Olmstead and A. L. Balch, *Chem. Commun.*, 2009, 7143-7145.
[124] (a) A. E. Carpenter, A. L. Rheingold and J. S. Figueroa, *Organometallics*, 2016, **35**, 2309-2318; (b) A. E. Carpentier, C. Chan, A. L. Rheingold and J. S. Figueroa, *Organometallics*, 2016, **35**, 2319-2326.
[125] F. L. Bowles, M. M. Olmstead, C. M. Beavers and A. L. Balch, *Chem. Commun.*, 2013, **49**, 5921-5923.
[126] C. E. Plečnik, S. Liu, X. Chen, E. A. Meyers and S. G. Shore, *J. Am. Chem. Soc.*, 2004, **126**, 204-213.
[127] (a) H. N. Adams, G. Fachinetti and J. Strähle, *Angew. Chem. Int. Ed.*, 1980, **19**, 404-405; (b) G. Fachinetti, G. Fochi, T. Funaioli and P. F. Zanazzi, *Angew. Chem. Int. Ed.*, 1987, **26**, 680-681.
[128] (a) V. G. Albano, P. Chini, S. Martinengo, M. Sansoni and D. Strumolo, *J. Chem. Soc., Chem. Commun.*, 1974, 299-300; (b) S. Martinengo, D. Strumolo, P. Chini, V. G. Albano and D. Braga, *J. Chem. Soc., Dalton Trans*., 1985, 35-41.
[129] V. G. Albano, D. Braga, F. Grepioni, R. Della Pergola, L. Garlaschelli and A. Fumagalli, *J. Chem. Soc., Dalton Trans.* 1989, 879-883.
[130] S. Kamiguchi and T. Chihara, *J. Clust. Sci.*, 2000, **11**, 483-492.
[131] A. Ceriotti, R. Della Pergola, G. Longoni, M. Manassero, N. Masciocchi and M. Sansoni, *J. Organomet. Chem.*, 1987, **330**, 237-252.
[132] A. Arrigoni, A. Ceriotti, R. Della Pergola, G. Longoni, M. Manassero, N. Masciocchi and M. Sansoni, *Angew. Chem. Int. Ed.*, 1984, **23**, 322-323.
[133] A. Arrigoni, A. Ceriotti, R. Della Pergola, G. Longoni, M. Manassero and M. Sansoni, *J. Organomet. Chem.*, 1985, **296**, 243-253.
[134] I. Ciabatti, F. Fabrizi de Biani, C. Femoni, M. C. Iapalucci, G. Longoni and S. Zacchini, *Dalton Trans.*, 2013, **42**, 9662-9670.
[135] C. Femoni, M. C. Iapalucci, G. Longoni, J. Wolowska, S. Zacchini, P. Zanello, S. Fedi, M. Riccò, D. Pontiroli and M. Mazzani, *J. Am. Chem. Soc.*, 2010, **132**, 2919-2927.
[136] (a) I. Ciabatti, C. Femoni, M. Hayatifar, M. C. Iapalucci and S. Zacchini, *Inorg. Chim. Acta*, 2015, **428**, 203-211; (b) I. Ciabatti, C. Femoni, M. Hayatifar, M. C. Iapalucci, A. Ienco, G. Longoni, G. Manca and S. Zacchini, *Inorg. Chem.*2014, **53**, 9761-9770; (c) M. Bortoluzzi, I. Ciabatti, C. Femoni, T. Funaioli, M. Hayatifar, M. C. Iaplaucci, G. Longoni and S. Zacchini, *Dalton Trans.*, 2014, **43**, 9633-9646.
[137] (a) A. Fumagalli, P. Ulivieri, M. Costa, O. Crispu, R. Della Pergola, F. Fabrizi de Biani, F. Laschi, P. Zanello, P. Macchi and A. Sironi, *Inorg. Chem.*, 2004, **43**, 2125-2131; (b) A. Fumagalli, M. Costa, R. Della Pergola, P. Zanello, F. Fabrizi de Biani, P. Macchi and A. Sironi, *Inorg. Chim. Acta*, 2003, **350**, 187-192.
[138] C. S. Hong, L. A. Berben and J. R. Long, *Dalton Trans.*, 2003, 2119-2120.
[139] G. Ciani, A. Sironi, S. Martinengo, L. Garlaschelli, R. Della Pergola, P. Zanello, F. Laschi and N. Masciocchi, *Inorg. Chem.*, 2001, **40**, 3905-3911.
[140] C. Dreher, M. Zabel, M. Bodensteiner and M. Scheer, *Organometallics*, 2010, **29**, 5187-5191.
[141] (a) L. A. Hanlan and G. A. Ozin, *J. Am. Chem. Soc.*, 1974, **96**, 6324-6329; (b) J. L. Vidal and W. E. Walker, *Inorg. Chem.*, 1981, **20**, 249-254.
[142] (a) P. Chini and S. Martinengo, *Inorg. Chim. Acta*, 1969, **3**, 315-318; (b) L. Garlaschelli, S. Martinengo, P. L. Bellon, F. Demartin, M. Manassero, M. Y. Chiang, C.-Y. Wei and R. Bau, *J. Am. Chem. Soc.*, 1984, **106**, 6664-6667.
[143] (a) G. Fachinetti, T. Funaioli and P. F. Zanazzi, *J. Organomet. Chem.*, 1993, **460**, C34-C36; (b) K. J. Bradd, B. T. Heaton, J. A. Iggo, C. Jacob, J. T. Sampanthar and S. Zacchini, *Dalton Trans.*, 2008, 685-690.
[144] (a) P. Chini and S. Martinengo, *Chem. Commun.*, 1969, 1092-1093; (b) S. Martinengo, A. Fumagalli and P. Chini, *J. Organomet. Chem.*, 1985, **284**, 275-279; (c) L. Malatesta, G. Caglio and M. Angoletta, *J. Chem. Soc., Chem. Commun.*, 1970, 532-533.

[145] M. R. Churchill and J. P. Hutchinson, *Inorg. Chem.*, 1978, **17**, 3528-3535.
[146] (a) D, Collini, F. Fabrizi de Biani, D. S. Dolzhnikov, C. Femoni, M. C. Iaplaucci, G. Longoni, C. Tiozzo, S. Zacchini and P. Zanello, *Inorg. Chem.*, 2011, **50**, 2790-2798; (b) D. S. Dolzhnikov, M. C. Iapalucci, G. Longoni, C. Tiozzo, S. Zacchini and C. Femoni, *Inorg. Chem.*, 2012, **51**, 11214-11216.
[147] R. Della Pergola, F. Cea, L. Garlaschelli, N. Masciocchi and M. Sansoni, *J. Chem. Soc., Dalton Trans.*, 1994, 1501-1503.
[148] R. Della Pergola, L. Garlaschelli, M. Manassero, N. Masciocchi and P. Zanello, *Angew. Chem. Int. Ed.*, 1993, **32**, 1347-1349.
[149] A. P. Palermo, C. Schöttle, S. Zhang, N. A. Grosso-Giordano, A. Okrut, D. A. Dixon, H. Frei, B. C. Gates and A. Katz, *Inorg. Chem.*, 2019, **58**, 14338-14348.
[150] (a) E. V. Grachova, P. Jutzi, B. Neumann and H.-G. Stammler, *Dalton Trans.*, 2005, 3614-3616; (b) E. V. Grachova and G. Linti, *Eur. J. Inorg. Chem.*, 2007, 3561-3564.
[151] (a) R. D. Adams, M. Chen, E. Trufan and Q. Zhang, *Organometallics*, 2011, **30**, 661-664; (b) R. D. Adams and M. Chen, *Organometallics*, 2012, **31**, 445-450.
[152] (a) R. D. Adams and M. Chen, *J. Organomet. Chem.*, 2013, **733**, 21-27; (b) R. D. Adams and G. Elpitiya, *Inorg. Chem.*, 2015, **54**, 8042-8048.
[153] Z. Li, C. Liu, J. Wu, Z. Lin and L. Xu, *Dalton Trans.*, 2019, **48**, 12013-12017.
[154] (a) C. Femoni, I. Ciabatti, M. C. Iapalucci, S. Ruggieri, S. Zacchini, *Progr. Nat. Sci: Mat. Internat.*, 2016, **26**, 461-466; (b) C. Femoni, G. Bussoli, I. Ciabatti, M. Ermini, M. Hayatifar, M. C. Iapalucci, S. Ruggieri and S. Zacchini, *Inorg. Chem.*, 2017, **56**, 6343-6351.
[155] (a) A. Boccalini, P. J. Dyson, C. Femoni, M. C. Iapalucci, S. Ruggieri and S. Zacchini, *Dalton Trans.*, 2018, **47**, 15737-15744; (b) C. Femoni, T. Funaioli, M. C. Iapalucci, S. Ruggieri and S. Zacchini, *Inorg. Chem.*, 2020, **59**, 4300-4310.
[156] J. L. Vidal, *Inorg. Chem.*, 1981, **20**, 243-249.
[157] (a) J. L. Vidal, W. E. Walker, R. L. Pruett and R. C. Shoening, *Inorg. Chem.*, 1979, **18**, 129-136; (b) J. L. Vidal, W. E. Walker and R. C. Shoening, *Inorg. Chem.*, 1981, **20**, 238-342.
[158] L. Garlaschelli, A. Fumagalli, S. Martinengo, B. T. Heaton, D. O. Smith and L. Strona, *J. Chem. Soc., Dalton Trans.*, 1982, 2265-2267.
[159] V. G. Albano, P. Chini, S. Martinengo, D. J. A. McCaffrey, D. Strumolo and B. T. Heaton, *J. Am. Chem. Soc.*, 1974, **96**, 8106-8107.
[160] (a) B. T. Heaton, L. Strona, S. Martinengo, D. Strumolo, V. G. Albano and D. Braga, *J. Chem. Soc., Dalton Trans.*, 1983, 2175-2182; (b) R. Della Pergola, A. Sironi, C. Manassero and M. Manassero, *Eur. J. Inorg. Chem.*, 2009, 4618-4621.
[161] L. Cerchi, A. Fumagalli, S. Fedi, P. Zanello, F. Fabrizi de Biani, F. Laschi, L. Garlaschelli, P. Macchi and A. Sironi, *Inorg. Chem.*, 2012, **51**, 9171-9180.
[162] G. Ciani, D. M. Proserpio, A. Sironi, S. Martinengo and A. Fumagalli, *J. Chem. Soc., Dalton Trans.*, 1994, 471-475.
[163] A. Fumagalli, S. Martinengo, G. Bernasconi, G. Ciani, D. M. Proserpio and A. Sironi, *J. Am. Chem. Soc.*, 1997, **119**, 1450-1451.
[164] (a) S. Martinengo, G. Ciani and A. Sironi, *J. Am. Chem. Soc.*, 1982, **104**, 328-330; (b) S. Martinengo, G. Ciani and A. Sironi, *J. Chem. Soc., Chem. Commun.*, 1984, 1577-1578.
[165] W. Hieber, *Adv. Organomet. Chem.*, 1970, **8**, 1-28.
[166] (a) G. Longoni, P. Chini and A. Cavalieri, *Inorg. Chem.*, 1976, **15**, 3025-3029; (b) G. Longoni and P. Chini, *Inorg. Chem.*, 1976, **15**, 3029-3031; (c) A. Ceriotti, P. Chini, R. Della Pergola and G. Longoni, *Inorg. Chem.*, 1983, **22**, 1595-1598.
[167] (a) J. K. Beattie, A. F. Masters and J. T. Meyer, *Polyhedron*, 1995, **14**, 829-868; (b) A. F. Masters and J. T. Meyer, *Polyhedron*, 1995, **14**, 339-365.
[168] F. Demartin, M. C. Iapalucci and G. Longoni, *Inorg. Chem.*, 1993, **32**, 5536-5543.
[169] C. Femoni, M. C. Iapalucci, G. Longoni, F. Ranuzzi, S. Zacchini, S. Fedi and P. Zanello, *Eur. J. Inorg. Chem.*, 2007, 4064-4070.
[170] (a) D. Collini, C. Femoni, M. C. Iapalucci, G. Longoni, P. H. Svensson and P. Zanello, *Angew. Chem. Int. Ed.*, 2002, **41**, 3685-3688; (b) N. T. Tran, M. Kawano, D. R. Powell and L. F. Dahl, *J. Chem. Soc., Dalton Trans.*, 2000, 4138-4144.

[171] (a) C. Femoni, M. C. Iapalucci, G. Longoni, P. H. Svensson and J. Wolowska, *Angew. Chem. Int. Ed.*, 2000, **39**, 1635-1637; (b) C. Femoni, M. C. Iapalucci, G. Longoni, P. H. Svensson, P. Zanello and F. Fabrizi de Biani, *Chem. Eur. J.*, 2004, **10**, 2318-2326; (c) C. Femoni, M. C. Iapalucci, G. Longoni and P. H. Svensson, *Chem. Commun.*, 2001, 1776-1777.

[172] (a) C. Femoni, M. C. Iapalucci, G. Longoni and P. H. Svensson, *Chem. Commun.*, 2004, 2274-2275; (b) I. Ciabatti, C. Femoni, M. C. Iapalucci, G. Longoni, S. Zacchini, S. Fedi and F. Fabrizi de Biani, *Inorg. Chem*., 2012, **51**, 11753-11761.

[173] N. T. Tran, M. Kawano, D. R. Powell, R. K. Hayashi, C. F. Campana and L. F. Dahl, *J. Am. Chem. Soc.*, 1999, **121**, 5945-5952.

[174] (a) I. Ciabatti, C. Femoni, T. Funaioli, M. C. Iapalucci, S. Merighi and S. Zacchini, *J. Organomet. Chem.*, 2017, **849-850**, 299-305; (b) C. Femoni, M. C. Iapalucci, G. Longoni, S. Zacchini, S. Fedi and F. Fabrizi de Biani, *Dalton Trans.*, 2012, **41**, 4649-4663; (c) C. Femoni, M. C. Iapalucci, G. Longoni and S. Zacchini, *Chem. Commun.*, 2008, 3157-3159.

[175] (a) A. Bernardi, I. Ciabatti, C. Femoni, M. C. Iapalucci, G. Longoni and S. Zacchini, *J. Organomet. Chem.*, 2016, **812**, 229-239; (b) A. Bernardi, I. Ciabatti, C. Femoni, M. C. Iapalucci, G. Longoni and S. Zacchini, *Dalton Trans.*, 2013, **42**, 407-421; (c) I. Ciabatti, C. Femoni, M. C. Iapalucci, A. Ienco, G. Longoni, G. Manca and S. Zacchini, *Inorg. Chem.*, 2013, **52**, 10559-10565.

[176] C. Cesari, I. Ciabatti, C. Femoni, M. C. Iapalucci and S. Zacchini, *J. Clust. Sci.*, 2017, **28**, 1963-1979.

[177] (a) M. Bortoluzzi, I. Ciabatti, C. Femoni, M. Hayatifar, M. C. Iapalucci, G. Longoni and S. Zacchini, *Dalton Trans.*, 2014, **43**, 13471-13475; (b) A. Bernardi, C. Femoni, M. C. Iapalucci, G. Longoni and S. Zacchini, *Dalton Trans.*, 2009, 4245-4251; (c) A. Bernardi, C. Femoni, M. C. Iapalucci, G. Longoni, F. Ranuzzi, S. Zacchini, P. Zanello and S. Fedi, *Chem. Eur. J.*, 2008, **14**, 1924-1934.

[178] (a) A. Bernardi, C. Femoni, M. C. Iapalucci, G. Longoni and S. Zacchini, *Inorg. Chim. Acta*, 2009, **362**, 1239-1246; (b) A. Bernardi, C. Femoni, M. C. Iapalucci, G. Longoni, S. Zacchini, S. Fedi and P. Zanello, *Eur. J. Inorg. Chem.*, 2010, 4831-4842.

[179] C. Femoni, M. C. Iapalucci, G. Longoni and S. Zacchini, *Eur. J. Inorg. Chem.*, 2010, 1056-1062.

[180] C. Femoni, M. C. Iapalucci, G. Longoni, S. Zacchini, I. Ciabatti, R. G. Della Valle, M. Mazzani and M. Riccò, *Eur. J. Inorg. Chem.*, 2014, 4151-4158.

[181] (a) C. Capacci, I. Ciabatti, C. Femoni, M. C. Iapalucci, T. Funaioli, S. Zacchiuni and V. Zanotti, *Inorg. Chem.*, 2018, **57**, 1136-1147; (b) C. Capacci, C. Cesari, C. Femoni, M. C. Iapalucci, F. Mancini, S. Ruggieri and S. Zacchini, *Inorg. Chem.*, 2020, **59**, 16016-16026.

[182] (a) C. Femoni, F. Kaswalder, M. C. Iapalucci, G. Longoni, M. Mehlstäubl and S. Zacchini, *Chem. Commun.*, 2005, 5769-5771; (b) C. Femoni, F. Kaswalder, M. C. Iaplaucci, G. Longoni, M. Mehlstäubl, S. Zacchini and A. Ceriotti, *Angew. Chem. Int. Ed.*, 2006, **45**, 2060-2062; (c) C. Femoni, F. Kaswalder, M. C. Iaplucci, G. Longoni and S. Zacchini, *Eur. J. Inorg. Chem.*, 2007, 1483-1486.

[183] C. Femoni, M. C. Iapalucci, G. Longoni, T. Lovato, S. Stagni and S. Zacchini, *Inorg. Chem.*, 2010, **49**, 5992-6004.

[184] B. Berti, M. Bortoluzzi, A. Ceriotti, C. Cesari, C. Femoni, M. C. Iapalucci and S. Zacchini, *Inorg. Chim. Acta*, 2020, **512**, 119904.

[185] (a) I. Ciabatti, C. Femoni, M. C. Iapalucci, G. Longoni, T. Lovato and S. Zacchini, *Inorg. Chem.*, 2013, **52**, 4384-4395; (b) I. Ciabatti, C. Femoni, M. C. Iapalucci, G. Longoni and S. Zacchini, *Organometallics*, 2013, **32**, 5180-5189.

[186] (a) C. Cesari, I. Ciabatti, C. Femoni, M. C. Iapalucci, F. Mancini and S. Zacchini, *Inorg. Chem.*, 2017, **56**, 1655-1668; (b) L. K. Batchelor, B. Berti, C. Cesari, I. Ciabatti, P. J. Dyson, C. Femoni, M. C. Iapalucci, M. Mor, S. Ruggieri and S. Zacchini, *Dalton Trans.*, 2018, **47**, 4467-4477.

[187] B. Berti, C. Cesari, F. Conte, I. Ciabatti, C. Femoni, M. C. Iapalucci, F. Vacca and S. Zacchini, *Inorg. Chem.*, 2018, **57**, 7578-7590.

[188] C. Femoni, F. Kaswalder, M. C. Iapalucci, G. Longoni and S. Zacchini, *Chem. Commun.*, 2006, 2135-2137.

[189] M. Bortoluzzi, C. Cesari, I. Ciabatti, C. Femoni, M. C. Iapalucci and S. Zacchini, *Inorg. Chem.*, 2017, **56**, 6532-6544.

[190] (a) A. Ceriotti, M. Daghetta, S. El Afefey, A. Ienco, G. Longoni, G. Manca, C. Mealli, S. Zacchini and S. Zarra, *Inorg. Chem.*, 2011, **50**, 12553-12561; (b) M. Bortoluzzi, A. Ceriotti, I. Ciabatti, R. Della Pergola, C. Femoni, M. C. Iapalucci, A. Storione and S. Zacchini, *Dalton Trans.*, 2016, **45**, 5001-5013.

[191] (a) M. Bortoluzzi, A. Ceriotti, C. Cesari, I. Ciabatti, R. Della Pergola, C. Femoni, M. C. Iapalucci, A. Storione and S. Zacchini, *Eur. J. Inorg. Chem.*, 2016, 3939-3949; (b) B. Berti, M. Bortoluzzi, C. Cesari, C. Femoni, M. C. Iapalucci and S. Zacchini, *Inorg. Chim. Acta*, 2020, **503**, 119432.
[192] D. Bonincontro, A. Lolli, A. Storione, A. Gasparotto, B. Berti, S. Zacchini, N. Dimitratos and S. Albonetti, *Appl. Catal. A*, 2019, **588**, 117279.
[193] (a) C. Femoni, M. C. Iapalucci, G. Longoni, S. Zacchini and S. Zarra, *J. Am. Chem. Soc.*, 2011, **133**, 2406-2409; (b) I. Ciabatti, C. Femoni, M. C. Iapalucci, G. Longoni, S. Zacchini and S. Zarra, *Nanoscale*, 2012, **4**, 4166-4177.
[194] (a) E. Cattabriga, I. Ciabatti, C. Femoni, M. C. Iapalucci, G. Longoni and S. Zacchini, *Inorg. Chim. Acta*, 2018, **470**, 238-249; (b) F. Gao, C. Li, B. T. Heaton, S. Zacchini, S. Zarra, G. Longoni and M. Garland, *Dalton Trans.*, 2011, **40**, 5002-5008.
[195] D. M. Washecheck, E. J. Wucherer, L. F. Dahl, A. Ceriotti, G. Longoni, M. Manassero, M. Sansoni and P. Chini, *J. Am. Chem. Soc.*, 1979, **101**, 6110-6112
[196] J. A. Widegren and R. G. Finke *J. Mol. Catal. A: Chem.* 2003, **198**, 317–341.
[197] L. Liu, T. J. Woods and T. B. Rauchfuss, *Eur. J. Inorg. Chem.*, 2020, **2020**, 3460–3465.
[198] N. Queyriaux, D. Sun, J. Fize, J. Pécaut, M. J. Field, M. C-. Kerlidou and V. Artero, *J. Am. Chem. Soc.,* 2020, **142**, 274−282.
[199] R.M. Laine, *J. Mol. Catal.*, 1982, **14**, 137–169.
[200] J. McGale, G. E. Cutsail, C. Joseph, M. J. Rose and S. DeBeer, *Inorg. Chem.*, 2019, **58**, 12918–12932.
[201] G. O. Evans and C. J. Newell, *Inorg. Chim. Acta*, 1978, L387–L389.
[202] H. C. Kang, C. H. Mauldin, T. Cole, W. Slegeir, K. Cann and R. Pettit, *J. Am. Chem. Soc.*, 1977, **99**, 8323–8325.
[203] K. Cann, T. Cole, W. Slegeir and R. Pettit, *J. Am. Chem. Soc.*, 1978, **100**, 3969–3971.
[204] D. J. Darensbourg, C. Ovalles and M. Pala, *J. Am. Chem. Soc.*, 1983, **105**, 5937–5939.
[205] M. G. Thomas, B. F. Beier and E. L. Muetterties, *J. Am. Chem. Soc.*, 1976, **98**, 1296–1297.
[206] C. P. Casey and C. R. Cyr, *J. Am. Chem. Soc.*, 1973, **95**, 2248–2253.
[207] Y. Sunada, H. Kawakami, T. Imaoka, Y. Motoyama and H. Nagashima, *Angew. Chem. Intl. Ed.*, 2009, **48**, 9511–9514.
[208] S. Zhou, K. Junge, D. Addis, S. Das and M. Beller, *Angew. Chem.*, 2009, **121**, 9671–9674.
[209] S. Zhou, D. Addis, S. Das, K. Junge and M. Beller, *Chem. Commun.*, 2009, 4883.
[210] S. Zhou, S. Fleischer, K. Junge, S. Das, D. Addis and M. Beller, *Angew. Chem. Intl. Ed.*, 2010, **49**, 8121–8125.
[211] S. Enthaler, *ChemCatChem*, 2011, **3**, 666–670.
[212] Y.-Y. Li, S.-L. Yu, W.-Y. Shen and J.-X. Gao, *Acc. Chem. Res.*, 2015, **48**, 2587–2598.
[213] Y. Li, S. Yu, X. Wu, J. Xiao, W. Shen, Z. Dong and J. Gao, *J. Am. Chem. Soc.*, 2014, **136**, 4031–4039.
[214] (a) C.-N. Lin, C.-Y. Huang, C.-C. Yu, Y.-M. Chen, W.-M. Ke, G.-J. Wang, G.-A. Lee and M. Shieh, *Dalton Trans.*, 2015, **44**, 16675–16679.; (b) M. Shieh, Y.-H. Liu, C.-C. Wang, S.-H. Jian, C.-N. Lin, Y.-M. Chen and C.-Y. Huang, *New J. Chem.*, 2019, **43**, 11832–11843.
[215] P. C. Ford, R. G. Rinker, C. Ungermann, R. M. Laine, V. Landis and S. A. Moya, *J. Am. Chem. Soc.*, 1978, **100**, 4595–4597.
[216] J. C. Bricker, C. C. Nagel, A. A. Bhattacharyya and S. G. Shore, *J. Am. Chem. Soc.*, 1985, **107**, 377–384.
[217] H. S. Hilal, S. Khalaf and W. Jondi, *J. Organometallic Chem.*, 1993, **452**, 167–173.
[218] T. Morimoto, N. Chatani and S. Murai, *J. Am. Chem. Soc.*, 1999, **121**, 1758–1759.
[219] H. Nagashima, A. Suzuki, T. Iura, K. Ryu and K. Matsubara, *Organometallics*, 2000, **19**, 3579–3590.
[220] M. Igarashi, R. Mizuno and T. Fuchikami, *Tet. Lett.*, 2001, **42**, 2149–2151.
[221] W. Imhof, A. Göbel, L. Schweda, D. Dönnecke and K. Halbauer, *J. Organometallic Chem.*, 2005, **690**, 3886–3897.
[222] G. Süss-Fink and J. Reiner, *J. Mol. Catal.*, 1982, **16**, 231–242.
[223] H. S. Hilal, W. Jondi, S. Khalaf and R. Abu-Halawa, *J. Organomet. Chem.,*1993, **452**, 161–165.

[224] K. G. Caulton, M. G. Thomas, B. A. Sosinsky and E. L. Muetterties, *Proc. Natl. Acad. Sci.*, 1976, **73**, 4274–4276.
[225] R. D. Adams, *Acc. Chem. Res.*, 1983, **16**, 67–72.
[226] R. C. Ryan and C. U. Pittman, *J. Am. Chem. Soc.*, 1977, **99**, 1986–1988.
[227] T. Murai, T. Sakane and S. Kato, *J. Org. Chem.*, 1990, **55**, 449–453.
[228] I. Ojima, R. J. Donovan and N. Clos, *Organometallics*, 1991, **10**, 2606–2610.
[229] I. Ojima, P. Ingallina, R. J. Donovan and N. Clos, *Organometallics*, 1991, **10**, 38–41.
[230] H. Yamazaki and P. Hong, *J. Mol. Cat.*, 1983, **21**, 133–150.
[231] K. Kaneda, H. Kuwahara and T. Imanaka, *J. Mol. Catal.*, 1994, **88**, L267–L270.
[232] S. Kawi, J. R. Chang and B. C. Gates, *J. Am. Chem. Soc.*, 1993, **115**, 4830–4843.
[233] S. Kawi, J. R. Chang and B. C. Gates, *J. Phys. Chem.*, 1994, **98**, 12978–12988.
[234] T. Yamamoto, T. Shido, S. Inagaki, Y. Fukushima and M. Ichikawa, *J. Phys. Chem. B*, 1998, **102**, 3866–3875.
[235] S. Bhaduri, *Current Science*, 2000, **78**, 1318.
[236] S. Basu, H. Paul, C. Gopinath, S. Bhaduri and G. Lahiri, *J. Catal.*, 2005, **229**, 298–302.
[237] Z. Zhang, F. A. P. Cavalcanti and W. M. H. Sachtler, *Catal. Lett.,* 1992, **12** 157–169
[238] (a) C. R. Carr, A. Taheri and L. A. Berben, *J. Am. Chem. Soc.*, 2020, **142**, 12299–12305. (b) S. Pattanayak, S.; L. A. Berben, *ChemElectroChem.* 2021, *8*, DOI: doi.org/10.1002/celc.202100402
[239] C. Costentin, S. Drouet, M. Robert, J.-M. Savéant, *J. Am. Chem. Soc.* 2012, **134**, 11235–11242.
[240] G. Gritzner and J. Kuta, *Pure & appl. Chem.*, 1983, **56**, 461–466
[241] I. Noviandri, K. N. Brown, D. S.Fleming, P. T. Gulyas, P. A. Lay, A. F. Masters and L. Phillips, *J. Phys. Chem. B*, 1999, **103**, 6713.
[242] (a) S. Roy, B. Sharma, J. Pécaut, P. Simon, M. Fontecave, P. D. Tran, E. Derat and V. Artero, *J. Am. Chem. Soc.*, 2017, **139**, 3685–3696; (b) D. C. Cunningham and J. Y. Yang, *Chem. Commun.,* 2020*,* **56***,*12965–12968.
[243] A. Taheri, C. R. Carr and L. A. Berben, *ACS Catal.*, 2018, **8**, 5787–5793
[244] (a) M. D. Rail and L. A. Berben, *J. Am. Chem. Soc.*, 2011, **133**, 18577–18579; (b) N. D. Loewen, T. Neelakantan, L. A. Berben, *Acc. Chem. Res.* 2017,**50**, 2362-2370; (c) A. Taheri, N. D. Loewen, D. B. Cluff, J. C. Fettinger, L. A. Berben, *Organometallics*, 2018, **37**, 1087-1091.
[245] A. Taheri, E. J. Thompson, J. C. Fettinger and L. A. Berben, *ACS Catal.*, 2015, **5**, 7140–7151.
[246] (a) A. D. Nguyen, M. D. Rail, M. Shanmugam, J. C. Fettinger and L. A. Berben, *Inorg. Chem.*, 2013, **52**, 12847–12854; (b) A. Taheri, L. A. Berben, *Inorg. Chem.* 2016, **55**, 378-385.
[247] M. L. Helm, M. Stewart, R. M. Bullock, M. Rakowski DuBois, D. L. DuBois, *Science*, 2011, **333**, 863-866.
[248] S. Ghosh and G. Hogarth, *J. Organomet. Chem.*, 2017, **851**, 57–67.
[249] S. Ghosh, S. Basak-Modi, M. G. Richmond, E. Nordlander and G. Hogarth, *Inorg. Chim. Acta*, 2018, **480**, 47–53.
[250] A. Rahaman, G. C. Lisensky, J. Browder-Long, D. A. Hrovat, M. G. Richmond, E. Nordlander, and G. Hogarth, *Dalton Trans*., 2020, **49**, 7133–7143
[251] M. Tachikawa, J. Stein, E. L. Muetterties, R. G. Teller, M. A. Beno, E. Gebert and J. M. Williams, *J. Am. Chem. Soc.*, 1980, **102**, 6648–6649.
[252] C. R. Carr, D. B. Cluff, L. A. Berben, *Organometallics* 2020, **39**, 1658-1663.
[253] N. D. Loewen, E. J. Thompson, M. Kagan, C. L. Banales, T. W. Myers, J. C. Fettinger and L. A. Berben, *Chem. Sci.*, 2016, **7**, 2728–2735.
[254] (a) N. D. Loewen and L. A. Berben, *Inorg. Chem.*, 2019, **58**, 16849–16857; (b) D. B. Cluff, A. Arnold, J. C. Fettinger and L. A. Berben, *Organometallics* 2019, **38**, 1230-1235
[255] P. D. Jadzinsky, G. Calero, D. A. Ackerson, D. A. Bushnell and R. D. Kornberg, *Science,* 2007, **318**, 430-433.

[256] N. D. Loewen, S. Pattanayak, R. Herber, J. C. Fettinger, L. A. Berben, L. A. *J. Phys. Chem. Lett.* 2021, **12**, 3066-3073.
[257] M. J. Drance, C. C. Mokhtarzadeh, M. Melaimi, D. W. Agnew, C. E. Moore, A. L. Rheingold, J. S. Figueroa, *Angew. Chem. Int. Ed.,* 2018, **57**, 13057–13061.
[258] S. Hossain, Y. Nihori, L. V. Nair, B. Kumar, W. Kurashige and Y. Negishi, *Acc. Chem. Res.,* 2018, **51**, 3114-3124.
[259] S. Wang, Q. Li, X. Kang and M. Zhu, *Acc. Chem. Res.,* 2018, **51**, 2784-2792.
[260] I. G. Powers and C. Uyeda, *ACS Catal.*, 2017, **7**, 936–958.
[261] M. T. Nielsen, R. Padilla and M. Nielsen, *J. Clust. Sci.*, 2020, **31**, 11–61.